UNIVERSIDAD
DE GRANADA

PROGRAMA DE DOCTORADO EN BIOMEDICINA

Departamento de Química Farmacéutica y Orgánica

Doctoral Thesis

Dynamic Chemical Labelling to profile circulating microRNAs in Body Fluids

PhD Candidate

Antonio Marín Romero

GenYo
PFIZER-UNIVERSIDAD DE GRANADA-JUNTA DE ANDALUCIA
CENTRE FOR GENOMICS AND ONCOLOGICAL RESEARCH

DESTINA

Editor: Universidad de Granada. Tesis Doctorales
Autor: Antonio Marín Romero
ISBN: 978-84-1306-728-5
URI: http://hdl.handle.net/10481/65394

No entres dócilmente en esa buena noche.
La vejez debería delirar y arder cuando se acaba el día.
Rabia, rabia, contra la luz que se esconde.

- Dylan Thomas -

Quality criteria to apply for the degree of “International PhD” by the University of Granada

To apply for the mention of “International Doctorate”, this Doctoral Thesis is supported by:

1. One international internship:

1.1. Internship at the Center for Integrative Biology (CIBIO), at the University of Trento, under the supervision of Prof. Michela Denti, Associate Professor of Applied Biology. This internship took place from the 1st of August to the 30th of November of 2019 and was funded by Programa de Ayudas para Doctorados Industriales en colaboración con la Escuela Internacional de Posgrado (2016) (P26 Programme) and Horizon 2020 programme (MSCA-RISE 2015). Project: “Developing a Novel Detection Platform for microRNAs Useful as Improved Biomarkers for Detection of Lung Cancer and Clinical Decision Making (miRNADisEASY)”

2. Two published scientific articles in relevant journals in the field of the Doctoral Thesis scope. These two published articles include part of the Doctoral Thesis results.

2.1. **Marín-Romero A**, Robles-Remacho A, Tabraue-Chávez M, et al. A PCR-free technology to detect and quantify microRNAs directly from human plasma. Analyst. 2018;143(23):5676-5682. doi:10.1039/c8an01397g. 2018/ 2019 Impact Factor 3.976. Cited by 7

2.2. **Marín-Romero A**, Tabraue-Chávez M, Dear J, et al. Amplification-free profiling of microRNA-122 biomarker in DILI patient serums, using the Luminex MAGPIX system. Talanta. 2020; 219: 121265. 10.1016/j.talanta.2020.121265. 2018/ 2019 Impact Factor 5.339.

3. According to the University of Granada criteria to obtain an “international doctorate” degree, this Doctoral Thesis has been written and will be later defended in English. Additionally and following the requirement of the University of Granada, some parts of the document (abstract and conclusions) have also been written in Spanish and the conclusions will be defended in Spanish.

Grants and funding

The doctoral candidate Antonio Marín Romero is grateful to the funding sources that have been made this Doctoral Thesis possible:

- P26 program – Industrial PhD of the Research and Knowledge Transfer Programme. Universidad de Granada

- DESTINA Genomica S.L. for providing scientific material, assistance, and collaboration, during this PhD.

Index

Abstract / Resumen

Abstract

In the last few years, numerous studies are speedily expanding in search of various biochemical markers found in circulation. Strictly speaking, biomarkers are molecules that detect or confirm the presence of a pathophysiologic condition aiding to establish a diagnosis, refining the prognosis and modifying the treatment. The ideal biomarker exhibits high sensitivity and specificity and should be minimally-invasive.

Micro-Ribonucleic Acids (miRNAs) have been proposed as a new class of biomarkers for multiple human diseases. miRNAs are small non-coding RNAs of 19–24 nucleotides in length that play a major role in fine-tuning the expression of protein-coding genes within the human organism as well as they perform a crucial role in the development and maintenance of numerous pathological processes. A substantial number of miRNAs are present outside the cells, circulating in blood and other body fluids. Recently, there has been a significant interest within the research community to discover and validate circulating miRNAs as clinical biomarkers. However, conventional techniques are not particularly suitable to interrogate small RNA species, such as miRNAs.

Outside of these conventional tools, a unique PCR-free method for the direct detection of nucleic acids (NAs) based on dynamic chemistry, the so-called dynamic chemical labelling (DCL), has been recently proposed. The approach combines the specific labelling of an immobilized abasic peptide nucleic acid (PNA) capture probe with a biotinylated reactive nucleobase, through the templating action of target NA molecules, allowing NA reading with single base resolution. The DCL method harnesses Watson–Crick base pairing to template a dynamic reductive amination reaction on a strand of an abasic PNA, reaction which is thermodynamically controlled. Complementary NA strands also act as catalysts to accelerate the rate of reductive amination. Therefore, when there are not complementary NA strands, reactions do not happen within the assay timeframe.

The aim of this project was to develop, optimise and implement the DCL method into different commercial reading platforms, some of them IVD (*in-vitro* diagnostic) certified, to reach an assay which allow interrogating patient's biological fluids for obtaining clinical decisions.

Different targets were studied:

a) miR-451a, an erythroid cell-specific miRNA associated with human erythroid maturation.

b) miR-122, a well-known specific miRNA of liver cells which is an early and more sensitive indicator of drug-induced liver injury (DILI) than other currently used biomarkers such as ALT or AST.

c) Simultaneous detection of proteins and miRNAs in a single sample, which we have coined seqCOMBO assay.

The DCL method was integrated into two different platforms:

a) FLUOstar OMEGA, a conventional multi-mode fluorescent micro-plate reader for a bead-based in order to develop a novel cost-effective manner for profiling miRNAs.

b) Luminex MAGPIX system, a bead-based fluorescent assay with multiplexing capabilities.

Combining the DCL method with different platforms, direct quantification of miRNAs from biological fluids can be achieved. When used with clinical samples, the developed assay presented an AUC value of 0.94 in distinguishing pathological *vs.* non-pathological conditions, with no false-positive detected. In this Doctoral Thesis and for the first time, a multiplex assay of molecules from different natures (miRNAs and proteins) has been presented, leaving open a new door for the development of new diagnostic opportunities both in the R&D and IVD markets.

Resumen

En los últimos años, son numerosos los estudios que se han expandido rápidamente en búsqueda de varios marcadores bioquímicos. Los biomarcadores se definen como moléculas que detectan o confirman la presencia de una condición fisiopatológica, permitiendo así establecer un diagnóstico, un mejor pronóstico, e incluso modificar un tratamiento. Un biomarcador ideal debe ser altamente sensible y específico, además de ser poco invasivo.

Los ácidos micro-ribonucleicos (miARNs) se han propuesto como una nueva clase de biomarcadores para múltiples enfermedades humanas. Los miARNs son moléculas

pequeñas de ARN, de 19-24 nucleótidos de longitud, que juegan un papel esencial en la modificación de la expresión de genes que codifican para proteínas en el organismo humano, al mismo tiempo que están involucrados en el desarrollo y mantenimiento de numerosos procesos patológicos. Por otro lado, una enorme cantidad de miARNs está presente fuera de las células, circulando en sangre y otros fluidos biológicos. Recientemente se ha despertado un enorme interés dentro de la comunidad científica para descubrir y validar miARNs circulantes como biomarcadores clínicos. Sin embargo, las técnicas convencionales existentes a día de hoy no son totalmente adecuadas para interrogar moléculas pequeñas de ARN, como los miARNs.

Dentro de estas herramientas convencionales disponibles, recientemente se ha propuesto un método único, libre de PCR y basado en química dinámica, para la detección directa de ácidos nucleicos: el método *dynamic chemical labelling* (DCL). Este método combina el marcado específico con un nucleótido reactivo biotinilado sobre una sonda de captura de ácido peptidonucleico (APN) inmovilizada y que contiene una posición abásica, a través de la acción complementaria de la molécula de ARN diana, permitiendo la lectura de ácidos nucleicos con resolución de una sola base. El método DCL está basado en el apareamiento de bases descrito por Watson-Crick, consiguiendo así llevar a cabo una aminación reductiva dinámica sobre una cadena abásica de APN, una reacción termodinámicamente controlada. Además, el ácido nucleico complementario a la cadena abásica de APN actúa como catalizador para acelerar la reacción de aminación reductiva. Así, cuando no existe una cadena de ácido nucleico complementaria, la reacción no tiene lugar dentro del marco de tiempo del ensayo.

El objetivo de este proyecto ha sido desarrollar, optimizar e implementar el método DCL en diferentes plataformas, algunas de ellas con certificado IVD (diagnóstico *in-vitro*, IVD por sus siglas en inglés), para conseguir un ensayo libre de error que permita interrogar fluidos biológicos de pacientes para tomar decisiones clínicas.

Se estudiaron diferentes dianas:

a) miARN-451a, un miARN específico de eritrocitos asociado a la maduración eritrocitaria en humanos.
b) miARN-122, un miARN específico de células hepáticas y bien conocido por ser un indicador de enfermedad hepática inducida por fármacos (DILI), siendo más sensible que otros de los biomarcadores actualmente en uso como ALT o AST.

c) Un múltiplex de moléculas de distinta naturaleza, en un mismo ensayo y desde una misma muestra, el cual hemos llamado ensayo COMBO, para la detección de miARNs y proteínas.

El método DCL se integró en dos plataformas distintas:

a) FLUOstar OMEGA, un lector de placas convencional que, aplicado a ensayos basados en micropartículas, permite desarrollar un ensayo económico para la cuantificación de miARNs.

b) El sistema Luminex® MAGPIX® para el desarrollo de un ensayo basado en la fluorescencia de micropartículas magnéticas con capacidades *multiplexing*.

Mediante la combinación del método DCL con las diferentes plataformas se ha conseguido la cuantificación directa de miARNs en fluidos biológicos. En su aplicación a muestras clínicas, se ha demostrado un ensayo libre de errores en la distinción entre condición patológica y no patológica, dejando a un lado la posibilidad de falsos positivos debido al trasfondo químico de la metodología. En esta Tesis Doctoral se ha conseguido por primera vez en el mundo un múltiplex de moléculas de distinta naturaleza (miARNs y proteínas), dejando una puerta abierta para el desarrollo de prometedoras oportunidades de diagnóstico.

Abbreviations

3SR	Self-sustained sequence replication
ADR	Adverse drug reaction
AEB	Average number of enzymes per bead
AGO	Argonaute
ALF	Acute liver failure
ALP	Alkaline phosphatase
ALT	Alanine transaminase
ARG1	Arginase 1
AUC	Area under the curve
bDNA	Branched DNA
CCD	Charge-coupled device
CDS	Coding sequence
cfNA	Circulating free NA
CTC	Circulating tumor cell
CV	Coefficient of variation
DCL	Dynamic chemical labelling
DGL	PNA probe with an abasic position
DILI	Drug-induced liver injury
DNA	Deoxyribonucleic acid
dNTP	Deoxyribonucleotide
dsDNA	Double-stranded deoxyribonucleic acid
ELISA	Enzyme-linked immunosorbent assay
HDA	Helicase dependent amplification
HDL	High density lipoprotein
HP	Haemolysed Plasma

HRP	Horseradish peroxidase
HV	Healthy volunteer
ISB	Institute for Systems Biology
IVD	*In vitro* diagnostic
LAMP	Lloop-mediated isothermal amplification
LCR	Ligase-mediated chain reaction
LED	Light-emitting diode
LNA	Locked nucleic acid
LoD	Limit of detection
MFI	Median Fluorescence Intensity
microRNA/ miRNA/ miR	Micro ribonucleic acid
mRNA	Messenger ribonucleic acid
NA	Nucleic acid
NAATs	Nucleic acid amplification technologies
NANATs	Nucleic acid non-amplification technologies
NASBA	Nucleic acid sequence-based amplification
NCCN	National Comprehensive Cancer Network
ncRNA	Small noncoding ribonucleic acid
NGS	Next generation sequencing
NHP	Non-haemolysed plasma
NSCLC	Non-small cell lung cancer
PCR	Polymerase chain reaction
piRNA	Piwi-interacting ribonucleic acid
PNA	Peptide nucleic acid
pre-miRNA	Precursor miRNA
pri-miRNA	Primary miRNA

RBC	Red blood cells
RFU	Relative fluorescence unit
RGP	Resorufin-β-D-galactopyranoside
RISC	RNA-inducing silencing complex
RNA	Ribonucleic acid
ROC	Receiver operating characteristic
RPA	Recombinase polymerase amplification
rRNA	Ribosomal ribonucleic acid
RT-PCR	Real-time polymerase chain reaction
RUCAM	Roussel-Uclaf Causality Assessment Method
SA-PE	Streptavidin-R-phycoerythrin
SAFE-T	Safer and Faster Evidence-based Translation
SβG	Streptavidin-β-galactosidase
SDA	Strand displacement amplification
SiPM	Silicon photomultiplier
siRNA	Small interfering ribonucleic acid
SMART-Nb	Aldehyde-modified nucleobase
SNF	Single nucleotide polymorphism
snRNA	Small nuclear ribonucleic acid
SNV	Single nucleotide variant
ssDNA	Single-stranded deoxyribonucleic acid
TFO	Triplex-forming oligonucleotide
TMA	Transcription-mediated amplification
tRNA	Transfer ribonucleic acid
UTR	Untranslated region
UV	Ultraviolet

Rationale

The detection of miRNAs from clinical samples is challenging and error-prone for assays that require laborious sample preparation. Besides, PCR based methodologies also suffer from bias and sample contamination risk from the production of high concentrations of amplicons. As a result, miRNA profiling has serious analytical challenges when highly precise and accurate quantification is required for diagnostic purposes.

This project aimed to develop a bead-based assay for the direct profiling of miRNAs in body fluids to overcome the various limitations of conventional methods for analysing miRNAs, such as (a) the challenges associated with the pre-extraction of RNAs and (b) the problems related to both the reverse transcription and amplification.

Objectives

Objective 1: Development of an amplification-free technology to detect and quantify microRNAs directly from human plasma.

Specific aims of the objective 1:

1.1. Development of a platform comprising magnetic microspheres and DCL method for the identification and quantification of miR-451a.

1.1.1. Design, synthesis and characterisation of a DGL probe for the miR-451a detection.

1.1.2. Coupling of the DGL probes to the magnetic microspheres.

1.1.3. Validation of the functionality of the DGL probes coupled to the magnetic microspheres using a conventional micro-plate reader (FLUOstar® OMEGA).

1.1.4. Protocol optimization and determination of the assay sensitivity using healthy plasma matrix.

1.2. Direct quantification of circulating miR-451a from haemolysed plasma samples.

1.2.1. Haemolysed and non-haemolysed plasma samples direct quantification using the DCL method.

1.2.2. Analytical comparison of DCL method *versus* the gold standard RT-qPCR.

Objective 2: Integration of the DCL method with the Luminex® MAGPIX® system for the direct profiling of miR-122 biomarker in DILI patient serums.

Specific aims of the objective 2:

2.1 Development of the DCL method for the integration in the Luminex® MAGPIX® system.

2.1.1 Design, synthesis and characterisation of a DGL probe for the miR-122 detection.

2.1.2 Coupling of the DGL probes to the magnetic microspheres.

2.1.3 Validation of the functionality of the DGL probes coupled to the magnetic microspheres using the Luminex® MAGPIX® system.

2.1.4 Protocol optimization and determination of the assay sensitivity.

2.2 Direct profiling of miR-122 biomarker in DILI patient serums.

1.2.1 Direct detection and quantification of miR-122 in DILI patient serums using the DCL / MAGPIX assay.

1.2.2 Contrasting levels of miR-122 in DILI and No DILI patients.

1.2.3 Correlation between levels of miR-122 and ALT protein for the DILI patients.

Objective 3: Simultaneous Detection of DILI related microRNA and Protein using DCL method in integration with the Luminex® MAGPIX® system.

Specific aims of the objective 3:

3.1 Integration of the DCL method with a MILIPLEX MAP kit to generate an unique protocol to direct detect microRNA and protein from a single sample.

3.1.1 Coupling of the DGL probes to the magnetic microspheres.

3.1.2 Validation of the functionality of the DGL probes coupled to the magnetic microspheres using the Luminex® MAGPIX® system.

3.1.3 Protocol optimization.

3.2 Direct profiling of miR-122 and ARG1 protein in DILI patient serums.

3.2.1 Direct detection of miR-122 and ARG1 protein from a single DILI patient serum sample using the DCL / MAGPIX assay.

Chapter 1:
Introduction

Chapter 1: Introduction

Over the last years, it has been put a high effort into genome and proteome research, leading to a deeper knowledge of the molecular basis of diseases, their incidence, development, and cure. Consequently, there is emerging a wide quantity of new therapies that are being discussed as either ‘‘personalized medicine’’ or “precision medicine”. (1, 2) The role of molecular diagnostic has a big impact on this concept since specific biomarkers for early detection of disease are needed, even when presymptomatic status have to be diagnosed to reach successful medical treatments. (3-5) Also, the screening of individual genetic markers of patients will help to improve personalized therapies. (6) On top of that, novel IVD testing as point-of-care can leverage molecular knowledge developed over the past decades for mass testing. Thus, most analysts coincide that the molecular *in vitro* diagnostics (IVD) market will grow with a double-digit CAGR (compound annual growth rate) through the next decade.

The biomarker concept is a key component for the future development of diagnostic. Biomarkers are all types of parameters that may be measured quantitatively from a patient and correlate with a specific disease. (5) The general concept of a biomarker includes all types of physiological data such as heartbeat and lung volume, among others. The more specific concept of molecular biomarkers concentrates on biochemical or genetic parameters and patterns, sometimes called signatures. Moreover, diagnostics become more complex when a deeper look at multiple biomarkers is necessary. Within the Human Genome Project, about 25,000 genes were identified. (7) These genes are transcribed to various forms of RNA, then translated into proteins and post-translationally modified in different ways. (8) Going one step further, also variation in metabolism may be linked to diseases as well. In this regard, genomic, proteomic, glycomic, and metabolomic research has aimed to the need to detect and quantify a wide range of analytes ranging from genes and proteins to small molecules and combinations thereof. (9)

1.1 Nucleic Acid

In 1953 James Watson, Francis Crick, Rosalind Franklin and Maurice Wilkins revealed the structure of DNA (10) highlighting two main characteristics: (i) the existence of complementarity between the nitrogenous bases of the two chains (thymine supplements with adenine and guanine with cytosine) and (ii) the adoption of a double helix structure of the DNA polymer.

DNA and RNA are polynucleotide chains that show relevant differences.

1.1.1 Deoxyribonucleic acid

DNA molecules are double-stranded. The nucleotides of both molecules are composed of five-carbon sugar rings, to which a nitrogen base and a phosphate group are bound. The sugar is a deoxyribose monophosphate (the phosphate binds to the sugar via ester bond in the 5’ hydroxyl group) and the bases can be adenine, guanine, cytosine and thymine. Nitrogen bases with a single sugar-ring structure (cytosine, thymine) are pyrimidines. The ones containing a double-ring structure (adenine, guanine) are purines (Figure 1.1). Each strand is a repeating phosphate-sugar polymer covalently linked by phosphodiester bonds between the hydroxyl group of the 3' carbon and a phosphate group at the 5' position of the incoming nucleotide. The order of these bases determines the genetic code.

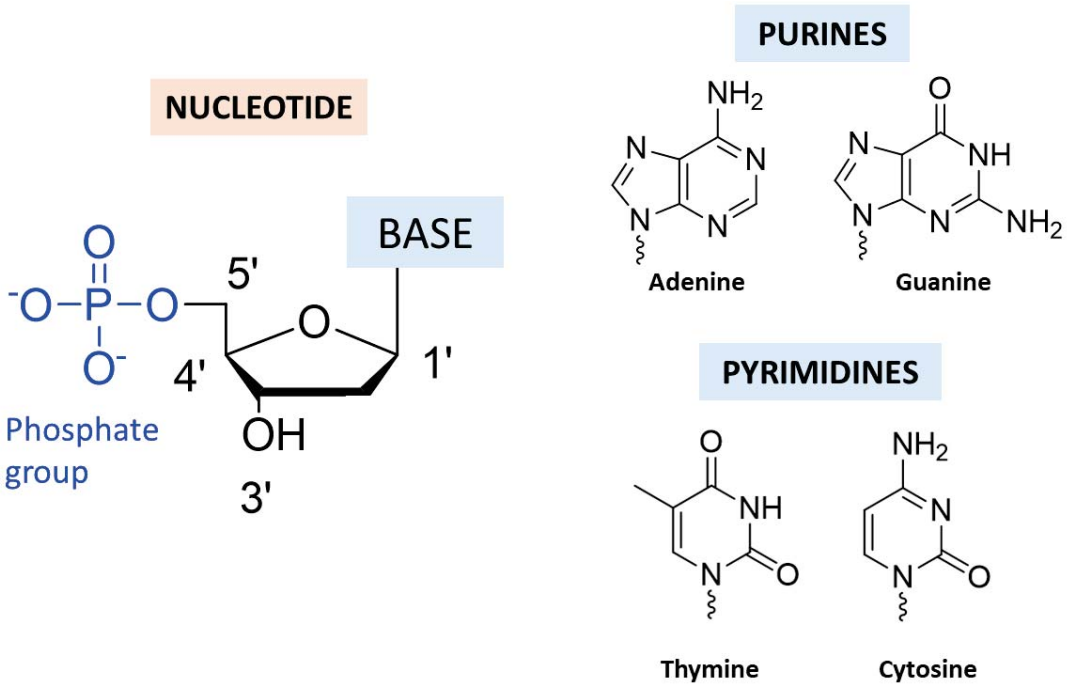

Figure 1.1 – Purine and pyrimidine bases.

DNA molecules adopt a three-dimensional structure with a double helix with a right-handed sense direction. The two chains of a DNA molecule are held together thanks to the complementarity of bases, in which each base is joined by hydrogen bonds to its complementary base of the antiparallel chain. Adenine forms two hydrogen bonds with thymine, while cytosine pairs with guanine through three hydrogen bonds. As a result, all the bases are oriented towards the inside of the helix while the sugar-phosphate backbones stay towards the outside. Both strands are antiparallel, so that the 5' end

with the phosphate terminal group of one strand aligns with the 3' end with the hydroxyl terminal of the other strand. There are van der Waals and hydrophobic interactions between both strands that contribute to the stability of the DNA structure. The helix rotates every 3.4 nm, with 10 pairs per turn, forming what is known as the B form of DNA. There are other alternative DNA structures, such as form A, which is found in conditions of very low humidity, being more compact with 11 bases per turn; the Z shape, which is a left helix. (11)

1.1.2 Ribonucleic acid

Ribonucleic acid (RNA) is a nucleotide polymer that shows great similarities to DNA. Even so, there are several structural differences, and among the main ones are the following:

- RNA has ribose instead of deoxyribose in the case of the sugar molecule.
- One of the nitrogenous bases, thymine, is replaced by uracil (thymine is 5-methyl uracil as shown in Figure 1.2).

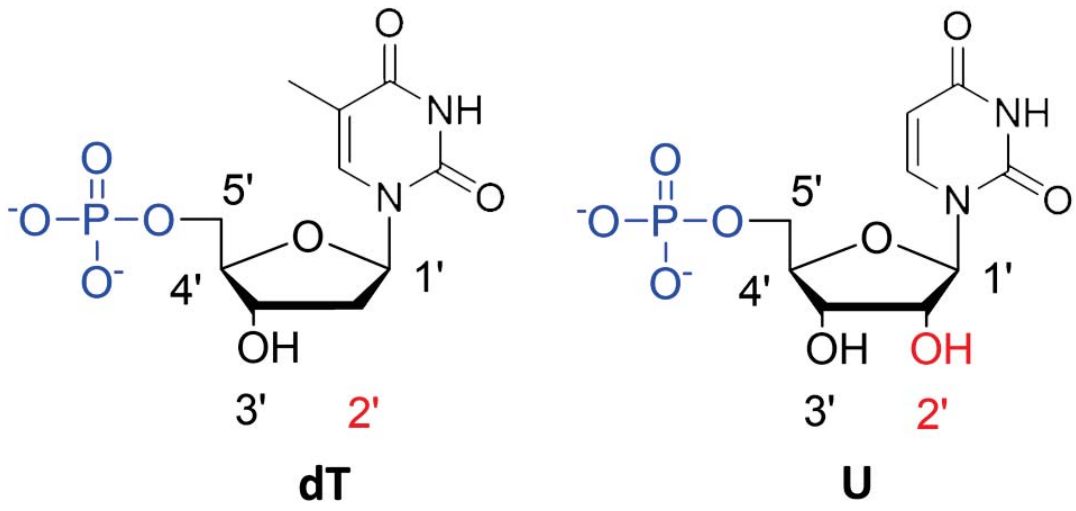

Figure 1. 2 – Uracil (U), the nucleotide replacing thymine in RNA.

- RNA is single-stranded. Despite the fact that practically none of RNA strands have a complementary strand, the structure is not completely single-stranded, but they form secondary structures due to the existence of internal complementarity.

There are numerous types of RNA in the cell:

Messenger RNA (mRNA): mRNA is generated as a consequence of DNA transcription. Ultimately, it will produce proteins through the translation complex, which are responsible for the phenotype.

Ribosomal RNA (rRNA): rRNA, which comprises 80% to 90% of total cellular RNA and constitutes an important structural and functional part of ribosomes, the cellular organelles where proteins are synthesized.

Transfer RNA (tRNA): the tRNA acts as adapter molecules to allow the reading of the information contained in the mRNA by ribosomes to produce proteins. There is at least one tRNA for each amino acid.

Small nuclear RNA (RNAnn): RNAnn remains in the nucleus after being transcribed by RNA polymerase I or III and is not translated into protein. Its main function is the processing of pre-messenger RNA in the nucleus.

Small non-coding RNA (ncRNA): Small ncRNAs are transcribed but, like snRNAs, they are not translated into proteins. These types of RNA are known to play roles in gene regulation. Many different classes of small cRNAs have been described in the last two decades. Of these, microRNAs (miRNAs), small interference RNAs (siRNAs), and Piwi-interacting RNAs (piRNAs) have been studied in more detail.

1.1.1 Thermodynamics of Nucleic Acid duplex formation

Nucleic acid probe technology is mainly based on the concept of complementary base pairing between two strands of NA. Double-stranded DNA (dsDNA) can be denatured into two complementary single strands by simply applying heat, alkali, or putting into solution with double-helix destabilizing agents, for example formamide. When incubated under the optimal conditions for renaturation, the complementary strands can re-associate to reform the initial duplex double helical form. (12) The term hybridization refers to the formation of this specific base-paired duplex. Hybridization can also occur between RNA/RNA (13) or RNA/DNA. (14) The temperature at which a specific dsNA is denatured is called melting temperature (Tm), reflecting thus the thermal stability of a dsNA. The factors that affect the stability of a dsNA have been widely studied. The three major factors affecting the Tm are:

1. The ionic strength of the solution.
2. The presence of specific denaturing agents.
3. The base composition of the particular nucleic acid sequence.

The next formula describes how all these factors contribute to the Tm:

$$Tm = 81.5 + 16.6\ (\log M) + 0.41(\%\ G + C) - 0.61\ (\%form) - 500/L$$

Where: Tm = melting temperature (ºC); M = molarity of monovalent cations; %G + C is the percentage of guanine and cytosine; (%form) refers to the percentage of formamide in the solution; and L is the base pair length of the NA.

The maximum rates of hybridization occur at temperatures below the Tm of the NA, approximately at 20 to 25ºC. When temperature go lower and lower from the Tm, the hybridization tends to be carried out slowly and cross-hybridization between non-complementary sequences takes place more frequently, since mismatched duplexes are stable at the lower temperatures. On the other hand, when temperatures are close to the Tm of the duplex, hybridization also tends to be slow because perfectly matched duplexed tend to dissociate. (15)

Other factors can highly affect the rate of hybridization. When a low ionic strength (a solution that contain low-salt concentration) (16) and high viscosity is present, (17) low rate of hybridization occurs. NA hybridizes at higher rate in the presence of inert polymers like dextran sulphate and polyethylene glycol. (18) Formamide often is added to the hybridization solution to go down the Tm of the duplexes and allow hybridizations at lower temperatures. (18)

1.2 Nucleic Acid analogs

As described in the previous chapter, the knowledge in NAs is growing. The molecular diagnostic field has come a long way thanks to technologies such as the polymerase chain reaction (PCR) and other antisense methodologies. However, despite all these advances, the nature of NAs imposes some limitations on this type of methodologies so that it cannot continue to be refined. That is why there is a large part of the research that dedicates its effort to designing and developing synthetic analogues of NAs, which offer characteristics that allow overcoming those limitations implicit in natural NA. The development of such synthetic analogs makes it possible facilitating oligonucleotide synthesis, improving selectivity and affinity, increasing resistance to nucleases, improving thermodynamic properties and offering a greater ability to cross biological membranes. (19)

There are several ways through which these NA analogs can be generated. All of them introduce some modification in any of the substructures of the molecule: a)

modifications on the nucleobase; b) in the sugar ring or c) in the phosphodiester backbone. (20) Some of the most promising analogs are blocked NAs (LNAs) and peptide NAs (PNAs).

1.2.1 Locked nucleic acid

In 1998 Singh et al. described LNA as a new class of synthetic analogs of NAs containing conformational restriction. (21) As shown in Figure 1.3, LNA is a ribonucleoside structurally locked covalently via the 2' oxygen and the 4' carbon, containing a methylene unit.

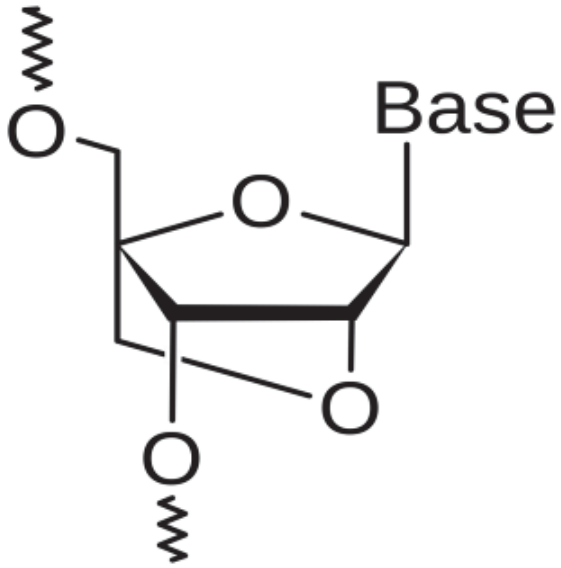

Figure 1. 3 – Locked nucleic acid (LNA) chemical structure. (*Copyright under CC BY-SA 3.0*).

Properties of LNAs

1. High-affinity hybridization: LNA has hybridization affinity for both complementary DNA and RNA, being considered a powerful tool for research purposes and molecular diagnostic. (22, 23)
2. Triplex-forming oligonucleotide: LNA has the ability to form triple helix structures through interaction with a duplex DNA molecule, thus being possible to inhibit the transcription process. (24) Because this triple helix is high stable, LNAs containing triplex-forming oligonucleotides (TFOs) allows its formation at physiological conditions.
3. Thermodynamics: A duplex conformation containing one strand of LNA is high stable. (25)

Applications of LNAs

The properties of LNAs described above offer high selectivity to discriminate mismatches, making them very useful for SNPs identification studies. Furthermore, it is recommended for any hybridization assay through the design of LNA-based capture probes, or the use of LNA-based primers for PCR. (26, 27)

1.2.1 Peptide nucleic acid

In the 1980s Peter Nielsen described peptide nucleic acids (PNAs) as a synthetic DNA analogue characterized by an amino acid backbone rather than a sugary one. (28) This amino acid skeleton is made up of N- (2-aminoethyl) glycine units. Nucleobases are linked through a methylene-carbonyl bond.

As occur with LNAs, PNAs have high affinity for complementary DNA and RNA strands, (29, 30) and are more stable compared to DNA / DNA or RNA / RNA duplexes. (31, 32) They have a high resistance to proteases and nucleases, making them very useful for molecular diagnostics purposes.

Properties of PNAs

Due to the neutral charge of PNAs, they have poor water solubility compared to DNA. The neutral PNA molecules tend to form aggregates depending on the sequence of the oligomer. PNA solubility is dependent on the length of the oligomer and purine/ pyrimidine ratio. (33) To increase solubility of PNA oligomers, positively charged lysine residues (34) are normally incorporated into the amino acid skeleton or negative charges are introduced. They are very stable to acidic conditions. PNA can also form secondary structure by internal complementarity to form stem-loop (“hairpin”) structures. (35)

PNAs form PNA–RNA, (29) PNA–DNA, (30) PNA–PNA duplexes, (36) and PNA–PNA–DNA triplex. (37) The PNA backbone has not negative charge as others NA analogs, making them stronger to form hetero-duplex PNA-DNA and PNA-RNA than standard DNA-DNA or RNA-RNA homo-duplex, respectively. (32) It occurs since the absence of negative charge in the structure avoids charge repulsion between strands. Besides, such hetero-duplexes are generally more thermally stable than the corresponding homo-duplexes. (32)

PNA–DNA structures are not affected by the ionic strength of the solution. The capacity to discriminate mismatches is also higher than standard homo-duplexes, hence making PNAs a useful tool for SNP identification. (38)

Applications of PNAs

PNAs possess a lot of the properties that an antisense reagent has to unify. They have high stability and selectivity for binding to complementary RNA, and very high stability under physiological conditions, enabling them to effectively inhibit translation of target mRNA. In addition, they have high resistance to being digested by proteases and nucleases, which is not the case with the natural NAs. For this reason, when PNAs enter the cell, they are capable to keep intact for at least 48 hours, while in the case of natural NAs the half-life time is less than 15 minutes. All these properties have been clearly reported elsewhere. (39) The hetero-duplex PNA-NA is very stable in solutions with low ionic strength, allowing them to be used in several techniques for isolation and detection of NAs for molecular diagnostic purposes. (40) Since PNA has high selectivity and affinity, their use for SNP identification analysis are high recommended. (41)

1.3 The use of nucleic acids in molecular diagnostic

Most molecular diagnostic techniques are based on modifying, isolating, amplifying, and detecting NA sequences. Purification and amplification are required to have enough quantity to be detected and analyzed by the detection platform. These types of methodologies are known as "nucleic acid amplification technologies" (NAAT). (42) However, there are other types of techniques that do not require NA purification or amplification prior to analysis, known as "non-nucleic acid amplification technologies" (NANAT). (43)

Around 1970, three key elements for the development of molecular diagnosis were discovered: 1) the synthesis of oligonucleotides; 2) the use of restriction enzymes and, 3) reverse transcriptase. The first molecular diagnostic technique reported was Southern blot, presented in 1975 through the use of restriction enzymes and separating the resulting sequences by size on agarose gels. (44) Shortly after, in 1977, the Northern blot was developed, being very similar but applied to the analysis of RNA instead of DNA. (45) Currently, Southern or Northern Blot is very rarely used, since they have many limitations such as the requirement of large amounts of genetic starting material, as well as being very laborious and time-consuming.

Practically in parallel to the appearance of the Northern blot, in 1977, DNA sequencing using chain termination inhibitors (dideoxynucleotides) was also presented, which allowed an automated fluorescence analysis and that positioned it with a higher value compared to the two previous methods. (46)

In 1985, it was described for the first time the polymerase chain reaction (PCR). It was not until 1988 that this methodology underwent a significant improvement through the discovery and use of thermostable polymerases. (47, 48) Of all the molecular techniques that have been developed to date for use in molecular diagnostics, PCR has become the most popular method. In addition, there are numerous variants and improvements that have been developed, being particularly and widely extended real-time PCR (RT-PCR), which was described in 1992. (49)

In 1990 DNA microarrays were reported. (50) Next generation sequencing (NGS) was first published in 2005 and has described a continue development becoming a leading technology. (51)

In the twenty years, there have been emerging numerous NANAT by carrying out single hybridization onto solid surfaces and then amplifying the signal by non-enzymatic procedures.

1.3.1 Nucleic acid amplification technologies (NAATs)

Most of the molecular methods available so far in clinical laboratories for detection of NAs employ some form of NA amplification. As mentioned above, one of the most widely used methods is PCR, but there is a great diversity of techniques for this purpose. Some of the most commonly used are ligase-mediated chain reaction (LCR), loop-mediated isothermal amplification (LAMP) or nucleic acid sequence-based amplification (NASBA). These conventional NA tests require some common steps: 1) NA isolation; 2) NA amplification; and 3) detection and analysis. Occasionally it is needed to include some sample conditioning steps prior to amplification or analysis. This is the case of the conversion of RNA to DNA, which has to be carried out by the enzyme reverse transcriptase in a process known as retro-transcription.

1.3.1.1 Nucleic acid isolation

There are three steps used for the majority of samples: (1) NA extraction from the sample under interrogation; (2) NA isolation from the obtained matrix; and (3) NA purification allowing removing substances that can inhibit the polymerase activity. (52)

To release the NA from the starting material (cells, vesicles, tissues, etc.), a lysis process is carried out. The lysis can be chemical, mechanical or enzymatic, and it is important to select properly the methodology to ensure that the genetic material is released efficiently. Once the lithic process is completed, the NA fraction has to be separated from the rest of the sample, for which different separation methods are used. (52) Subsequently, the genetic material has to be purified, although the importance of the degree of purity may be greater or less depending on the objective of the analysis and the methodology used for such analysis. Finally, the purity of the sample is measured, which is usually done by ultraviolet (UV) absorbance. (53)

1.3.1.2 Amplification of NAs

Polymerase Chain Reaction (PCR)

A massive amplification of a DNA segment can be carried out by knowing the sequence of at least the end portions of the pertinent segment. This is possible by using the polymerase chain reaction (PCR), a process conceived by Kary Mullis in 1983. (47)

The PCR procedure, shown in Figure 1.4, is executed by enzymes called DNA polymerases. These enzymes have the capacity to synthesize DNA strands from deoxyribonucleotides (dNTPs), using a DNA template. DNA polymerases do not generate DNA *de novo*, but instead add nucleotides to pre-existing strands, as the so called primers. In PCR, two synthetic oligonucleotides are used as primers, which can be extended by a DNA polymerase. These oligonucleotide primers are complementary to sequences on opposite strands of the DNA portion under interrogation, positioned so that their 5′ ends define the ends of the portion to be amplified, and they become part of the amplified sequence. The 3′ ends of the annealed primers are oriented toward each other and positioned to prime DNA synthesis across the targeted DNA region.

Four key components are required to carry out the PCR: 1) the source material containing the DNA region under interrogation; 2) the mentioned primers; 3) a pool of deoxynucleoside triphosphates, and a DNA polymerase.

As shown in Figure 1.4, there are three steps to carried out a complete protocol for one PCR cycle. In step 1, both DNA strands are separated by applying heat to the reaction mixture. In step 2, the temperature is decreased so that the primers hybridize with the complementary region of DNA. It is important to establish an optimal concentration for the primers, since if the concentration is too low there is a risk to re-hybridize the two

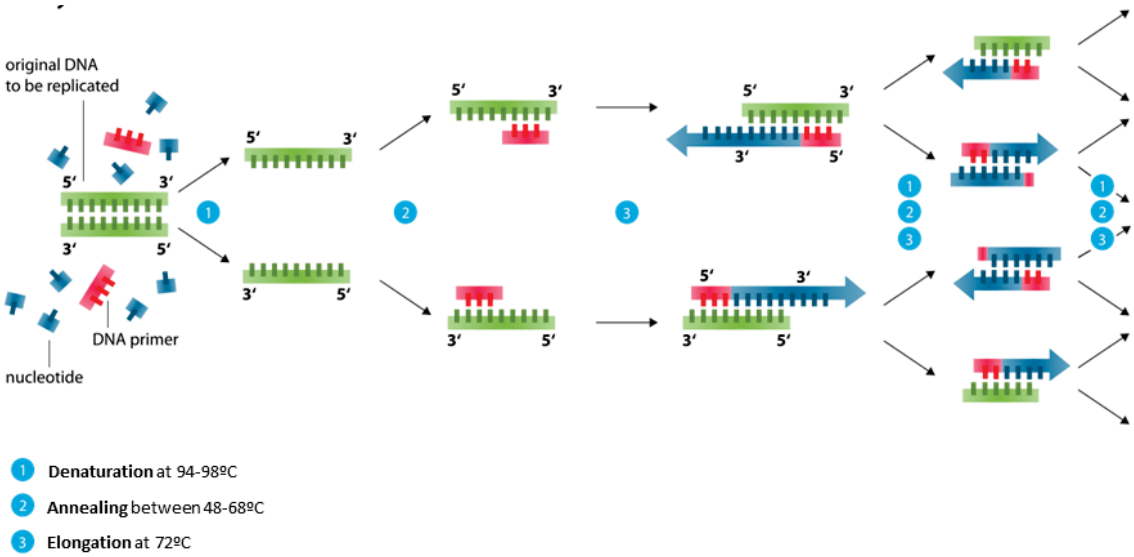

Figure 1.4 – DNA amplification via polymerase chain reaction (PCR) The complete protocol of PCR is divided in three main steps. Primers coloured in red. Flank region appears in green. (*Copyright under CC BY-SA 3.0*).

DNA strands. The annealing temperature is also decisive, for which the Tm of the pair of primers must be determined. In step 3, the polymerase uses the pool of dNTPs to carry out the amplification of the flanked region. All these three described steps are repeated in cycles, from about 20 to 40 times in an automated process inside a machine known as thermocycler, which allows obtaining a large amount of the target genetic region. Finally, the amplified products can be detected by different techniques. (54)

Each replication cycle duplicates the number of target DNA segment copies, so the concentration grows in an exponential way. After 20 cycles, the targeted DNA segment has been amplified more than a million-fold (2^{20}); after 30 cycles, more than a billion-fold. PCR uses a heat-stable DNA polymerase such as the *Taq* polymerase, isolated from a thermophilic bacterium (Thermus aquaticus) that thrives in hot springs where temperatures approach the boiling point of water. Thus, the *Taq* polymerase remains active after every heating step (step 1) and does not have to be replenished. (54)

This technology is highly sensitive: PCR can detect and amplify just one DNA molecule in almost any type of sample. Contamination of samples is a serious issue due to the extreme sensitivity of PCR methods. Specific controls must be run to ensure that the amplified DNA is not derived from the researcher or from contaminating bacteria. (55)

PCR was later combined with fluorescent labelling which led to real-time PCR (RT-PCR). (49) All real-time systems quantify by fluorescence the amount of genetic material that is produced during the amplification process. Therefore, a fluorescent

signal that increases with each cycle suggests that the target region is in the sample. On the contrary, the absence of signal after 35/40 cycles suggests that there is no amplification of the target genetic region and, therefore, our target is not present in the sample. The methodology includes positive controls to confirm that the amplification reaction is being carried out efficiently, and negative controls to rule out possible contamination that could give us false positive results.

Transcription-Based Amplification Methods

Transcription-based amplification methods were presented after the discovery of the replication mechanism of retroviruses. (56) These methods are known by various names, including NA sequence–based amplification (NASBA), transcription-mediated amplification (TMA) and self-sustained sequence replication (3SR) assays. Amplification of the target region is carried out under isothermal conditions using the activity of reverse transcriptase, RNase H and RNA polymerase. As shown in Figure 1.5, the name most commonly used to describe this form of amplification is TMA. To do this, the two primers are put into the reaction mixture together with the reverse transcriptase and an RNA polymerase. The primer has the peculiarity of containing a 5' tail including an RNA polymerase promoter sequence, so that when it hybridizes with the target RNA it is extended by reverse transcriptase, creating an RNA-DNA duplex. The RNase H activity then degrades the RNA strand so that the second primer can hybridize to the remaining DNA strand. In this way, the reverse transcriptase extends the second primer thus creating a DNA-DNA homo-duplex, which includes the RNA polymerase promoter. RNA polymerase recognizes this promoter and initiates transcription, generating hundreds of RNA copies for each DNA template. Each strand of RNA is then attached to the second primer, spreading to re-form an RNA-DNA heteroduplex; RNA in the hybrid is degraded by RNase H and the promoter primer is bound and extended to produce double-stranded DNA, which can be re-transcribed to repeat the described cycle. It is a mainly advantageous methodology when the target is RNA.

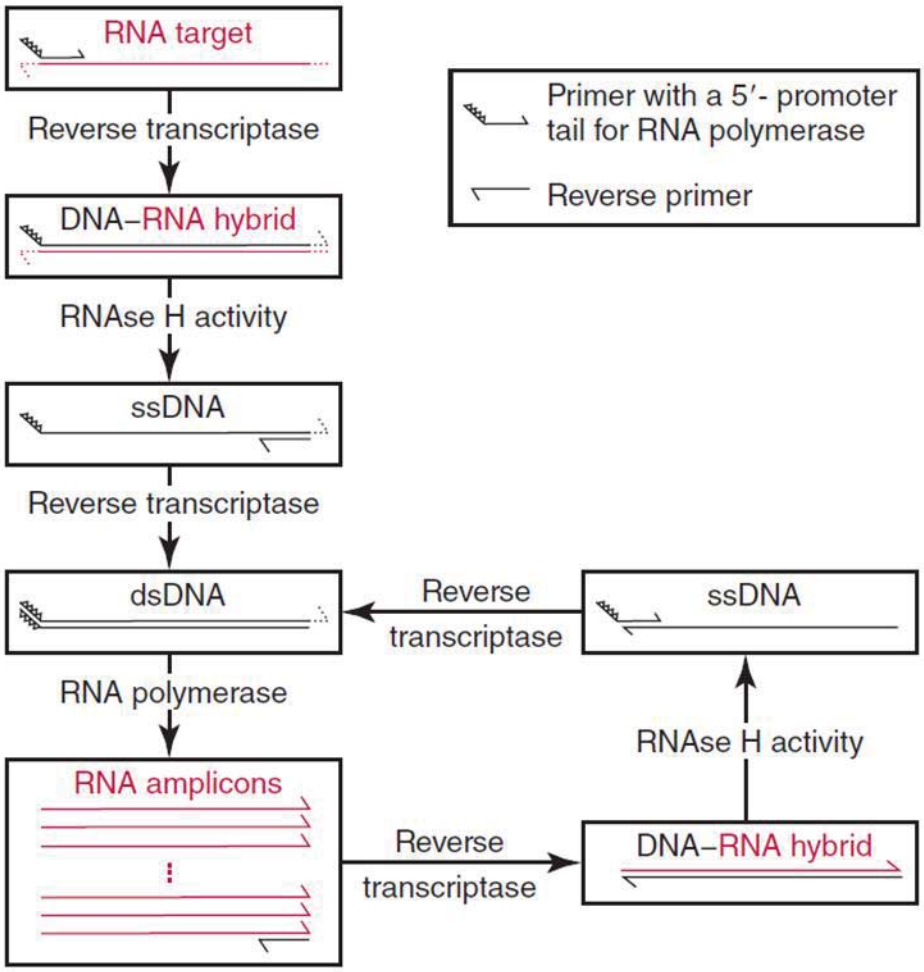

Figure 1.5 – Complete procedure of transcription-mediated amplification (TMA). (57)

Loop-Mediated Amplification Methods

Loop-mediated amplification (LAMP) generates highly diverse DNA structures during the amplification process. (58) The target sequence is amplified under isothermal conditions, between 60-65 °C. Two different primer pairs are used, one pair of outer primers with strand displacement capability, and the other pair of inner primers with looping capability, recognizing a total of six target regions. The inner primer pair amplifies the target sequence and, after this extension, the outer primer pair displaces the generated products. These generated products are used to carry out cyclic amplification by extending the 3' free ends, generating increasingly complex products containing more loops and branched structures.

Strand Displacement Amplification

As in the case of LAMP, strand displacement amplification (SDA) needs to generate starting material before amplification. (59) DNA strands are separated by applying heat in the presence of four primers: two external primers with characteristics similar to

those of LAMP, and two internal primers that have 5 'tails with a restriction site. Once the annealing process has been carried out, a polymerase with exonuclease capacity, together with a pool of dGTP, dCTP, dUTP and a modified deoxynucleotide (dATPαS), carries out exponential amplification under isothermal conditions at 37ºC: (1) a restriction enzyme cuts on a single strand (dATPαS prevents double-stranded cutting); (2) from the cleavage site, extension occurs by strand displacement polymerase; (3) the internal primer containing the restriction site pairs with the displaced strand and; (4) final extension of the displaced strand, forming the product of the desired region.

Variants of PCR Non-Requiring Heat Denaturation

There are methodologies that present the same end products as PCR but working under isothermal conditions. This is the case of helicase-dependent amplification (HDA), which using a helicase enzyme, allows the two strands to be unwound and separated without the need to apply heat. Since the helicase used is thermostable, extension by a polymerase can be carried out between 60 and 65 °C. (60) Another example is recombinase polymerase amplification (RPA), which uses a recombinase enzyme to analyze double-stranded DNA for primer sites, allowing primers to hybridize together with single-stranded binding proteins to avoid a re-hybridization of the two strands during the amplification process, which takes place at 37 °C. (61)

1.3.1.2 Detection of NAs

Molecular beacons

As shown in Figure 1.6, molecular beacons are hairpin-shaped oligonucleotide probes and are about 25 nucleotides long. (62) Their typical structure can be divided in 4 parts:

1. The loop, made up by a 15–30 base pair region. This region is complementary to the target sequence.
2. The stem, at both 3’ and 5’ ends of the loop, each one formed by 4 to 7 nucleotides complementary to each other.
3. A fluorophore at the 5' end.
4. A quencher at the 3' end.

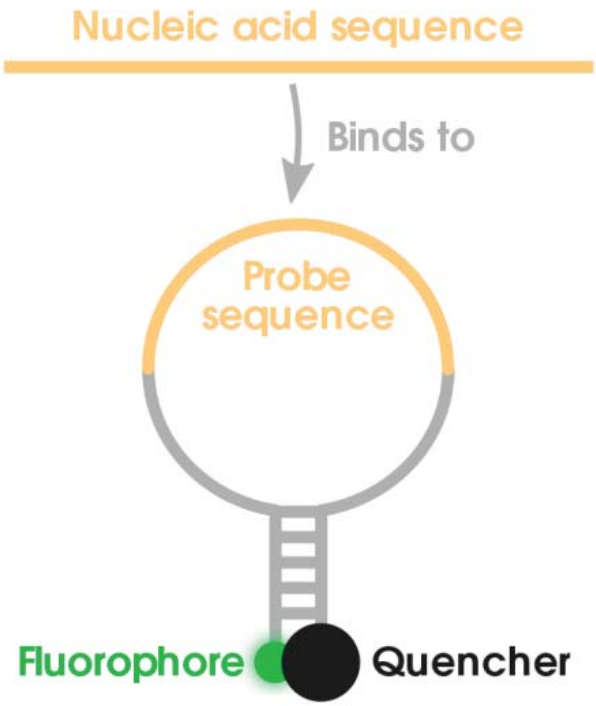

Figure 1. 6 - Structure of a typical molecular beacon probe. (*Copyright under CC BY 4.0*).

If the target is not present in the solution containing the beacon probe, the probe keeps in a closed loop shape, and the proximity of the quencher and the fluorophore results in quenching the fluorescent emission of the latter. When the target, which is complementary to the strand in the loop, is present in the solution, the event of hybridization occurs. This event takes place since the duplex formed between the nucleic acid and the loop region is more stable than that of the stem since it involves more base pairs. (63) As the quencher is no longer in proximity to the fluorophore, fluorescence emission takes place. The measured fluorescence signal is directly proportional to the amount of target DNA.

TaqMan

TaqMan probes contain a fluorophore covalently attached to the 5' end and a quencher at the 3' end (Figure 1.7). Because of this close proximity, the fluorescence of the fluorophore is quenched in the free probes. (64) The probe sequence is intended to hybridize specifically in the DNA target region of interest contained between both PCR primers. The new strand synthesis displaces the TaqMan probes hybridized with the target sequence. Since the Taq DNA polymerase has 5′-exonuclease activity, it degrades the annealed probe and liberates the fluorophore (64) Once the fluorophore is released from the TaqMan probe, the quencher does not absorb its fluorescence and the fluorescent emission takes place (Figure 1.7). It is important to note that

mismatches between the DNA template sequence and the TaqMan probe can cause failure to detect the DNA template appropriately.

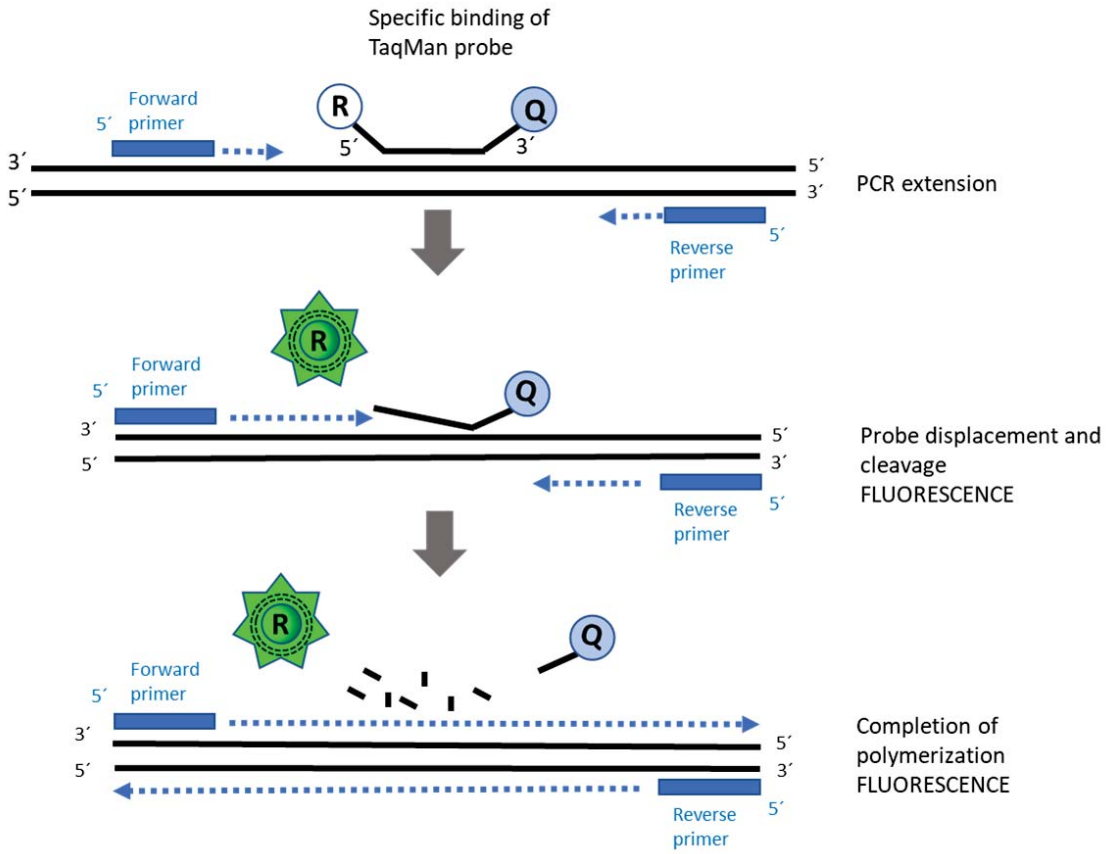

Figure 1.7 - Scheme of TaqMan assay.

Intercalating Dyes (i.e. SYBR Green)

When the amplification event takes place, a duplex of DNA is formed. An intercalating fluorescent dye has the capacity to be inserted into this generated DNA duplex (Figure 1.8), so the intensity of fluorescence increases proportionally to the generated duplex, offering the capacity to make measurements in real-time. (65).

dsDNA + intercalating dye = measurable fluorescence

Consequently, as you have more DNA products at the end of the last cycle, your intensity of fluorescence also increases and will become higher. (66)

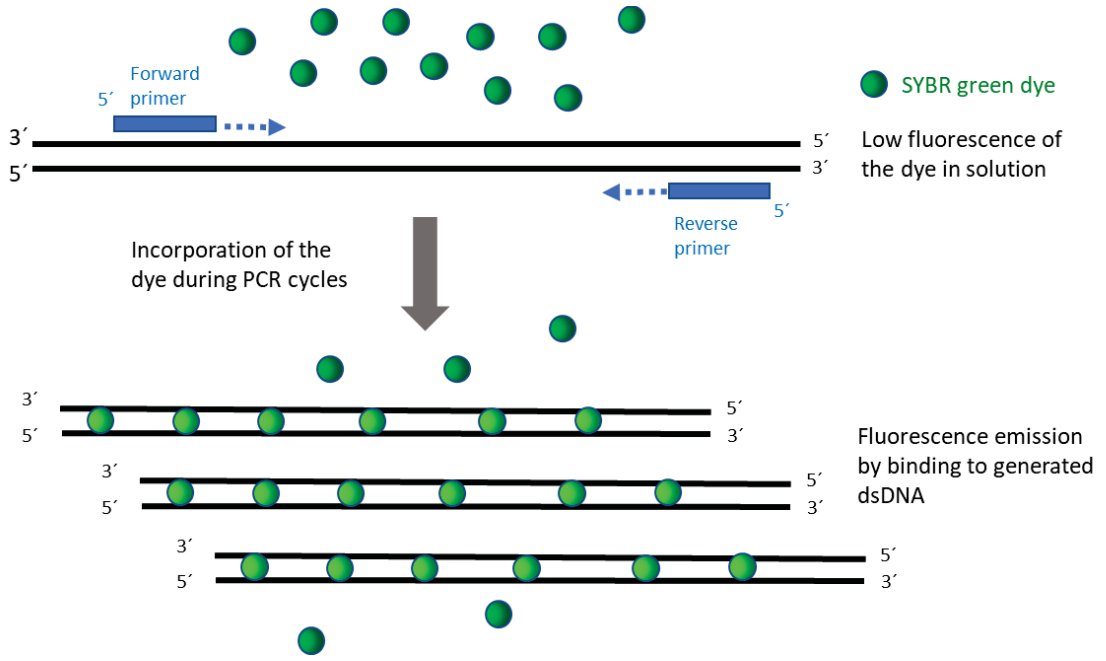

Figure 1.8 - Scheme of SYBR Green assay.

PlexPCR® technology

PlexPCR® technology has a high specificity due to the bi-specificity of PlexZyme® activity, which reduces the chance of false positives. In addition, universal probes are used, which makes the methodology robust and consistent. (67)The PlexZyme® are made up of two components called "partzymes" (Figure 1.9 A). Each part possesses DNA catalytic activity and an extensor arm that allows binding a universal probe. These partzymes are inherently inactive but, when both partzymes bind adjacent to a target, they form an active PlexZyme® complex (Figure 1.9 B). PlexZymes® catalyzes the cleavage of universal probes thanks to the DNA catalytic activity, resulting in a fluorescence signal that can be monitored in real time (Figure 1.9 C).

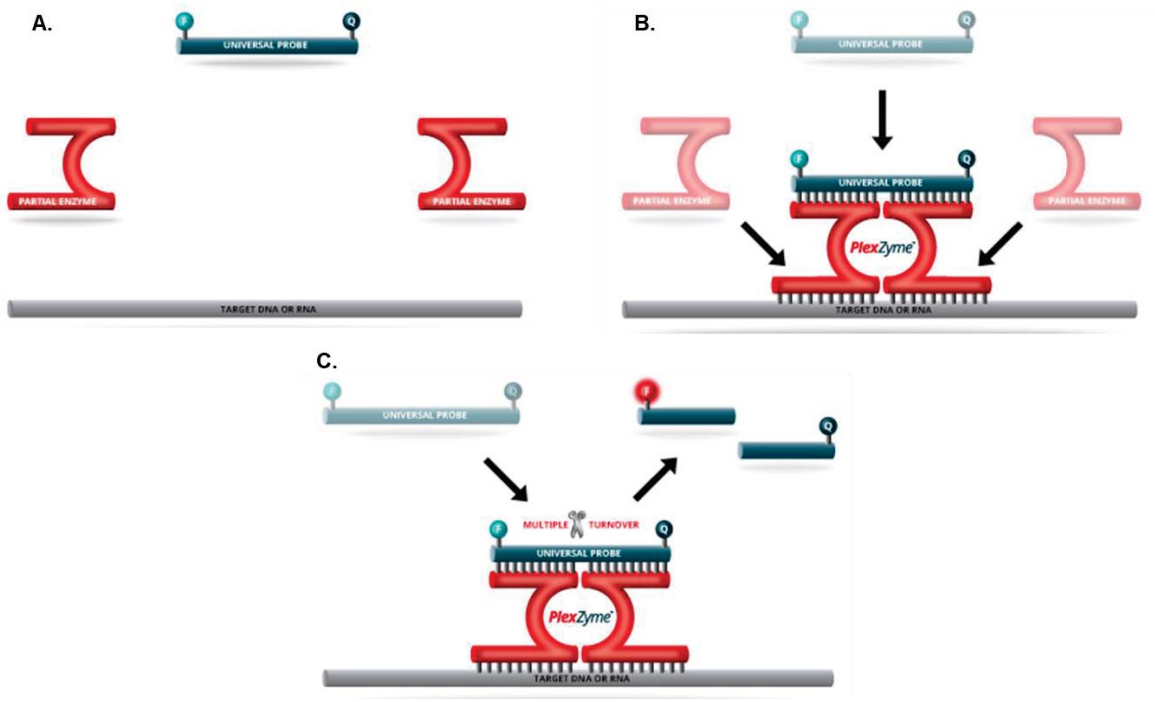

Figure 1.9 - Scheme of PlexPCR® technology.

Multiplex assays can be designed with this technology by labelling universal probes with different fluorophores (Figure 1.10). Thus, the emission of each fluorophore corresponds to the detection of a specific target sequence. (68)

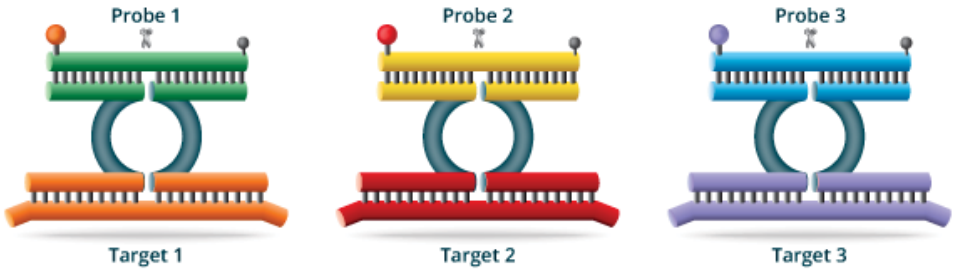

Figure 1.10 - Multiplexing with PlexPCR®

Hybridization based methods.

The DNA hybridization has become one of the main principles in the construction of DNA biosensor devices, consisting of single-stranded DNA (ssDNA) probes layer immobilized on a transducer surface. (69, 70) These immobilized probes recognize its complementary DNA target to form a DNA double helix (Figure 1.11). This hybridization event can be converted into a quantified signal by the transducer in the form of optical,

electrochemical, piezoelectric and thermal for detection. (71-74)

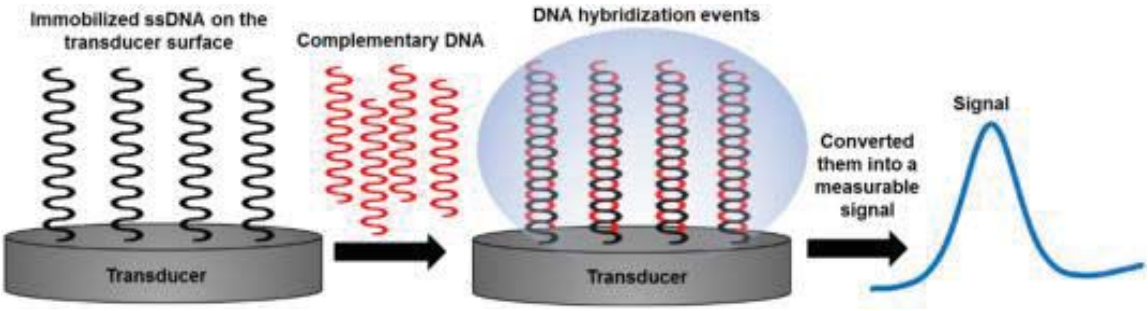

Figure 1.11 - A schematic of general design of a hybridization based method. (*Copyright under CC BY NC-ND 4.0*).

1.3.2 Nucleic acid non-amplification technologies (NANATs)

Nucleic acid non-amplification technologies (NANATs) have lower sensitivity in comparison with NAATs, not becoming them suitable to generating quantitative data. In the other hand, more linear quantitative signals are produced because the molecular manipulations of sample from the obtention of it to the final read-out are insignificant in comparison with NAATs, offering the capacity for more directly interpretable quantitative signals. (75) The majority of non-amplified methods employed are not enzymatic dependent, and there they can have less stringent requirements and less dependence on the good reagent logistics chain. Furthermore, the lower sensitivity does not always have to be valued as a negative aspect, but can also be favourable, since it eliminates the high risk of giving false positives due to the common contamination that occurs due to the existence of remaining amplicons.

There are several techniques classified in this category, almost all based on direct nucleic acid probe hybridization. These direct hybridization methods are based on the use of nucleotide probes (the synthetic analogs presented above are frequently used) to detect nucleic acids in biological samples. (76) The drawback of these direct detection methods is that a sufficient amount of target sequence is required, thus limiting its use in molecular diagnostics. Therefore, it is important to know when to use these methodologies so that an analysis can be carried out reliably. Thus, when sensitivity is not a limiting factor and the target sequence is in an acceptable concentration, it is advisable to use this type of methodologies due to the easy handling Furthermore, the protocols are much less extensive, thus obtaining fast results, and the probability of contamination is very remote compared to NAATs.

Nanosphere's Verigene system.

As shown in Figure 1.12, Nanosphere's Verigene (Northbrook, IL) system uses a gold nanoparticle probe technology, typically 13–20 nm in diameter that carries a defined

number of target-specific oligonucleotides. (77) The nanoparticles support increased sensitivity compared to fluorophores. Light scattered from one nanoparticle is reported to be equivalent to the light emitted from one half million fluorophores.

As shown in Figure 1.12, the Verigene system from Nanosphere (Northbrook, IL) uses gold nanoparticles of ±15 nm in diameter, coupled with oligonucleotides probes specific to the target sequence. (77) The light scattered by a nanoparticle is equivalent to the light emitted by half a million fluorophores, so the sensitivity compared to methods using fluorophores is much higher.

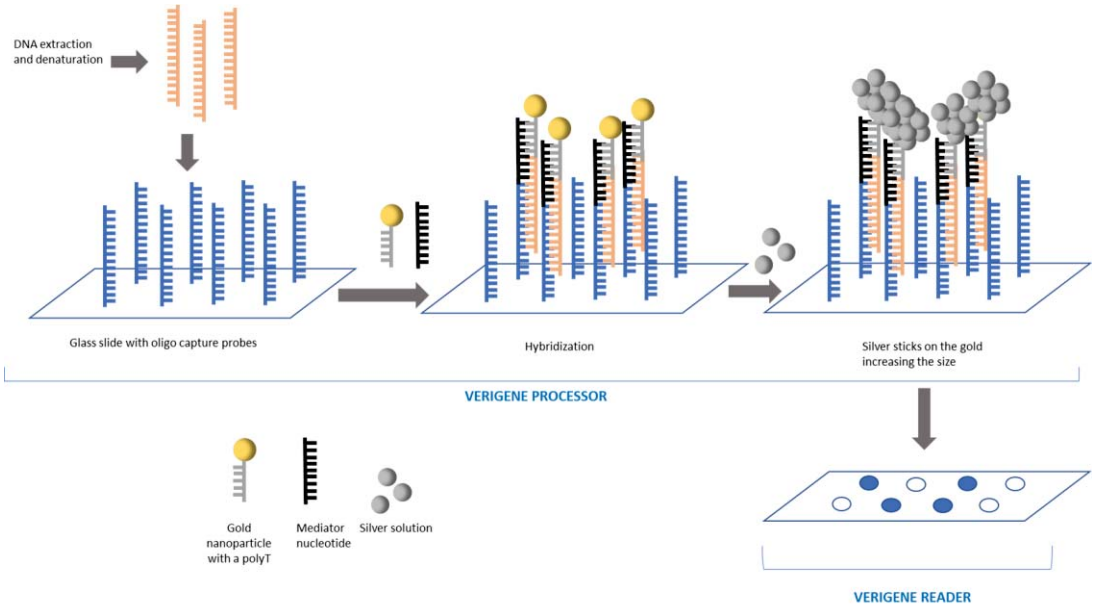

Figure 1.12 - Nanosphere's Verigene system workflow.

The sample is placed in a tray where the genetic material is extracted and inserted into a Verigene system (Figure 1.13). The extracted genetic material is then automatically transferred to a cartridge where it hybridizes with the capture probes immobilized on a glass microarray. The nucleic acid target sequence is detected using a second hybridization with a gold nanoparticle conjugated detection probe. Finally, signal amplification of probes occurs via a silver staining process with automated qualitative analysis performed on the Verigene Reader (Figure 1.13). The reading of the array is conducted in the Verigene Reader and the entire assay time is about 2.5 h.

Figure 1.13 - Nanosphere's Verigene SP system.

Nanostrings nCounter Technology

NanoString nCounter technology is based on a high-throughput, multiplex, fluorescence-based digital hybridization method designed for gene expression analysis. (78) The technology is based on fluorescent molecular barcode chemistry developed at the Institute for Systems Biology (ISB) in Seattle. (79) As shown in Figure 1.14, the combination of short, gene-specific molecular barcoded reporter probes and biotin-labelled capture probes make up a CodeSet (target-probe complex) representing the target genes for the assay. The CodeSet probes can be designed to hybridize to purified RNA or DNA. Alternatively, unpurified extracts from serum, plasma, cell culture or even single cells can be used. After an overnight hybridization, the samples are purified on a preparation station robot (nCounter Prep station) where all excess probes and unbound nucleic acids are removed. The remaining tripartite complexes composed of reporter probe, capture probe and RNA or DNA hybrids are then immobilized and electro stretched on a streptavidin coated cartridge. The molecular barcodes are then counted in a quantitative fashion using an automated digital analyzer (nCounter Digital Analyzer). The raw barcode counting represents the relative expression of each gene under interrogation within the analysed sample. The count of each target is then normalized to reference genes and system controls in order to accurately determine the expression of each one.

NanoString nCounter technology is based on a high-throughput digital hybridization method, with multiplex capability for gene expression studies. (78) This technology is based on a fluorescent barcode language developed at the Institute for Systems

Biology (ISB) in Seattle. (79) The combination of reporter probes with specific fluorescent codes together with biotin-labeled capture probes form a single code known as a CodeSet. Hybridization of the reporter and capture probes with the target sequence is carried out overnight, and the excess of probes and nucleic acids unbound are removed. The complexes formed by the reporter probe, capture probe and target sequence are immobilized on a surface and, by appliying an electric field, are stretched inside a cartridge containing streptavidin. Fluorescent codes are read on an automated digital analyzer (nCounter Digital Analyzer).

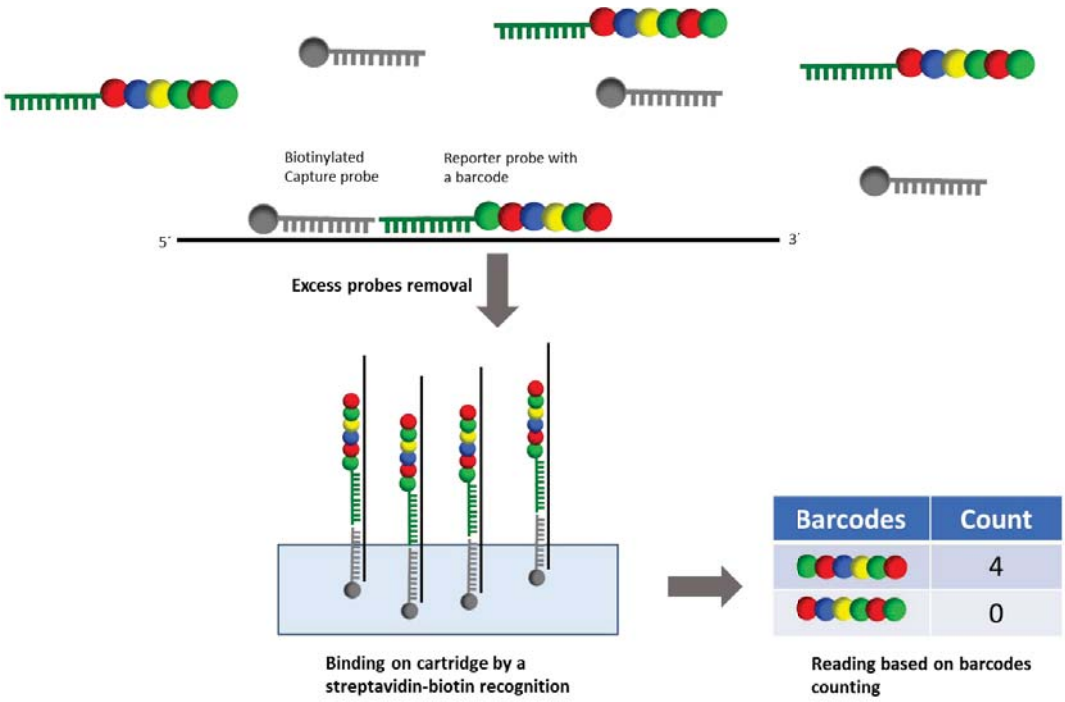

Figure 1.14 - Nanostrings nCounter technology workflow

Branched DNA (bDNA).

Branched DNA (bDNA) probes where developed around 20 years ago and they are still useful in several applications in molecular diagnostic and clinical research. bDNA probes are formed by different regions: i) a 20 to 25 nucleotides region which hybridize specifically with the target sequence; ii) a region containing different zones which can bind multiple sequences containing reporter molecules and; iii) a short linker region (Figure 1.15). Through this structure, the signal can be increased enough to perform a direct detection method with a detection limit around 100 target copies/mL. (80, 81) This assay is more cost-effective method than NAATs, since all the amplification methods requires around one day from the DNA extraction until the final read-out. (81, 82) However, the same inconvenient of NAAT to give false positive results is intrinsic to the methodology.

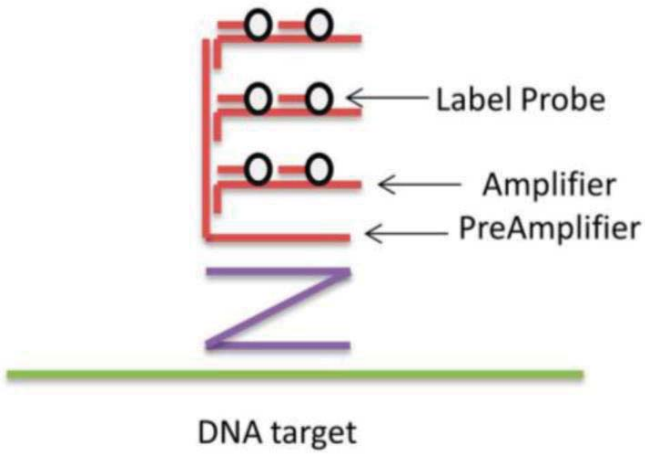

Figure 1.15 – General principle of the bDNA. (*Copyright under CC BY 4.0*).

1.3.3 Dynamic Chemical Labelling

Among the several nucleic acid testing available, a unique PCR-free method for the direct detection of nucleic acids, the so-called dynamic chemical labelling (DCL), which is based on dynamic chemistry, was presented by Bowler et al. in 2010. (83) DCL combines patented aldehyde-modified nucleobases with unique PNA capture probes which contain an abasic position (DGL probes). The DGL probe hybridizes with a complementary nucleic acid target, and the abasic position opposite the nucleobase under analysis creating a chemical pocket. Once the chemical pocket is formed, a reversible reaction between the DGL (specifically the secondary amine of the 'blank' position) and four aldehyde-modified nucleobases (Figure 1.16) takes place and an iminium intermediate is generated and can be reduced to a stable tertiary amine. Four iminium species will be thus generated, but the one with the correct hydrogen bonding motif, basing on the templating power of Watson–Crick base pairing and base stacking, will be the most thermodynamically stable product. This higher stability will lead to a

higher proportion, if not only, of the reduced product (tertiary amine) that will be ready to be analysed.

DCL reagents can be modified as required to implement onto different platforms. In this sense, DGL probes can be designed with backbone modifications to efficiently hybridise to a complementary nucleic acid target. Besides, they can be functionalised at the end terminals to be linked with most surfaces used in molecular diagnostic platforms, that's the case of the use of nucleophilic groups such as -NH_2 or -SH. If mass spectrometry is used, a triphenylphosphonium charge tag is used as N terminal cap since it was observed that it enhances MALDI-TOF detection limit. In addition, aldehyde-modified nucleobases can be labelled with fluorescent molecules, biotin, as well as other tags. Therefore, aldehyde-modified nucleobases can be tagged with four different tags for genotyping assays. Other applications might require just one tagged aldehyde-modified nucleobase to label the duplex formation, as used when testing miRNAs sequences. (84-88)

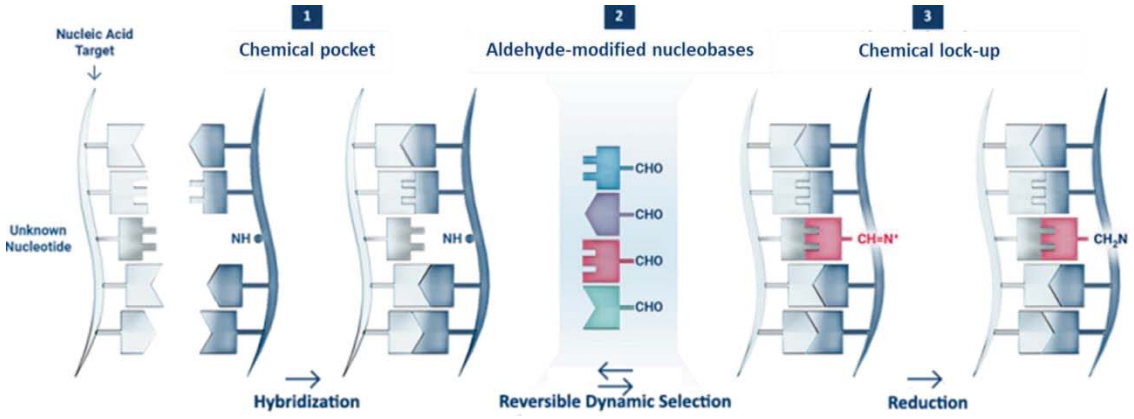

Figure 1.16 - Scheme of DCL method. 1) The DGL probe hybridises with a complementary nucleic acid target, creating a chemical pocket containing the unknown nucleotide under interrogation. 2) In the presence of four aldehyde-modified nucleobases (i.e. adenine, thymine guanine and cytosine) the chemical pocket creates reversible iminium intermediates between the aldehyde chemical group on the modified nucleobases and the secondary amino group on the abasic position. 3) The unknown nucleotide stabilises the iminium intermediate formed with the complementary nucleobase. The most stable iminium intermediate is thus reduced (chemical Lock-up) and analysed.

As described previously elsewhere, the DCL method has been merged with multiple platforms for different purposes and applications. (84, 85, 87) Below is described the multiple applications of the DCL method for the read out onto different platforms

1.3.3.1 DCL / MALDI-TOF mass spectrometry

MALDI-TOF mass spectrometry was the first platform in which the DCL method was implemented for its validation. (83) The resulting mass spectra demonstrated selective incorporation of the aldehyde-modified nucleobase complementary to the templating unknown nucleotide on the DNA strand under interrogation. In some reactions, some unreacted DGL probes were observed. The peak of the unreacted DGL may appear together with a peak of ≈+14 Da which is hypothesized to be the results of a borane adduct due to the available free amine at the blank position of the probe (Figure 1.17). (83)

In addition, by using the MALDI-TOF mass spectrometry for the read out of the DCL reaction, it was demonstrated that guanine and cytosine are incorporated in greater yield and more selectively than either adenine or thymine (attributed to the greater number of templating hydrogen-bonds) [32]. Furthermore, purine bases were incorporated with greater yield and selectivity than pyrimidines (A > T; G > C), which may be due to greater π-stacking interactions associated with the bicyclic pyrimidine rings. It was also studied that modifying the starting concentrations of the aldehyde-modified nucleobases gave different product rations. In accordance with Le Chatelier's principle for a system in dynamic equilibrium, increasing the concentrations of those bases with lower yield and selectivity under equimolar conditions lead to in improved

yields and peak ratios for the 'correct' template product (89).

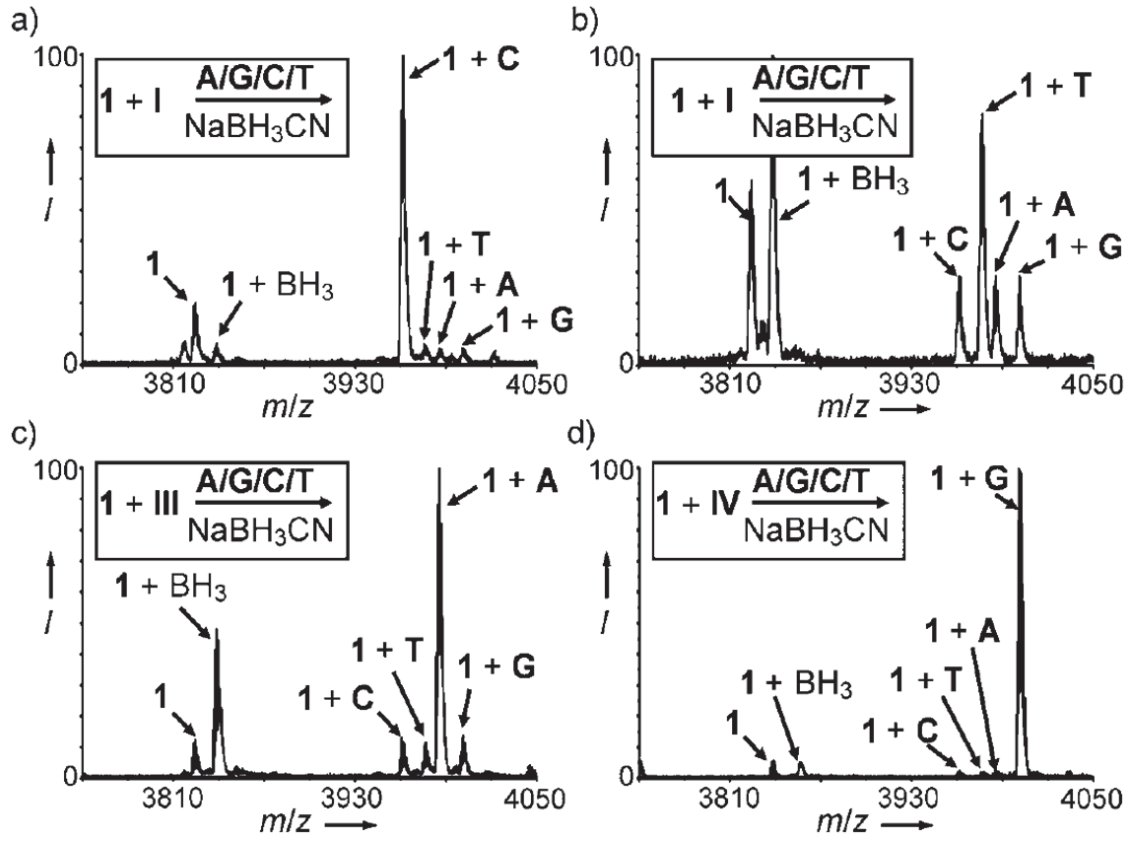

Figure 1.17 - Mass spectra recorded after DNA-templated reductive aminations using an unoptimized equimolar of the four aldehydes. a) DNA template I directs incorporation of **C**; b) DNA template II directs incorporation of **T**; c) DNA template III directs incorporation of **A** and; d) DNA template IV directs incorporation of **G**. *I = percentage intensity. (90)*.

Control reactions either in the absence of complementary DNA or in the presence of a non-complementary DNA have further demonstrated the role of DNA template in speeding up the reaction and promoting selective aldehyde-modified nucleobase incorporation. (83)

The effect of pH on the reaction efficiency was also studied. As expected for the iminium ions formation, conversions were better at mildly acidic pH, being pH 6 optimal. A mildly acidic pH strikes the balance between being high enough to provide sufficient free amine in the abasic position of the DGL probe to attack the carbonyl group of the aldehyde in the modified nucleobase, but low enough for protonation of the carbonyl oxygen prior to nucleophilic attack, and also protonation of the resulting tetrahedral intermediate for elimination of water. (83)

By using the MALDI-TOF platform, the DCL method was successfully used to genotype 12 cystic fibrosis patients. Despite the high number of mutations associated to it, around two-thirds are related to a 3 base-pair deletion, ΔF508. Patients were

genotyped for genotyped for two mutations associated to this disease: (i) the indel ΔF508, which is a 3 base-pair deletion which accounts for two-thirds of cases and (ii) the SNP, G551D, responsible for 1-2% of cases. The analysis of the SNP was straightforward (Figure 1.18 A) whereas to analyse the indel, since the 3 bases deletion avoid the analysis with a single probe, two DGL probes were used: one to clamp the mutant and the second one to the wild-type sequence (Figure 1.18 B). (90)

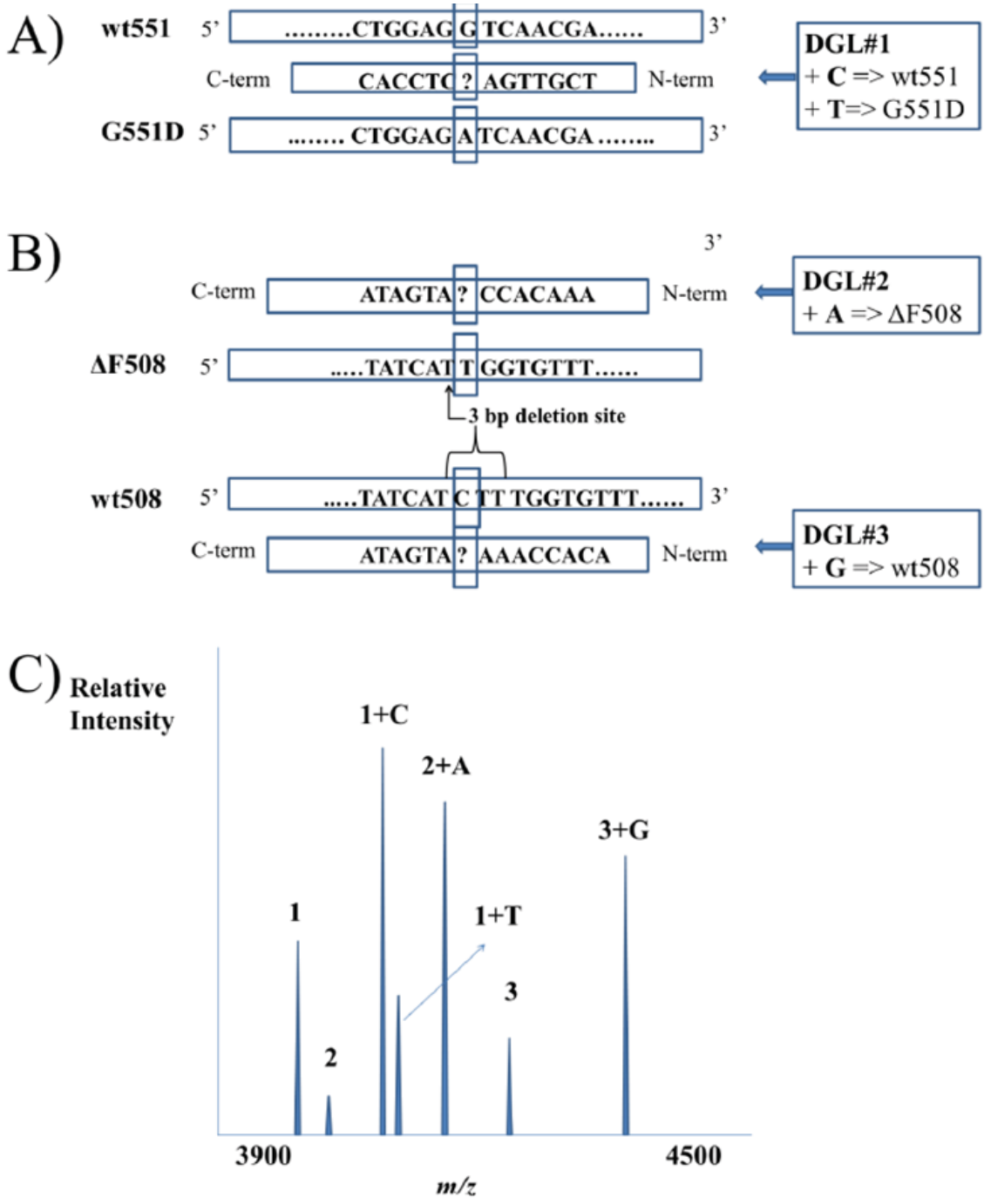

Figure 1.18 - DGL probes sequences for cystic fibrosis indel ΔF508 and SNP G551D identification. A) One probe is used for SNP G551D genotyping: DGL#1. Aldehyde-modified cytosine incorporation means wild-type and aldehyde-modified thymine calls for the SNP G551D. B) Two probes are needed to identify the indel ΔF508 and differentiate

the 3 base-pair deletion (DGL#2) from the wild-type sequence (DGL#3). If spectrum shows aldehyde-modified adenine incorporation on DGL#2, it indicates the presence of the deletion, whereas if it is seen the incorporation of aldehyde-modified guanine on DGL#3, it means that it does not have the deletion and so it is a wild-type sequence. C) MALDI-TOF spectrum for genotyping an individual heterozygous for both mutations. All possible aldehyde-modified nucleobases incorporation patterns are observed. (90)

1.3.3.2 DCL / STMicroelectronics In-check™ platform

The DCL method has also been integrated with the STMicroelectronics In-check™ platform which contains a microarray area where nucleic acids are captured and identified by single nucleobase fluorescent labelling. (71) This platform was evaluated and validated for detection of DNA sequences mimicking miR-122 and mengo virus RNA (MGV). Two DGL probes (DGL-miR122 and DGL-MGV) and a fluorescein-labelled aldehyde-modified cytosine (SMART-C-FITC) were used. DGL probes specifically hybridize with their complementary target nucleic acids, then the templating nucleotide which lies opposite the abasic site, templates the incorporation of its complementary aldehyde-modified nucleobase, in this case, SMART-C-FITC, labelling the probe. This event is later scanned with the ST's optical reader. No mis-incorporation was observed due to non-specific SMART-C-FITC incorporation on DGL-MGV (Figure 1.19). (71)

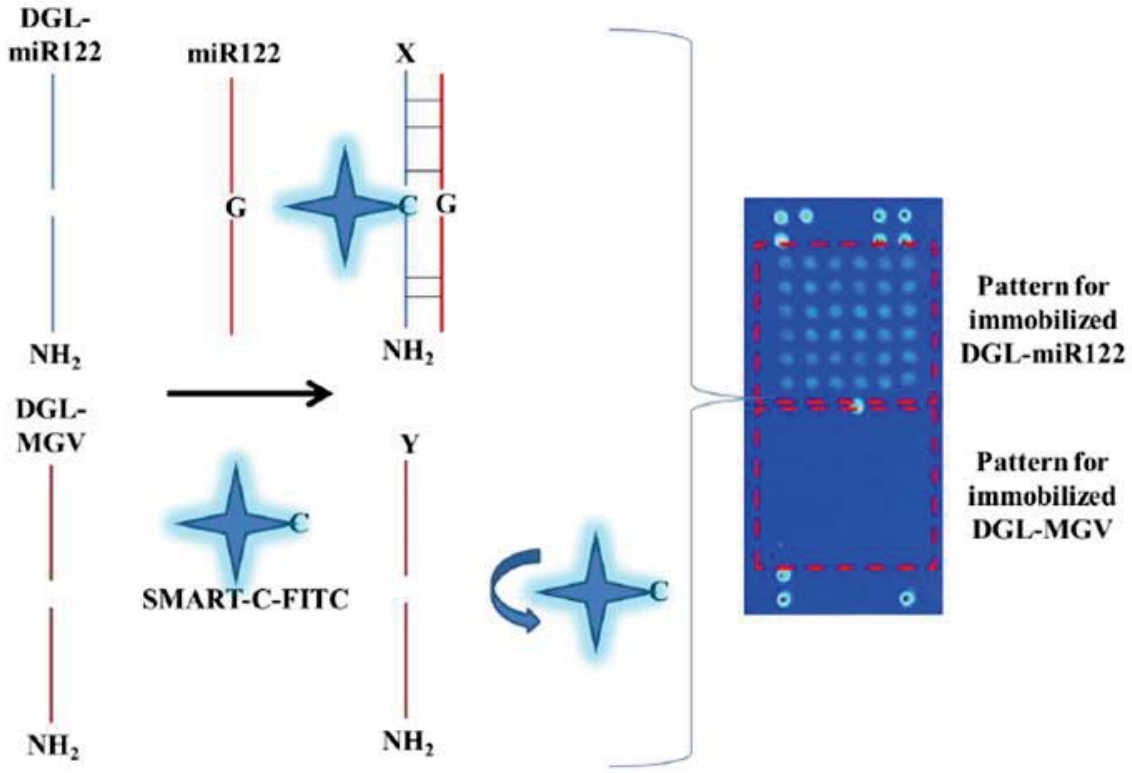

Figure 1.19 - miR-122 detection by DCL method on STMicroelectronics In-Check™ platform. Two DGL probes, DGL-miR-122 and DGL-MGV, were immobilised on the microarray surface. DNA mimicking miR-122 sequence was used as target nucleic acid, hybridizing with its complementary probe and labelling it by SMART-C-FITC incorporation. No signal was observed on the other spotted DGL probes which highlighted the specificity of DCL method (77). (*Copyright under CC BY 3.0*).

1.3.3.3 DCL / Spin-Tube

It has been developed a novel colorimetric molecular assay that integrates nucleic acid analysis by DCL with reverse dot-blot hybridization (91-93) in an array format for a rapid and easy discrimination of *Leishmania major* (*L. major)* and *Trypanosoma cruzi (T. cruzi)*. (94)

This novel platform combines the DCL method with a simple colorimetric end-point assay on a porous nylon membrane contained within a micro Spin-Tube device (Spin-Tube). The assay uses a singleplex PCR to amplify a highly conserved sequence of DNA, which encodes the RNA component of the large ribosome subunit with single nucleotide polymorphism (SNF) markers for the two different parasite species under interrogation. This amplicon is later interrogated by the DCL. As shown in Figure 1.20, the SNF sequence analysis is based on combining biotinylated aldehyde-modified cytosine with unique DGL probes to target PCR amplicon strands- The 'blank' position of the DGL probe lies opposite to two different nucleotides under interrogation on the DNA amplicons. A reversible reaction between the biotinylated aldehyde-modified cytosine and the free secondary amine on the DGL generates an iminium intermediate, which is chemically reduced to a stable tertiary amine. Within the novel Spin-Tube, the dynamic chemistry reaction mixture is added to the nylon membranes on which the abasic DGL probes have been immobilized following a specific spot pattern (Figure 1.20, Step 1). The PCR amplicons act as template molecules and drive the specific incorporation of biotinylated aldehyde-modified cytosine molecules into the specific 'blank' position of the DGL probes (Figure 1.20, Step 2). The labelling is then achieved by streptavidin alkaline phosphatase (Streptavidin-ALP) to produce colorimetric signal (blue precipitate) patterns when the chromogenic substrate (NBT/BCIP, nitro blue tetrazolium chloride/5-Bromo-4-chloro-3-indolyl phosphate) is added. Each parasite gives a unique coloured spot pattern that can be read by naked-eye (Figure 1.20, step 3).

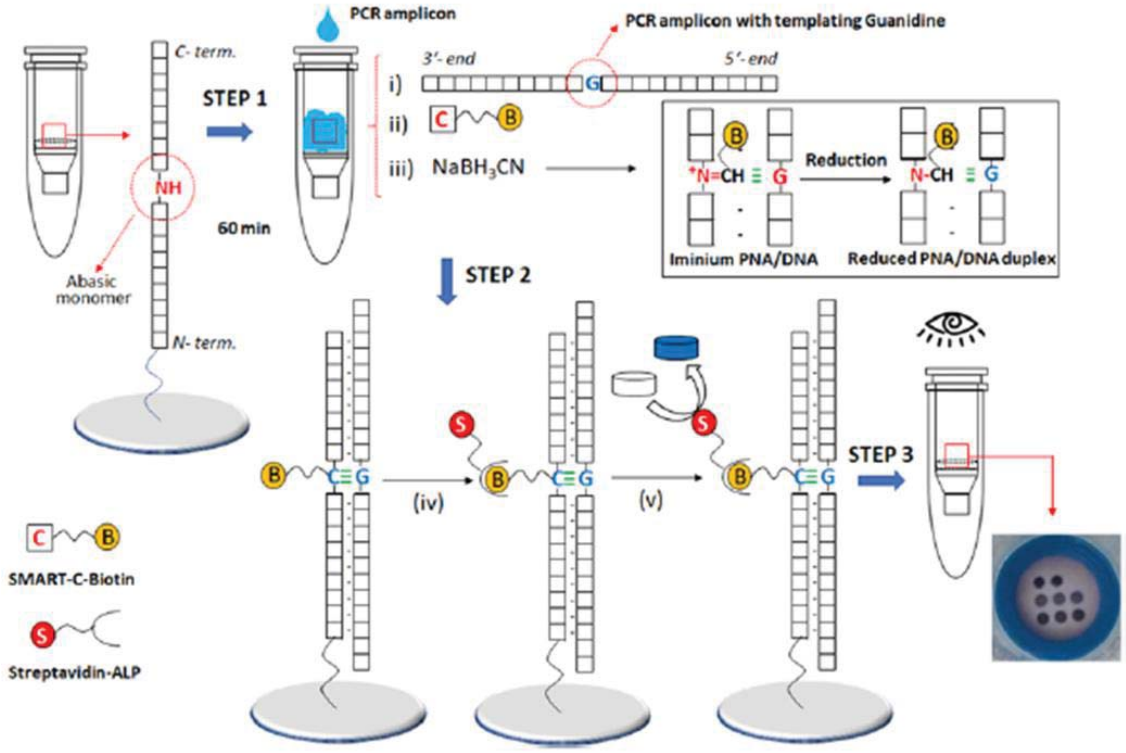

Figure 1.20 - Scheme of the Spin-Tube assay. Step 1: DGL probes are immobilized onto nylon membranes following specific spot patterns, with the biotinylated aldehyde-modified cytosine. This process requires three steps: (i) perfect hybridization between DGL probes and PCR amplicons; (ii) generation of reversible iminium specie between the secondary amine of the abasic unit and the aldehyde group of the modified cytosine driven by the templating nucleobase. In this case, biotinylated aldehyde-modified cytosine incorporation can be just templated by a guanidine as otherwise the iminium specie is not stable enough to be reduced; and (iii) reduction of the iminium specie by sodium cyanoborohydride to yield a non-reversible tertiary amine within the DGL printed onto the nylon membrane. Step 2: (iv) Biotin labelling with streptavidin alkaline phosphatase (Streptavidin-ALP); (v) Incubation with the chromogenic substrate (NBT/BCIP, nitro blue tetrazolium chloride/ 5-Bromo-4-chloro-3-indolyl phosphate) which generates a blue precipitate. Step 3: Data analyses by naked-eye reading. Time for the assay: 90 min PCR amplification; 60 min dynamic chemistry reaction; 30 min color development procedure, ±3 h total). (106) (*Copyright under CC BY 4.0*).

1.3.3.4 DCL / FLUOstar OMEGA micro-plate reader

The DCL method was used with a conventional multi-mode micro-plate reader (FLUOstar OMEGA instrument) in order to develop a cost-effective manner for quantifying miRNAs.

In 2018 Marin et al. applied the DCL method in combination with the micro-plate reader to the direct detection of miR-451a in human plasma without performing RNA extraction nor amplification. (85) In 2019, Delgado et al merged the method with the same micro-plate reader for the direct detection of miR-21 from lung cancer cell cultures. (86) Thus, interrogating different starting materials (plasma and cell cultures), the general assay was relatively similar. For both, specific DGL probe complementary to target miR-451a or miR-21 was synthesised and covalently bound to magnetic

microspheres (Figure 1.21, Step 1). The respective microspheres were added to the sample under interrogation and the miRNA target hybridised (Figure 1.21, Step 2), templating the incorporation of the aldehyde-modified nucleobase with biotin (Figure 1.21, Step 3). The microspheres were labelled with streptavidin-β-galactosidase (SβG) (Figure 1.21, Step 4). Following streptavidin–biotin recognition, a resorufin-β-D-galactopyranoside (RGP) fluorogenic substrate was added to prepare a fluorescent solution upon enzymatic hydrolysis of RGP by β-galactosidase, which gives rise to the fluorescent molecule, resorufin. Relative fluorescence units (RFU) were recorded during a 9 minute period with a FLUOstar OMEGA instrument (Figure 1.21, Step 5) equipped with 544 ± 10 nm excitation and 590 ± 10 nm emission filters and the slope of the linear region of the reaction time course was calculated.

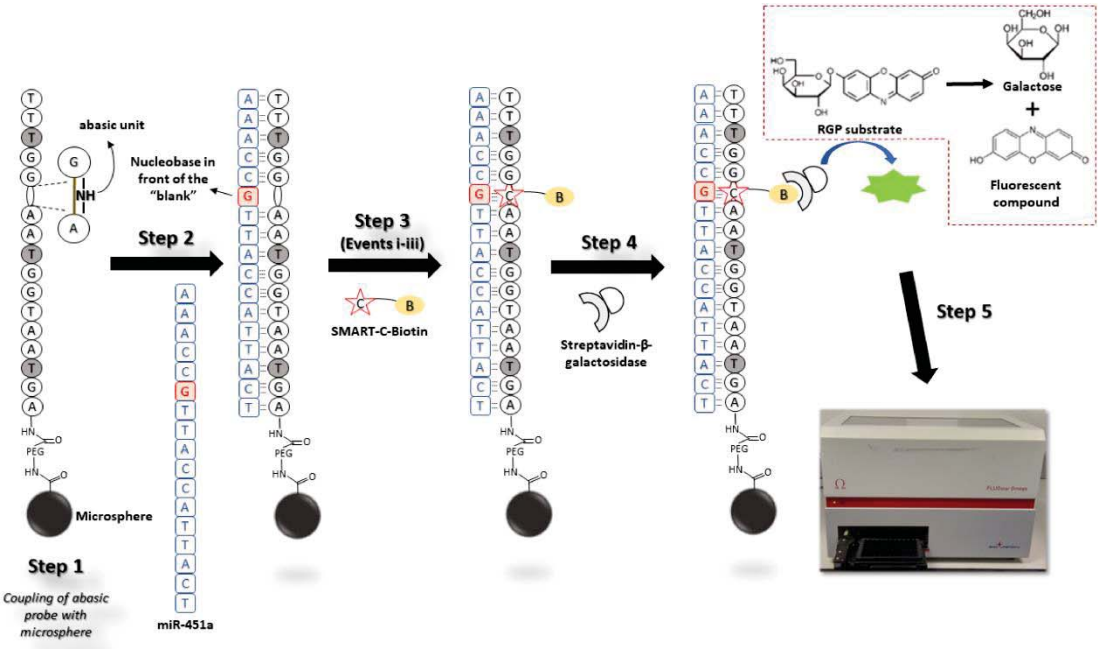

Figure 1.21 - DCL / FLUOStar OMEGA micro-plate reader to direct profile miRNA expression. Step 1: DGL probe complementary to the miRNA target (miR-451a has been represented in this figure) is coupled to magnetic microspheres. Step 2: DGL probe hybridises miRNA target. Step 3: Covalent modification of the DGL probe with biotinylated aldehyde-modified nucleobase through the templating role of miRNA target . This covalent modification requires three events to take place: (i) perfect hybridisation between the DGL probe and miRNA target; (ii) generation of a reversible iminium species between the secondary amine of the "abasic unit" and the aldehyde group of the biotinylated modified nucleobase which is driven by the templating nucleobase which lies in the front of the blank position; (iii) reduction of the iminium species by sodium cyanoborohydride to lock-up the modified nucleobase covalently into the duplex. Step 4: Microsphere labelling with streptavidin-β-galactosidase (SβG); Step 5: Addition of RGP substrate and fluorescence detection using a FLUOstar OMEGA instrument. (97) (R*eproduced from Ref. Analyst, 2018,143, 5676-5682 with permission from The Royal Society of Chemistry*).

This study is part of the present doctoral thesis and will be described in detail, in one chapter of this manuscript.

1.3.3.5 DCL / ODG device

In 2019, Detassis et al implemented the DCL method onto a novel silicon photomultiplier (SiPM)-based reader to create an innovative ODG platform, for detection and quantification of miRNAs without requiring extraction, pre-amplification, or pre-labelling of the target from their biological sources. (87) In this study, it was demonstrated how this platform can be used to profile miR-21-5p, a putative cancer marker detectable in plasma of non-small cell lung cancer (NSCLC) patients. With its compact benchtop format, the ODG platform promises to transform and expand routine testing and screening of circulating miRNAs in clinical diagnostic practice, including cancer diagnosis.

The protocol to interrogating serum samples is high similar to the one for the DCL / FLUOStar OMEGA platform, with the feature that in this case the recognition of the biotin tag is carried out with streptavidin-HRP (horseradish peroxidase) and as substrate was used luminol:peroxidase 1:1. Briefly, a DGL probe complementary to miR-21-5p was covalently bound to magnetic microspheres (Figure 1.22, Step 1). The complementary miR-21 is captured by the DGL probe, templating the incorporation into the duplex of a biotinylated aldehyde-modified adenine (SMART-A-Biotin) (Figure 1.22, Step 2). Following this recognition, washing steps are performed to eliminate off-targets (Figure 1.22, Step 3). Magnetic microspheres allow an effective phase-separation and an efficient washing process by using magnetic separation racks. The labelling is achieved via streptavidin-HRP, which specifically recognizes the biotin in the duplex (Figure 1.22, Step 4). A luminol-peroxidase substrate is added to generate a chemiluminescent signal. The oxidation of luminol by the peroxide is catalyzed by the HRP producing light. The read-out is performed by the SiPM-based reader (Figure 1.22, Step 5).

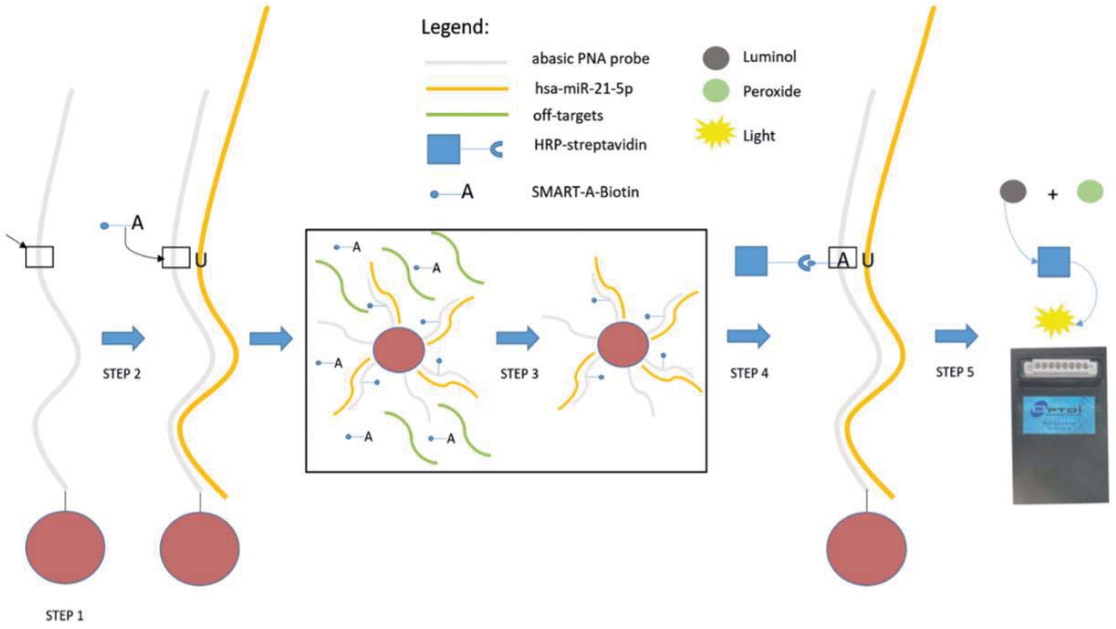

Figure 1.22 - ODG platform workflow. DGL probes are bound to magnetic microspheres (Step 1, the arrow shows the abasic position). The target hybridizes to the probe, and the biotinylated aldehyde-modified nucleobase enters the pocket (Step 2); off-targets are washed away (Step 3); Streptavidin-HRP binds the biotin of the aldehyde-modified nucleobase (Step 4). Chemiluminescent substrate is added, and the signal generated by the oxidation of the luminol with peroxide via HRP catalysis is analyzed via the SiPM-based reader (Step 5). (99)

1.3.3.6 DCL / Quanterix Simoa platform

It has been demonstrated that Simoa™ is very sensitive to an enzyme label, reaching a limit of detection (LoD) of 220 zM for proteins and DNA profiling. The Simoa™ DNA assay was, however, limited to relatively long target sequences (>100 base pairs) because of the requirement for a capture and multiple detection probes, each being 15–20 bases long.

The DCL method was successfully combined with the Simoa (single molecule array) platform by Rissin et al. in 2017. (84) enabling an assay with single label sensitivity and single base specificity using a single, short (<20 base) probe for detecting short RNA target molecules. The method was applied to detect miR-122, a biomarker of liver toxicity, in serum samples.

The protocol carried out to interrogate serum samples is almost equally than the one for the DCL / FLUOStar OMEGA platform (Figure 1.21). Some parameters regarding to concentrations and temperatures are different, all of them detailed elsewhere (88).

The array is fluorescently imaged to locate the beads and its enzyme activity. The analysis software determines the average number of enzymes per bead (AEB) and by interpolation in a linear curve made with AEB values of calibrators of known

concentrations, the concentration of the target nucleic acid can be determined. The LoD of the DCL / Quanterix Simoa platform is 500 fM.

1.3.3.7 DCL / Luminex® MAGPIX® system

In 2020, Marin et al. combined the DCL method with the Luminex MAGPIX system to generate a unique assay for the direct measurement of miR-122 in DILI patient's serums. (95) The Luminex MAGPIX was chosen as it is a validated system for clinical use, easy to use and the microsphere-based platform most installed in Hospitals and Research Centres.

The protocol to interrogating serum samples is high similar to the one for the previous presented platforms, with the feature that in this case the recognition of the biotin tag is carried out with streptavidin-R-phycoerythrin (SA-PE) and values of median fluorescence intensity (MFI) were recorded by the Luminex MAGPIX system with a with λexcitation 488 nm and λemission 585 nm. (Figure 1.23)

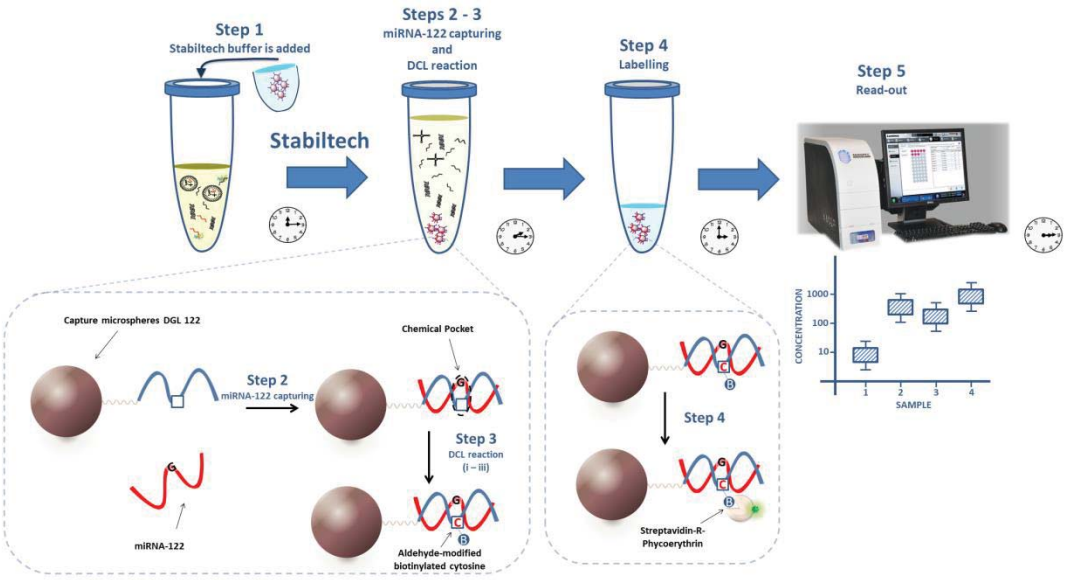

Figure 1.23 - Merging of DCL method with Luminex MAGPIX system. Fluorescence microspheres are read out by measuring the values of Median Fluorescence Intensity (MFI) – Phycoerythrin with λexcitation 488 nm and λemission 585 nm. (107)

This study is part of the present doctoral thesis and will be described in detail, dedicating one chapter of this manuscript.

1.3.4 The liquid biopsy revolution

In recent years, personalized medicine has undergone great advances, with several targeted therapies that have been approved by the FDA. (96) Especially for cancers, the National Comprehensive Cancer Network (NCCN) places great emphasis on detecting genomic markers for specific cancers that allow a personalized targeted therapy. This is why many patients have the possibility of receiving specific targeted therapies after genetic analysis from tissue biopsy samples. However, in some patients, tissue biopsy samples cannot be removed, missing the opportunity to take advantage from the new lifesaving therapies. There are a lot of circumstances for which may be the case, such as:

a) The anatomical location of the tissue to take the required samples is inaccessible. A representative example could be the mid-lung. (97)

b) The lack of quality or the insufficient quantity to test the tissue material acquired through biopsy. (98)

c) The time to get results is too long to obtain treatment decisions in an effective time. (98)

In addition, some types of cancers have other drawbacks associated with taking tissue samples:

i. Especially in the case of aggressive cancer stages or those that have received previous treatment, it is very likely that the state at the time of diagnosis does not correspond to the actual current state of the disease. (99)

ii. Due to the fact that many methods act very precisely to obtain the sample, such as needle aspiration, it is very likely that the sample obtained will not detect gene mutations in the entire tumor, a condition that is also affected by the heterogeneity of the tumor itself. (100)

Therefore, and trying to solve it, great effort is being focused in the research and development of obtaining samples from liquid biopsy to alleviate all the aforementioned inconveniences.

Liquid biopsy focuses on the study of circulating tumor cells (CTC) and / or cell-free nucleic acids (cfNA) in peripheral blood, saliva, urine, tears, etc. (Figure 1.24). It is one of the most promising non-invasive diagnostic methodologies that is in continuous advance, and that allows clinical decisions to be taken in an early stage

of the disease, which allows applying personalized treatments in effective time. (101-104)

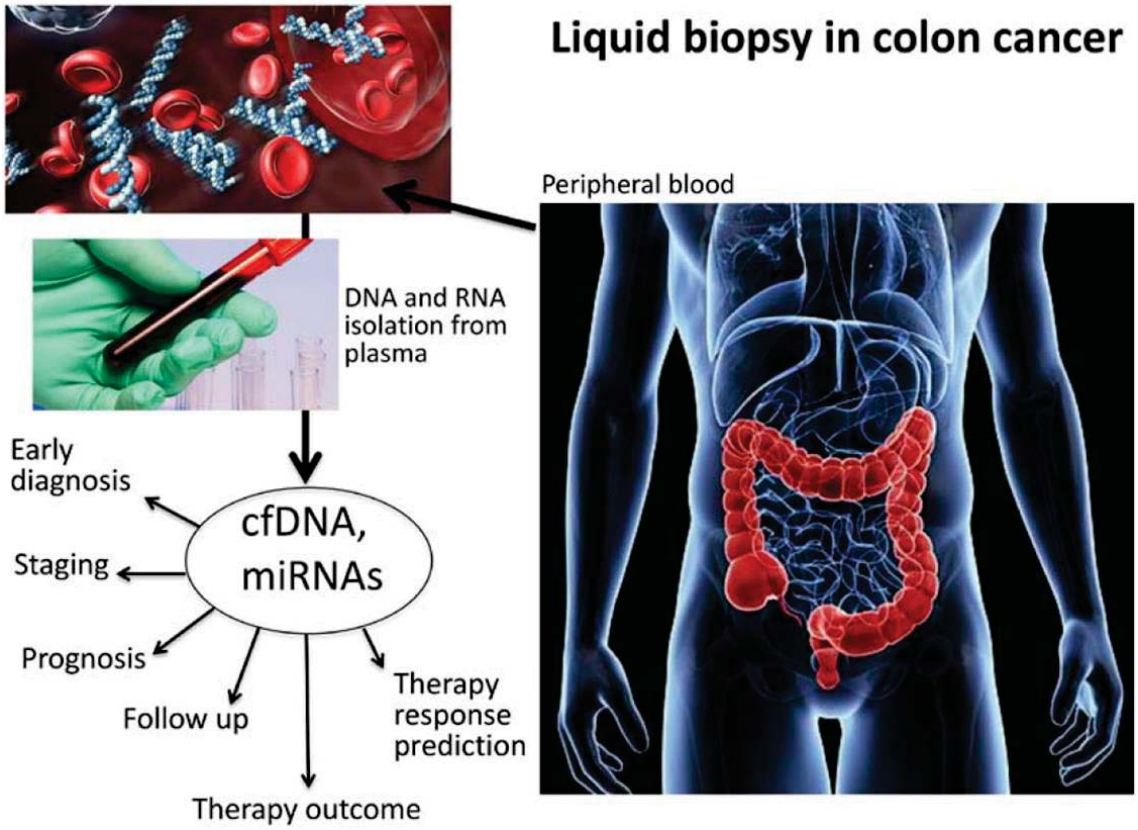

Figure 1.24 – Application of liquid biopsy in colorectal cancer. (115) (*Copyright under CC BY-NC-ND 4.0*).

1.3.4.1 Circulating tumor cells

Commonly, the study of CTCs has been a key element in characterizing the status of cancer patients using liquid biopsy. (103) There are numerous clinical reports that have focused on the use of CTC for the diagnosis and prognosis of the disease. (105)

1.3.4.2 Cell-free DNA and RNA

Numerous studies have been focused on the presence of circulating-free nucleic acids (cfNA) in biological fluids for personalized medicine studies. (106, 107) As with the CTC study, this strategy allows a non-invasive diagnosis, offering solutions to the issues mentioned above, being able to obtain a sample that as a whole assesses tumor heterogeneity. (108) However, this methodology also suffers from some drawbacks, among which are mainly the low concentrations of analyte or the low stability of cfNA. (109)

Chapter 2:

A PCR-free technology to detect and quantify microRNAs

directly from
human plasma

Chapter 2: A PCR-free technology to detect and quantify microRNAs directly from human plasma

2.1 Introduction

A novel sensitive, specific and rapid method for the detection and quantification of microRNAs without requiring extraction from their biological sources is now available using a novel chemical based PCR-free technology for nucleic acid testing. In this chapter, we both demonstrate how this method can be used to profile miRNA-451a, an important miRNA in erythropoiesis, and compare with the gold standard RT-qPCR.

2.1.1 MicroRNAs

MicroRNAs (miRNAs, miRs) are small noncoding RNA molecules (approximately 22 nucleotides in length) that inhibit gene expression at post-transcriptional level by inhibiting or degrading a complementary mRNA. (110) Numerous studies have demonstrated the important role of miRNAs in cellular processes such as differentiation, growth and apoptosis, and even in metabolism. (111)

The biogenesis of miRNAs has been widely reported elsewhere. (110, 112) miRNA genes are transcribed in the nucleus by RNA polymerase II leading to a long transcript known as primary miRNA (pri-miRNA). This molecule is then further processed by Drosha RNase III and DGCR8, the RNA-binding protein, resulting into stem-loop structured precursor miRNA (pre-miRNA) of approximately 70 nucleotides in length. This precursor is exported to the cytoplasm by Exportin 5. Once in the cytoplasm, the pre-miRNA is processed by the enzyme Dicer, another RNase III, which cleaves the molecule into a miRNA duplex, miRNA/ miRNA*. A helicase separate both strands and the mature one, miRNA, is recognized by an argonaute (AGO) protein to be associated with the RNA-induced silencing complex (RISC). At this point, the mature form of miRNA regulates gene expression by acting in a complementary mRNA (Figure 2.1). MiRNAs base-pair to a target mRNA, commonly the 3'- untranslated region (UTR), resulting in translational inhibition or degradation of the mRNA. (113)

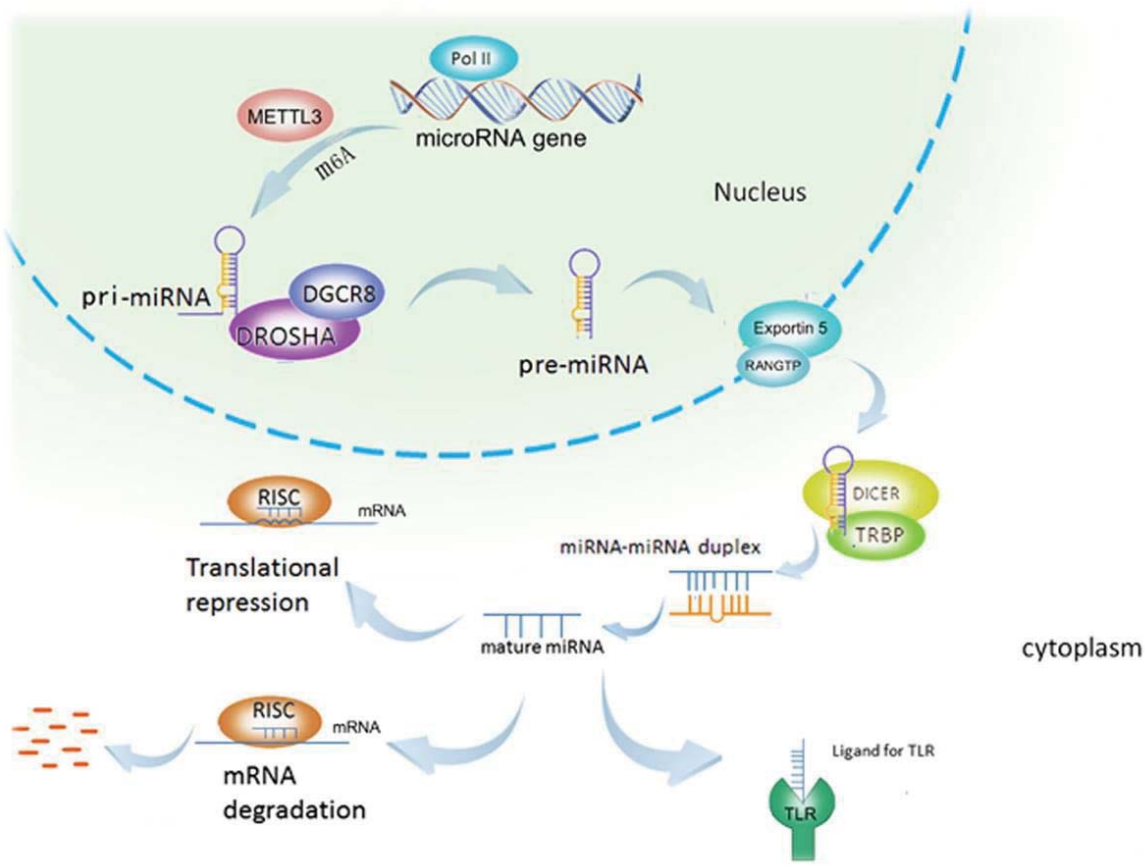

Figure 2.1 – miRNAs biogenesis. (114) (*Copyright under CC BY 4.0*).

2.1.2 Circulating miRNAs

The presence of miRNAs in biological fluids was demonstrated by Chim et al., (115) who found placental miRNAs in maternal blood plasma at readily detectable concentrations. Since then, there have been reported several studies which consistently reveal the circulating miRNAs in all variety of body fluids such as tears, breast milk, saliva, bronchial lavage, amniotic fluid, seminal plasma, pleural fluid, cerebrospinal fluid and colostrum. (116-119) miRNAs are distributed differently between the different body fluids, and the concentration of a specific miRNA is different from one body fluid to another. (118) Furthermore, miRNAs can act as biomarker since concentrations vary in various pathological conditions, offering the possibility to assess and monitorize a pathological status. (116-119)

It has been demonstrated that extracellular miRNAs do not exist only free in circulation, (120) but that they can be encapsulated in exosomes or vesicles. (121) This would give a precise explanation to the fact of the high stability of miRNAs in such a hostile environment, since these microvesicles are impervious to RNases.

In the same year, two totally independent articles were published demonstrating that the majority of circulating miRNAs are found free in biological fluids, without membrane encapsulation, but associated with proteins of the AGO family. (122, 123) As shown in Figure 2.1, the mature form of miRNAs is ultimately associated with one of the four AGO proteins, so it is not surprising that they remain bound to these proteins in circulation. This would also explain why miRNAs, despite not being encapsulated by microvesicles, continue to maintain remarkable stability in environments rich in nucleases and proteases. (122, 123) Additionally, some miRNAs associate with high-density lipoproteins (HDL), and even package into apoptotic bodies (Figure 2.2).

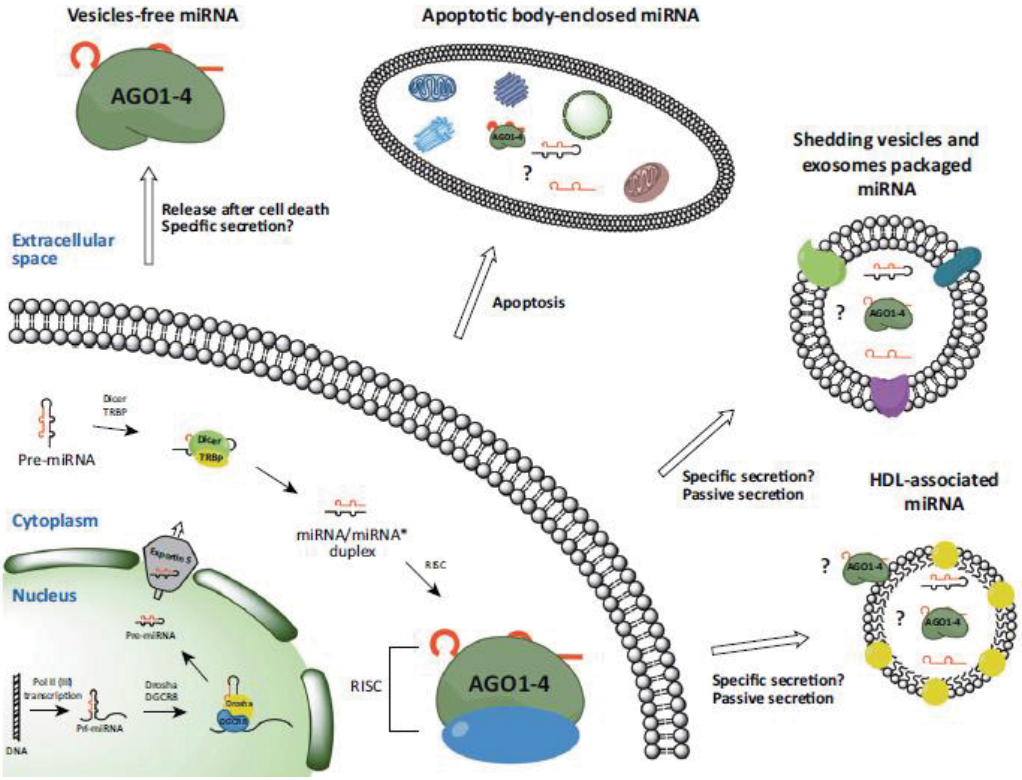

Figure 2.2 – miRNA biogenesis and extracellular miRNA modes. (124) (*Copyright under CC BY 3.0*).

2.1.3 MicroRNA detection methods

Several technologies for miRNA profiling have been developed to date, most of them typically based on DNA genotyping methods, relying on polymerase chain reaction (PCR) for the exponential amplification of target nucleic acid molecules. Hence, most of the efforts to perform miRNA analysis have been based on implementing PCR based methodologies. Despite advances, these tools are not particularly suitable to investigate small RNA species, such as miRNAs. The detection of miRNAs from clinical samples is challenging and error prone for assays that require laborious sample preparation, such as the elongation of the target molecules (ligation step with an extension sequence), conversion of target molecules into cDNA, and steps for the

amplification. (125, 126) In addition, PCR based methodologies also suffer from bias and sample contamination risk from the production of high concentrations of amplicons. (127, 128) As a result, miRNA profiling has serious analytical challenges when highly precise and accurate quantification is required for diagnostic purposes.

Current tools struggle to offer the innovation required to translate the use of miRNAs from the research sphere into reliable and practical clinical diagnostic assays. (128) These unmet innovations have been and remain the major obstacle to developing miRNAs as diagnostic and prognostic biomarkers for cancer, acute organ disease and toxicity testing. As Lowe and Lujambio stated recently, “further advances in the technology of miRNA profiling could help to revolutionize molecular pathology”. (129) There has been a clear unmet need up to now to develop new, innovative methods that enable reliable, direct profiling and absolute quantification of miRNAs.

2.1.4 Why miRNA-451a?

The family of miRNA-451 comprises two major members in human genome consisting of miRNA-451a and miRNA-451b, and are placed on chromosome 17. Their mature sequences contain 22 nucleotides in length. Previous evidence indicated that miR-451 is expressed in normal human peripheral blood cells approximately 10^4-fold higher than in granulocytes. Particularly, in the latter phase of erythroid maturation, the expression level of miRNA-451 is enhanced approximately 270 times. Thus, this miRNA is a key molecule for normal erythroid differentiation. (130)

The miRNA-451 family, which genetic information is located on chromosome 17, is made up of two main miRNAs: miRNA-451a and miRNA-451b. Both are 22 nucleotides in length. It has been demonstrated that play an essential role in erythrocyte maturation, being its level of expression in erythrocytes about 100 times higher than in granulocytes. In addition, during the last phase of maturation of the erythrocyte, its level increases ≈270 times. (130)

There is increasing evidence showing how miR-451 is deregulated in various cancer pathologies, playing an important role in the development of tumors through its role as a tumor suppressor. In addition, its levels are altered in response to stress to modulate cell proliferation and migration. (131)

As miRNA-451 is high expressed in erythrocytes, our team designed and developed a new protocol which allows having easy access to samples from healthy volunteers (HVs) with huge quantity of such miRNA in circulation. This protocol brought us the possibility to optimise the DCL protocol using real endogenous miRNA, avoiding

developing the protocol using synthetic spike-ins experiments which are not representative of a real clinical condition.

2.1.5 The DCL ELISA platform

The DCL method (see section 1.3.3) was applied to the direct detection of miRNA-451a in human plasma without performing RNA extraction (section 1.3.3.4). (85) MiRNA-451a is an erythroid cell-specific miRNA, (132, 133) and associated with human erythroid and maturation. (132-135) In addition, several studies have provided evidence about the potential use of miR-451a as a biomarker for cancer diagnosis, prognosis, and treatment. (136-138)

To show the feasibility of this approach, DCL was used with a conventional multi-mode micro-plate reader (FLUOstar OMEGA instrument) in order to develop a novel cost-effective manner for quantifying miRNAs, which we have called “DCL ELISA” (DCL enzyme-linked immunosorbent assay). The method is mentioned as “Chem-NAT ELISA platform” in the reference). (85) An abasic PNA probe (Table 2.1, ID: 1) complementary to target miRNA-451a (Table S1 – ID: 2) was synthesised and covalently bound to microspheres (Figure 2.3, Step 1) as described in sections 2.2.2 and 2.2.3. After abasic probes conjugation to magnetic microspheres, the miRNA-451a was hybridised (Figure 2.3, Step 2), templating the incorporation of aldehyde-modified cytosine with biotin (SMART-C-Biotin) (Figure 2.3, Step 3), whose structure is included in Figure 2.4. The microspheres were labelled with streptavidin-β-galactosidase (SβG) (Figure 2.3, Step 4). Following streptavidin–biotin recognition, a resorufin β-D-galactopyranoside (RGP) fluorogenic substrate was added to prepare a fluorescent solution upon enzymatic hydrolysis of RGP by β-galactosidase, which gives rise to the fluorescent molecule, resorufin. Relative fluorescence units (RFU) were recorded during a 9 minute period with a FLUOstar OMEGA instrument (Figure 2.3, Step 5) equipped with 544 ± 10 nm excitation and 590 ± 10 nm emission filters and the slope of the linear region of the reaction time course was calculated. The detailed protocol is included in section 2.2.6.

Table 2.1 – Sequences

Sequence ID	Name	Peptide with abasic position (N’-C’)
1	Abasic probe	xx-AGTgluAATGGTgluAA*GL*GGTgluTT
		miRNA sequence (5’-3’)
2	Target miR-451a	*AAACC**G**UUACCAUUACUGAGUU*
3	MiRNA-122	*UGGAGUGUGACAAUGGUGUUUG*
4	MiRNA-451a_T	*AAACC**T**UUACCAUUACUGAGUU*

ID 1: Abasic probe; ID 2: Synthetic mimic miR-451a; xx = amino-PEG-linker; Tglu = thymidine containing a propanoic acid side chain at the gamma position; *GL* = abasic "blank" monomer containing a propanoic acid side chain at the gamma position. The letters in **bold** represent the nucleobases under interrogation.

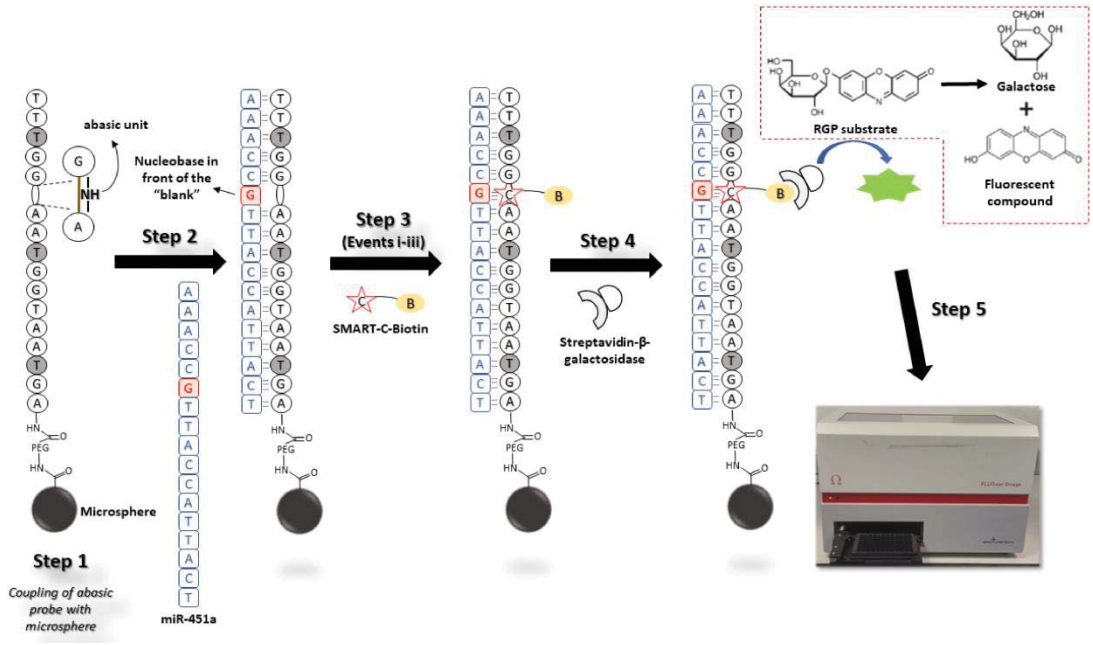

Figure 2.3 – DCL ELISA to profile miRNA-451a expression in blood samples. Step 1: Abasic PNA probe complementary to miRNA-451a is coupled to magnetic microspheres. Step 2: Abasic PNA probe hybridises miRNA-451a. Step 3: Covalent modification of the abasic PNA probe with SMART-C-Biotin through the templating role of miRNA-451a. This covalent modification requires three events to take place: (i) perfect hybridisation between the abasic probe and miR-451a; (ii) generation of a reversible iminium species between the secondary amine of the "abasic unit" and the aldehyde group of the SMART-C-Biotin which is driven by the templating "G" nucleobase at the 6th position from the 5'-end of miR-451a; (iii) reduction of the iminium species by sodium cyanoborohydride to lock-up the SMART-C-Biotin covalently into the duplex. Step 4: Microsphere labelling with streptavidin- β-galactosidase (SβG); Step 5: Addition of RGP substrate and fluorescence detection using a FLUOstar OMEGA instrument.

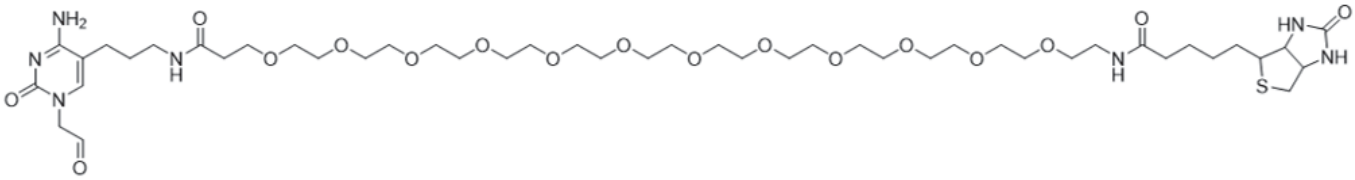

Figure 2.4 – Chemical structure of SMART-C-Biotin.

2.2 Material and Methods

2.2.1 Materials

Microspheres were purchased from ThermoFisher Scientific (Dynabeads® M-270 Carboxylic Acid). 1-ethyl-3-(3-dimethylaminopropyl) carbodiimide (EDC) was purchased from Sigma-Aldrich. Synthetic mimic miR-451a was purchased from Integrated DNA Technologies. TaqMan® MicroRNA Reverse Transcription Kit was

purchased from Life Technologies. Stem-loop RT primer specific for miR451 (Pub. No. 127AP11-01) was purchased from Applied Biosystems. FastStart TaqMan probe master mix was purchased from Roche. Hoechst 33342 (10 mg/mL in Water) was purchased from ThermoFisher Scientific. miRNeasy Serum/Plasma kit and reagents for RNA isolation were purchased from Qiagen.

Red Blood Cell (RBC) lysis buffer contains 150 mM ammonium chloride, 10 mM sodium bicarbonate and 10 mM disodium-EDTA in milli-Q water. Lysis buffer was prepared by mixing 21.4 g/L lithium chloride, 2.94 g/L ethylenediaminetetraacetic acid, 10.15 g/L lithium dodecyl sulphate, 0.79 g/L dithiothreitol and 0.4 g/L Proteinase K, in Tris-HCl 0.1M pH 7.5. Microsphere solution contains 10% PEG10K and 0.1% Tween in PBS 1X.

The thermoshaker (Biometra TS1 ThermoShaker), magnet rack (MagnaRackTM) and 96-black well plates (Nunc™ MicroWell™) were purchased from ThermoFisher Scientific. 7900 Fast Real-Time PCR System was purchased from Applied Biosystems. Microscopy chamber (Ref. No. 80826) was purchased from Ibidi.

Confocal microscopy model LSM 710 *Confocal Laser Scanning Microscopy*, from Zeiss.

2.2.2 Design, synthesis and characterization of DGL 451

Probe design was done using the public database miRbase.org, where hsa-miR451 has the miRbase Accession Number MIMAT0001631 and considering the antiparallel hybridization necessary to clamp mature miRNA 451a. Two amine-miniPEG spacers are included in the N-terminal, and some negatives charges are distributed across the backbone using DESTINA proprietary monomers as these are needed when immobilised on solid supports. The abasic site has a chiral and negatively charged glutamic monomer at gamma (γ) position and the probe also has a C-terminal primary amide.

DGL probes synthesis was based on standard solid-phase peptide chemistry and was done in an INTAVIS AG robotic synthesiser. The sequence was purified using an Agilent 1260 Infinity Agilent HPLC and a Jupiter Proteo C12 semipreparative column in reverse phase mode. The molecular weight of the probe was confirmed by MALDI-TOF using a UltrafleXtreme mass spectrometer (Bruker). Synthesis and characterization was done by the Chemistry department of DESTINA.

2.2.3 Microspheres coupling with abasic probe

A volume of 100 µL of super paramagnetic beads (containing 2 × 10^8 beads) were washed by adding 100 µL 0.01 M NaOH and mixing. The beads were pelleted, supernatant removed, and the beads were washed once in 100 µL 0.01 M NaOH and three times in 100 µL distilled water. The beads were then resuspended in 150 µL of freshly-prepared 50 mg/mL 1-ethyl-3-(3-dimethylamino-propyl) carbodiimide (EDC) in cold MES buffer 50 mM with 0.1% Tween 20 (pH 5) and incubated with slow tilt rotation at 23℃ for 30 min. After activation with EDC, the beads were washed twice with 100 µL cold MES buffer 50 mM with 0.1% Tween 20 (pH 5). Then, 100 µL of a solution containing 2100 pmol abasic probe (Table 2.1, ID: 1 in $NaHCO_3$ buffer 125 mM with 0.1% Tween 20 (pH 9.84) was added to the activated beads. The mixture of probe and beads was incubated at 23℃ for 3 h with slow tilt rotation, and then washed with MES buffer 50 mM with 0.1% Tween 20 (pH 5). The remaining activated carboxyl groups were quenched by incubating the beads with 100 µL of 50 mM ethanolamine in PBS with 0.1% Tween (pH 8) for 1 h, followed by three washes with 100 µL of 10% PEG10K and 0.1% Tween-20 in PBS. The capture beads were stored at 4℃ in 100 µL of 10% PEG10K and 0.1% Tween-20 in PBS.

2.2.4 Use of Red Blood Cell (RBC) lysis buffer to obtain haemolysed plasma

Informed consents were obtained from the human participants of this study.

The samples were haemolysed in order to liberate intra-erythropoietic miRNA-451a (haemolysed samples). Briefly, 1 mL of whole blood was incubated for 10 min with 19 mL of red blood cell (RBC) lysis buffer (dilution 1 : 20) to breakup red blood cells (Figure 2.5). The solution was then centrifuged at 1500 *g* for 10 min at room temperature in order to obtain the haemolysed plasma with free miRNA-451a. Haemolysis was validated by microscopy as shown in section 2.2.5.

Control samples (without free miRNA-451a) were prepared using whole blood without haemolysis. In this case, 3 mL of whole blood was centrifuged at 1500g for 10 min at room temperature. The supernatant plasma was collected and diluted 20 times with RBC lysis buffer to obtain the non-haemolysed plasma (Figure 2.5).

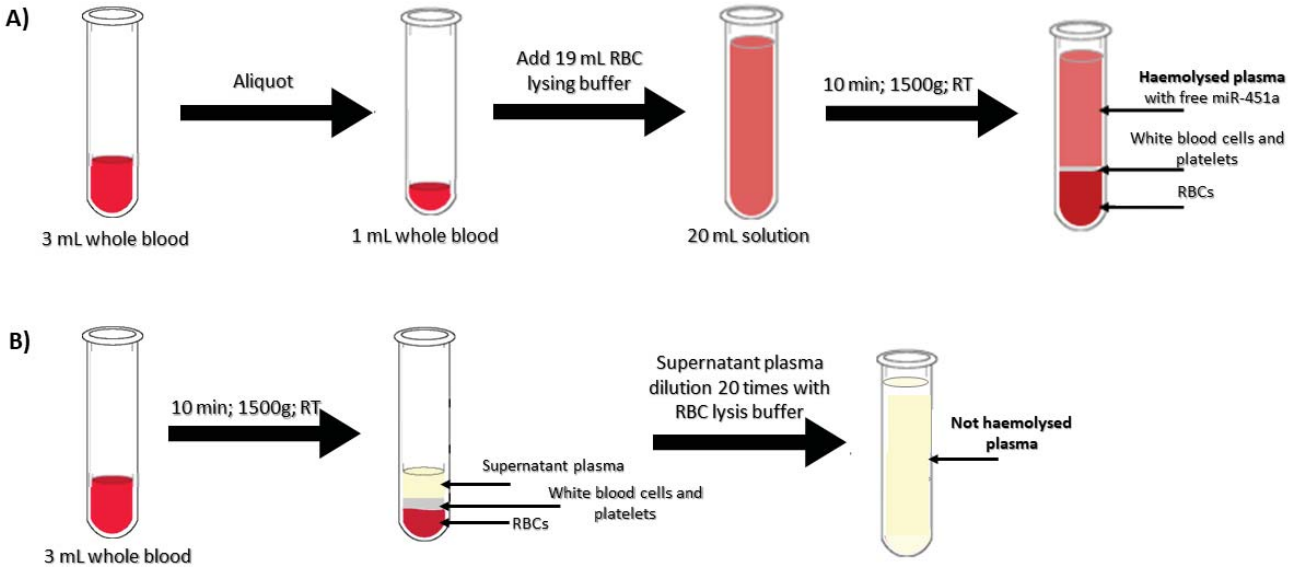

Figure 2. 5 – Procedure for preparing haemolysed and not haemolysed plasmas. To obtain haemolysed plasma, 1 mL of whole blood is incubated 10 min with 19 mL of RBC lysis buffer, in a proportion sample: buffer of 1:20. The 20 mL solution is centrifuged for 10 min at RT to separate figurative elements of blood (pellet) from the supernatant plasma containing free miRNA-451a. The supernatant is aliquot into 0.2 mL Eppendorf 0.2 mL and storage at -80 ºC; B) To obtain not haemolysed plasma, 3 mL of whole blood is centrifuged at 1,500g for 10 min at RT to separate the supernatant plasma from the figurative elements of blood (pellet). The supernatant is collected and diluted 20 times with RBC lysis buffer. The diluted supernatant (not haemolysed plasma) is aliquoted into 0.2 mL Eppendorf and storage at -80 C.

2.2.5 Haemolysis validation by confocal microscopy

In order to validate haemolysis was taking place, it was check out using confocal microscopy. Samples were prepared in different manner depending if was going to be haemolysed or not:

A) Haemolysed blood - 80 µL of Hoechst diluted in PBS 1X (1:1000) were added to 20 µL of whole blood in a 0.5 mL eppendorf. The eppendorf was incubated for 15 min at RT. 1.9 mL of RBC lysing buffer (1X) were added to the eppendorf and incubated for 10 min at RT.

B) Not haemolysed blood (control) - As control, 80 µL of Hoechst diluted in PBS 1X (1:1000) were added to 20 µL of whole blood in a 0.5 mL eppendorf. The eppendorf was incubated for 15 min at RT. 1. 9 mL of PBS (1X) were added to the eppendorf and incubated for 10 min at RT.

20 µL of both preparations were diluted 5 times with PBS 1X and loaded into a microscopy chamber for confocal microscopy analysis using a 40X objective (see Figure 2.6).

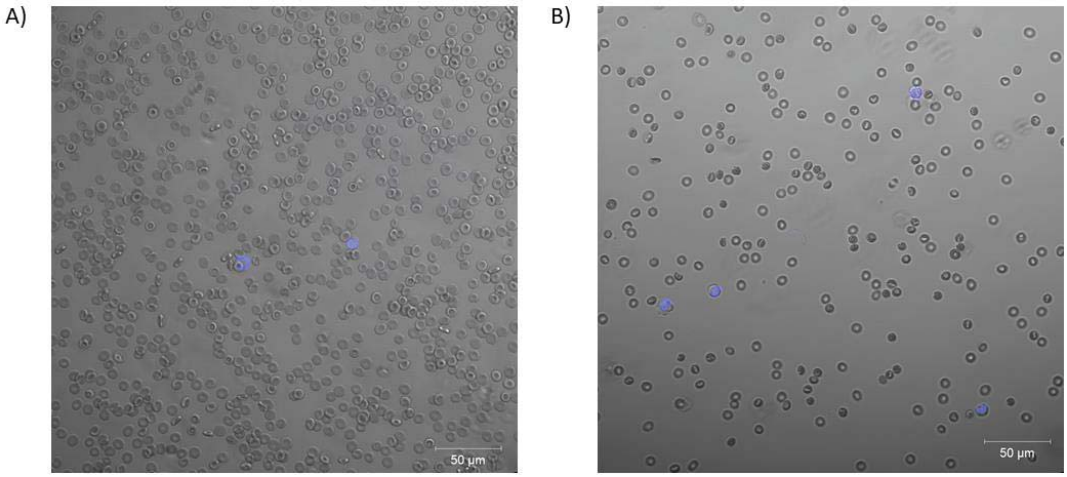

Figure 2. 6 – A) Not haemolysed blood - High number of erythrocytes are observed (not stained cells) as well as two leukocytes (stained cells); B) Haemolysed blood - A considerable low number of erythrocytes are observed (not staining cells). Some erythrocyte shows an unhealthy morphology based on the haemolysis treatment. Three leukocytes are observed (stained cells).

2.2.6 Calibration curve via DCL ELISA

For the calibration curve, spike-in solutions were prepared by dissolving varying quantities of synthetic mimic miRNA-451a (96, 48, 24 and 12 fmoles) in 5 µL of water. Each solution was diluted with a ratio 1:20 in 95 µL of RBC lysis buffer 1X in order to recreate the same conditions and environment of plasma samples. As control, 5 µL of only water were diluted with 95 µL of RBC lysis buffer 1X.

The reaction was carried out in three steps:

1) miRNA-451a hybridization - 100 µL of each spike-in solution was diluted in an eppendorf of 1.5 mL with 198.75 µL of lysis buffer and 1.25 µL of microsphere solution (200,000 beads/µL) containing 250,000 beads. The eppendorf was placed in a thermoshaker, mixed at 1,200 rpm, RT for 1 h. The microspheres were pelleted by centrifugation at 6,000 rpm for 10 sec and held on a magnet rack for 30 sec to discard the supernatant. The pellet was washed three times with 200 µL of 0.1% Tween®-20 in PBS (10 mM, pH 7.4).

2) The dynamic chemistry reaction was carried out by resuspending the pellet in 50 µL of solution containing 45.45 µL of 2X SSC and 0.1% SDS buffer (pH 6), 5 µM of SMART-C-Biotin (1.25 µL from a stock of 200 µM) and 1 mM of reducing agent (3.3 µL from a stock of 15 mM sodium cyanoborohydride). The eppendorf was incubated in a thermoshaker at 40ºC, 1,200 rpm for 1 h.

3) The microspheres were pelleted by centrifugation at 6000 rpm for 10 sec and held on a magnet rack for 30 sec to discard the supernatant. The pellet was washed three

times with 200 µL of 0.1% Tween®-20 in PBS (10 mM, pH 7.4) to remove the excess of SMART-C-Biotin. After washings, the pellet was resuspended in 100 µL of SβG (250 pM), vortexed and incubated in a thermoshaker for 20 min at RT. Microspheres were washed two times with 200 µL of 0.1% Tween®-20 in PBS (10 mM, pH 7.4) to remove the excess of SβG. Finally, microspheres were resuspended in 200 µL of 0.1% Tween®-20 in PBS (10 mM, pH 7.4) and transfer to a 96-black well plate. Supernatant was removed and 200 µL of resorufin-β-D-galactopyranoside (RGP) substrate was added. The fluorescence signal was measured by the FLUOstar OMEGA instrument. The values obtained were represented by the slope of the linear range of a plot of fluorescence measured (Figure 2.7).

2.2.7 Healthy volunteer sample analysis via DCL ELISA

Analysis of healthy volunteer samples was carried out as described in Section 2.2.6. Instead of 100 µL o spike-in solution was used 100 µL of plasma solution prepared as described in Figure 2.5.

2.2.8 Calibration curve via RT-qPCR

Spike-in solutions were prepared by dissolving varying quantities of synthetic mimic miR-451a (15, 1.5, 0.15, 0.015, 1.5 x 10^{-4}, 1.5 x 10^{-5} and 1.5 x 10^{-6} fmoles) in 500 µL of water.

The reverse transcription was carried out using the TaqMan® MicroRNA Reverse Transcription Kit and a specific stem-loop RT primer specific for miR-451. The cDNA was generated according to manufacturer's protocol using 5 µL of each Spike-in solution. cDNA generated was amplified by quantitative real time PCR using a FastStart TaqMan probe master mix according to manufacturer's protocol. Briefly, PCR master mix was prepared, in 0,2 mL tube on ice, by mixing 10µL of master mix, 1µL of miR-451 specific miR451 TaqMan probe (Assay ID #001141; Life Technologies) and 6,5µL PCR-grade water. 2,5µL of total cDNA were added to the PCR master mix, in a final volume of 20µL. Quantitative PCR analysis was performed on a 7900 Fast Real-Time PCR System, with an initial activation step of 95ºC for 15 min followed by 40 cycles of 2-step cycling (denaturation: 15s at 95°C and Annealing/Extension: 1min at 60ºC).

2.2.9 Isolation of RNA from HV plasma samples

RNA was isolated from haemolysed and not haemolysed plasma using the miRNeasy Serum/Plasma kit according to manufacturer's protocol. 100µL of each sample were mixed with 500µL of Qiazol, mixed and incubated at RT for 5 min. 100µL of chloroform

ere added and mixed and incubated for 3 min. The mix was centrifuged at 12,000xg for 15 min at 4ºC and the upper aqueous phase was transferred to a new collection tube. 100% ethanol was added to the collection tube, mixed and transferred to the RNeasy MinElute column and centrifuged at 10,000 x g for 15 min at RT. Using the same centrifugation conditions, the column was washed with respectively RWT and RPE buffers followed by a further washing with 80% ethanol. The column was dried by centrifugation and small RNAs eluted with 14µL RNase-free water and stored at -80ºC.

2.2.10 Reverse transcription and amplification of HV plasma samples

RNA samples were isolated as described in section 2.2.9. Frozen RNA was thawed at day 1 and reverse transcripted and amplified as reported in section 2.2.10. The aliquot was frozen and storage at -80ºC. For the inter-experimental repeatability study, the same aliquot of RNA was thawed after 24 hours and reverse transcripted and amplified.

2.3 Results

2.3.1 Analytical sensitivity of DCL ELISA

The analytical sensitivity of DCL ELISA was determined by creating a calibration curve (for protocols details see section 2.2.6) using known quantities of synthetic miRNA-451a molecules: 96, 48, 24 and 12 fmoles in a total hybridization volume of 300 µL, equal to 320, 160, 80 and 40 pM respectively (water was used as a negative control). Experiments were performed in triplicate with coefficients of variants for each condition below 10%, except for the negative control which has shown a CV value of ~25% (Table 2.2). The average slope values obtained for the four quantities of template RNA were, respectively, 0.973 ± 0.06 RFU s^{-1}, 0.567 ± 0.09 RFU s^{-1}, 0.257 ± 0.02 RFU s^{-1} and 0.17 ± 0.02 RFU s^{-1} and 0.070 ± 0.02 RFU s^{-1} for the control. The curve was obtained by plotting the slope values versus the quantity of synthetic RNA molecules (Figure 2.7). To determine the limit of detection (LoD), we used the formula based on the standard deviation of the blank and the slope (Formula 2.1).

$$LoD = \frac{3.3 \times SDblank}{slope} \qquad \text{(Formula 2.1)}$$

Table 2.2 – Slope values obtained by DCL ELISA

Fmoles	Slope 1	Slope 2	Slope 3	Average slope	SD	CV
96	0.940	0.910	1.070	0.973	0.085	8.74%

48	0.550	0.570	0.580	0.567	0.015	2.70%
24	0.26	0.25	0.26	0.257	0.006	2.25%
12	0.170	0.160	0.190	0.173	0.015	8.81%
Water	0.060	0.090	0.060	0.070	0.017	24.74%

Using the formula based on the standard deviation of the blank (water) and the slope of the curve represented in Figure 2-A [(3xSD)/slope)], the limit of detection (LoD) is calculated about 6.89 fmoles (22.97 pM in a total hybridization volume of 300 µL).

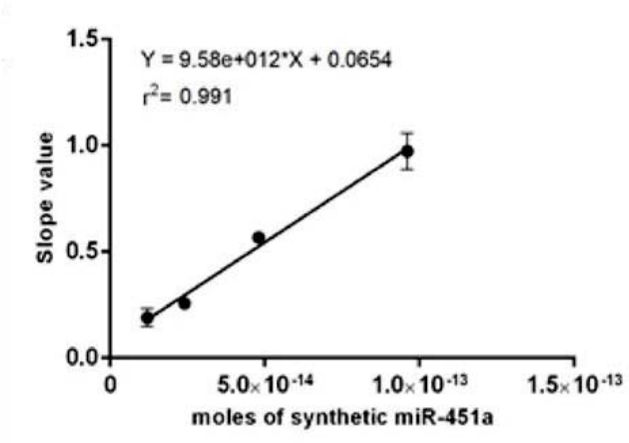

Figure 2.7 – Calibration curve generated using DCL ELISA. Plot of slope values of fluorescent signals *vs.* number of moles of synthetic miRNA-451a spiked-in. Error bars (±1 s.d.) based on triplicate measurements. For some points, error bars are smaller than the size of data points. *n = 3.*

2.3.3 Analytical specificity of DCL ELISA

The specificity of DCL ELISA was investigated using a non-complementary synthetic miRNA-122 as well as a target containing a single nucleotide mismatch (miRNA-451a_T) which presents a thymine in front of the abasic probe position instead of a guanine (Table 2.1). As shown in Figure 2.8, when the perfectly complementary target miRNA-451a was used the signal showed a linear correlation with miRNA-451a concentration while with miRNA-122 and miRNA-451a_T the signals were unaffected. These results show the high discrimination capability offered by this approach, which can be exploited to analyse isomiRNAs.

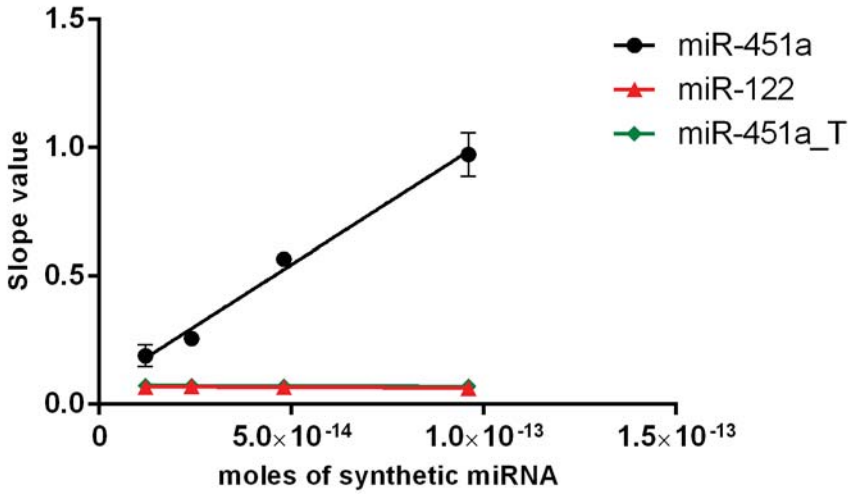

Figure 2.8 – Plot of slope values of fluorescent signals *vs.* number of moles (96, 48, 24 and 12 fmoles in a total hybridization volume of 300 µL) of synthetic miRNAs. ●: Full-complementary target miR-451a; ▲: Noncomplementary miR-122; ◆: miR-451a_T target containing a single nucleotide mismatch. n = 3.

2.3.3 MiRNA-451a direct profiling in plasma samples from healthy volunteers via DCL ELISA

Upon the generation of calibration curves and the determination of sensitivity (LoD) and specificity, both methods were employed for the direct detection of miRNA-451a in blood samples of three HVs. All experiments were performed in accordance with the Guidelines of Spain, and approved by the ethics committee at the Centro de Investigación de Granada, Servicio Andaluz de Salud.

Plasma samples containing RBC lysis buffer (1 : 20) with/ without free miRNA-451a were then tested using the DCL ELISA technology, as described in section 2.2.6. As shown in Figure 2.9, 100 µL of plasma samples containing RBC lysis buffer (1 : 20) samples were then incubated with a lysis buffer for both protein denaturation and exosome lysis containing microspheres (250,000) functionalised with abasic PNA probes complementary to miRNA-451a for 1 h, in a final volume of 300 µL, to capture the free miRNA-451a. For the reaction, the microspheres were firstly pelleted down and then re-suspended in a reaction buffer containing SMART-C-Biotin and a reducing agent with a final volume of 50 µL. The fluorescent signal was created by incubating the microspheres with SβG and adding an RGP substrate. Signals were read-out using FLUOstar OMEGA and the slopes were calculated.

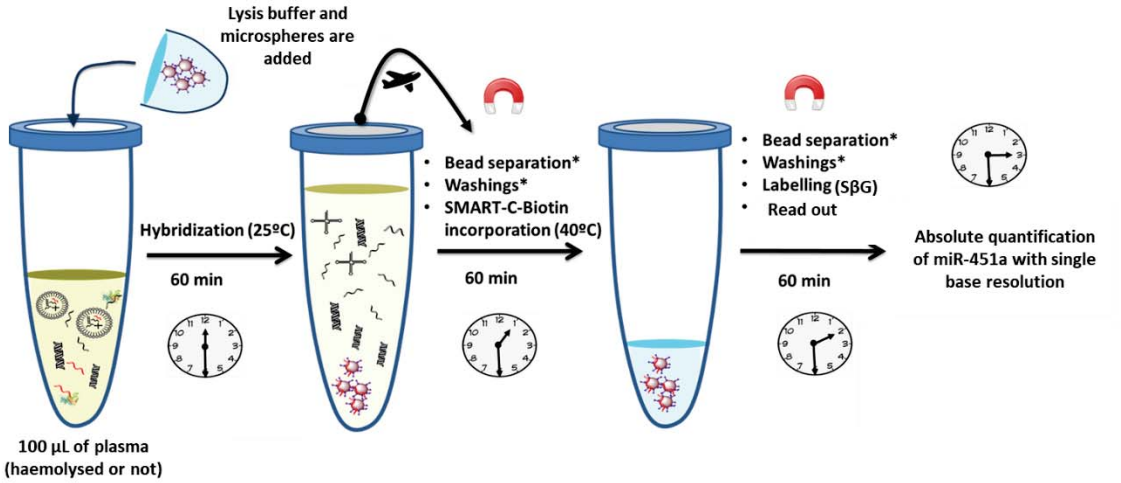

Figure 2.9 – DCL ELISA workflow. A mixture containing lysis buffer (200 µL) and microspheres (2.5×10^5) functionalized with the abasic PNA probe complementary to miRNA-451a is added to 100 µL of plasma sample containing RBC lysis buffer (1 : 20) to capture miRNA-451a for 1 h at RT. Microspheres were pelleted down, washed three times and resuspended in 50 µL of reaction buffer containing SMART-C-Biotin. Microspheres were labelled with SβG which trigger a fluorescence reaction for a final read out.

The absolute quantification was possible by extrapolating from the calibration curve (Figure 2.7) the number of moles of miRNA-451a using the slope values measured and reported in Table 2.3. The measurements were made in triplicates on two different days (day 1 and day 2). Concentrations of miRNA-451a for all samples are reported in Table 2.4. The number of moles (in the total 100 µL added) was extrapolated by using the calibration curve shown in Figure 2.7. To calculate the concentration of the plasma sample, the dilution factor 1 : 20 provided by the RBC lysis buffer plus the dilution factor 1 : 3 provided by the exosomal lysis buffer were taken into account. This means that the concentration of miRNA-451a in the solution containing both lysis buffers was 60 times lower than the sample concentration shown in the table. Controls are represented by not haemolysed plasmas.

Table 2. 3 – Slope values measured by DCL ELISA

Sample code	Measurement	Slope 1	Slope 2	Slope 3	Average slope	SD	CV
HV 1 – HP	Day 1	1.130	1.260	1.230	1.207	0.068	5.64%
	Day 2	1.110	1.380	1.290	1.260	0.137	10.91%
HV 2 - HP	Day 1	1.180	1.050	1.170	1.133	0.072	6.38%
	Day 2	1.330	1.070	1.160	1.187	0.132	11.13%
HV 3 - HP	Day 1	1.380	1.550	1.500	1.477	0.087	5.92%
	Day 2	1.640	1.620	1.380	1.547	0.145	9.35%
HV 1 – NHP	Day 1	0.080	0.120	0.040	0.080	0.040	50.00%
	Day 2	0.050	0.070	0.080	0.067	0.015	22.91%
HV 2 - NHP	Day 1	0.070	0.060	0.060	0.063	0.010	9.12%
	Day 2	0.080	0.070	0.070	0.073	0.006	7.87%
HV 3 - NHP	Day 1	0.130	0.140	0.080	0.117	0.030	27.55%
	Day 2	0.050	0.040	0.070	0.053	0.015	28.64%

HP: Haemolysed Plasma; NHP: Not haemolysed plasma.

Table 2. 4 – Concentration determined by DCL ELISA

Sample code	Concentration at day 1 (nM)	Concentration at day 2 (nM)	Average	SD	CV
HV 1 - HP	23.826	24.939	24.383	0.787	3.23%
HV 2 - HP	22.295	23.408	22.852	0.787	3.45%
HV 3 - HP	29.463	30.924	30.193	1.033	3.42%

2.3.4 Analytical sensitivity of RT-qPCR

In parallel to the analytical sensitivity of DCL ELISA, it was created a calibration curve using RT-qPCR, plotting the Ct values *vs.* $-\log_2$ of synthetic miRNA-451a quantities (Figure 2.10).

Seven quantities of synthetic miR-451a: 15, 1.5, 0.15, 0.015, 1.5×10^{-4}, 1.5×10^{-5} and 1.5×10^{-6} fmoles in a total reverse transcription reaction volume of 15 µL, thus equal to 1, 0.1, 0.01, 0.001, 0.0001, 0.00001 and 0.000001 nM were used. As described in detail section 2.2.10, the amplification was carried out using 2.5 µL of cDNA in a final volume of 20 µL. The Ct values obtained presented coefficients of variance below 1.5% (Table 2.4). The average Ct signals obtained for the seven quantities were respectively 17.252 ± 0.1, 21.254 ± 0.2, 26.590 ± 0.2, 29.907 ± 0.2, 36.627 ± 0.3, 37.958 ± 0.3 and not detectable for the lowest concentration of miRNA (1.5×10^{-6} fmoles). To estimate the LoD, the Ct values obtained with the two lowest detectable quantities (1.5×10^{-5} and 1.5×10^{-4} fmoles) were averaged and the standard deviation was determined. The Ct value at 3 SD below the average was 36.250, resulting in a LoD of 4.741×10^{-4} fmoles in a total volume of 15 µL (volume related to the generation of cDNA), thus equal to 31.60 fM (2.85 × 10 molecules).

Table 2.5 – Ct values obtained by RT-qPCR

Fmoles	Ct 1	Ct 2	Ct 3	Average Ct	SD	CV
15	17.183	17.296	17.278	17.252	0.061	0.35%
1.5	21.476	21.287	20.998	21.253	0.241	1.13%
1.5×10^{-1}	26.440	26.770	26.561	26.590	0.180	0.68%
1.5×10^{-2}	30.181	29.714	29.825	29.907	0.244	0.82%
1.5×10^{-4}	36.379	36.875	35.388	36.627	0.351	0.96%
1.5×10^{-5}	37.701	38.215	n.d	37.958	0.363	0.96%
1.5×10^{-6}	n.d	n.d	n.d	n.d	n.d	n.d

PCR was performed in triplicate on three aliquots from this reaction solution. To estimate the LoD, the Ct values of the two lowest detectable quantities (1.5×10^{-5} and 1.5×10^{-4} fmoles) were averaged and the standard deviation determined. The Ct value at 3 s.d. below the average was 36.250, resulting in a LoD of 4.741×10^{-4} fmoles in a total volume of 15 µL (volume related to the generation of cDNA.), i.e. 31.60. n.d = not determined.

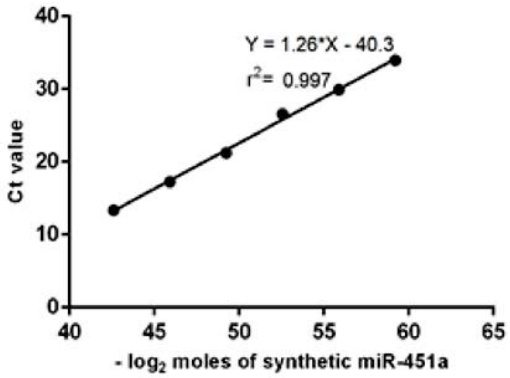

Figure 2.10 – Calibration curve generated using RT-qPCR. Plot of Ct values *vs.* $-\log_2$ of moles of miRNA-451a spiked-in. Error bars (±1 s.d.) based on triplicate measurements; the error bars are smaller than the size of data points. n = 3.

2.3.5 MiRNA-451a profiling in plasma samples from healthy volunteers via RT-qPCR

The RT-qPCR analysis was carried out on RNA isolated from plasma samples of the three HVs. For both haemolysed and not haemolysed plasma, RNA was isolated using the miRNeasy Serum/Plasma kit according to manufacturer's protocol. Briefly, 100µL of each sample were mixed with 500µL of Qiazol, mixed and incubated at RT for 5 min. 100µL of chloroform ere added and mixed and incubated for 3 min. The mix was

centrifuged at 12,000xg for 15 min at 4ºC and the upper aqueous phase was transferred to a new collection tube. 100% ethanol was added to the collection tube, mixed and transferred to the RNeasy MinElute column and centrifuged at 10,000 x g for 15 min at RT. Using the same centrifugation conditions, the column was washed with respectively RWT and RPE buffers followed by a further washing with 80% ethanol. The column was dried by centrifugation and small RNAs eluted with 14µL RNase-free water and stored at -80ºC.

Reverse transcription and amplification were carried out according to the manufacturer's protocols. The aliquot was frozen and storaged at -80ºC. For the inter-experimental repeatability study (see section 2.5), the same aliquot of RNA was thawed after 24 hours and reverse transcripted and amplified as manufacturer's recommendations .

The absolute quantification was possible by extrapolating from the calibration curve (Figure 2.11) the number of moles of miRNA-451a using the Ct values measured and reported in Table 2.6. The measurements were made in triplicate at two different days (day 1 and day 2). Concentrations of miRNA-451a for all samples are reported in Table 2.7. Controls are represented by non-haemolysed plasmas (NHP).

Table 2.6 – Ct values measured by RT-qPCR

Sample code	Measurement	Ct 1	Ct 2	Ct 3	Average Ct	SD	CV
HV 1 – HP	Day 1	13.962	14.139	14.095	14.065	0.092	0.66%
	Day 2	13.518	14.128	15.108	14.251	0.803	5.63%
HV 2 - HP	Day 1	13.377	13.621	13.369	13.456	0.144	1.07%
	Day 2	14.392	14.237	14.307	14.312	0.077	0.54%
HV 3 - HP	Day 1	12.498	12.650	13.810	12.986	0.718	5.53%
	Day 2	15.321	15.180	15.811	15.438	0.332	2.15%
HV 1 – NHP	Day 1	23.452	23.658	23.448	23.520	0.120	0.51%
	Day 2	23.299	22.839	23.265	23.135	0.256	1.11%

HV 2 - NHP	Day 1	22.962	23.087	22.891	22.981	0.099	0.43%
	Day 2	22.656	22.716	22.838	22.737	0.093	0.41%
HV 3 - NHP	Day 1	24.581	23.491	23.366	23.429	0.668	2.85%
	Day 2	22.034	22.499	22.527	22.514	0.277	1.23%

HP: Haemolysed Plasma; NHP: Not haemolysed plasma.

Table 2. 7 – Concentration determined by RT-qPCR

Sample code	Concentration at day 1 (nM)	Concentration at day 2 (nM)	Average	SD	CV
HV 1 - HP	20.534	18.536	19.535	1.413	7.23%
HV 2 - HP	28.713	17.925	23.319	7.628	32.71%
HV 3 - HP	37.180	9.652	23.416	19.465	83.13%

2.3.6 Analytical comparative between the two assays

A comparative analysis between the average concentrations at day 1 *vs.* day 2 to measure the inter-experiment variability between the two technologies is reported in Table 2.8. The comparative analysis was not undertaken for the not haemolysed plasmas. As shown in the Table 2.8, DCL ELISA shows CV values between 2-4%, indicating a high inter-experimental repeatability through the two experiment days. However, RT-qPCR shows CV values of 7%, 33% and 83% respectively for HV1, HV2 and HV3.

Table 2.8 – Comparative analysis between the two methods

Method	Sample code	Concentration at day 1 (nM)	Concentration at day 2 (nM)	Average	SD	CV
DCL ELISA	HV 1 - HP	23.826	24.939	24.383	0.787	3.23%
	HV 2 - HP	22.295	23.408	22.852	0.787	3.45%
	HV 3 - HP	29.463	30.924	30.193	1.033	3.42%
RT-qPCR	HV 1 - HP	20.534	18.536	19.535	1.413	7.23%
	HV 2 - HP	28.713	17.925	23.319	7.628	32.71%
	HV 3 - HP	37.180	9.652	23.416	19.465	83.13%

In addition, we studied the correlation between the two technologies, as well as the relative signal measured according the number of RBC/µL. Figure 2.11 shows the correlation between the numbers of RBC/µL and the concentration measured using DCL ELISA. Higher levels of miRNA-451a were detected in those samples with a higher RBC/µL. By contrast, the RT-qPCR results did not show the same correlation. HV2 with the lowest RBC/µL showed the second highest concentration of miRNA-451a, instead of the expected lowest concentration.

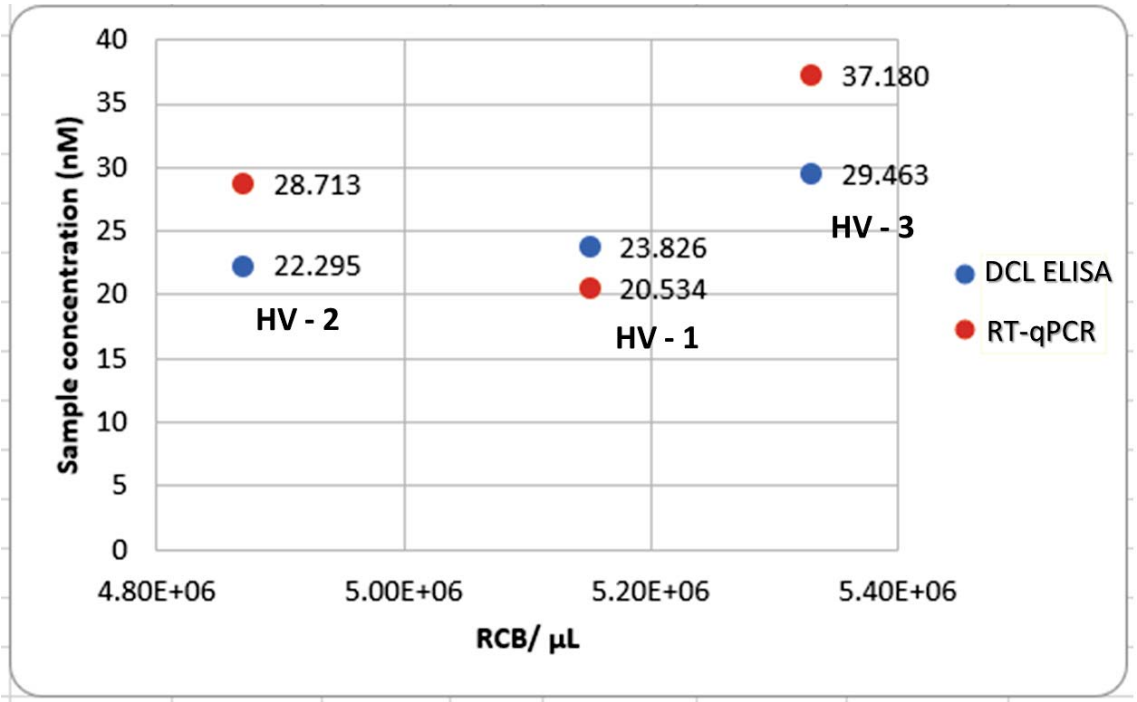

Figure 2. 11 – Plot of concentration between the number of RBC/µL *vs.* the miRNA-451a concentration (nM). Only the DCL ELISA shows this correlation, it is: higher is the number of RBC/µL, higher is the concentration of miRNA-451a.

2.4 Discussion

To facilitate the use of miRNA biomarkers in clinical diagnostic, we have developed a method to quantify directly miRNA which is different to all other systems for nucleic acid testing. Our DCL reagents were combined with a conventional multimode micro-plate reader, creating a novel cost-effective ELISA type system that we have coined as DCL ELISA. This system allows profiling of miRNAs with single base, without needing of neither extracting RNA molecules, amplifying them (PCR-free) nor adding modification to native mature miRNA (label-free). This direct detection method overcomes the various limitations of conventional methods for analysing miRNAs, such as: a) the challenges associated with the pre-extraction of RNAs and; b) the problems related to both the reverse transcription and amplification.

Here, the novel DCL ELISA was used for an accurate quantification of miRNA-451a. In a first instance, the system was used to generate a calibration curve so to determine the instrumental LoD, resulting in about 20 pM. The calibration curve was used also to quantify the level of miRNA-451a expression in three HV blood samples. The samples used for this proof of concept study were haemolysed in order to liberate intra-erythropoietic miRAN-451a, while not haemolysed plasma samples were used as controls.

For the three HV samples, miRNA-451a was detected respectively at 24.40, 22.86 and 30.20 nM, while it was not detected (n.d.) in not haemolysed plasma. When using RT-qPCR, miRNA-451a was detected also in the not haemolysed plasmas (Table 2.6). This indicated there is free miRNA-451a also in not haemolysed plasmas, which were not detectable via the plate reader due to insufficient sensitivity. To address the issue related to the sensitivity, our group has used an innovative single molecule resolution platform (SIMOA HD-1) which allows up to 1,000-fold better sensitivity in comparison with conventional reader systems. Recently, using the DCL approach, we were able to profile the expression of circulating miRNA-122 in drug induced liver injury (DILI) patients within a LoD of about 500 fM. (84) Hence, by using more sensitive detection platforms such as the SIMOA HD-1 instead of a plate reader, the presented chemistry and protocols will be able to address the issue concerning the sensitivity. In that way, detection of miRNA-451a which levels in not haemolysed plasmas are about 5,000-10,000 fM will be possible.

The presented detection system has shown superior: a) inter-experimental repeatability through the two experiment days and, (b) correlation between the RBC/µL and measured concentration of miRNA-451a. This is most likely due to our method not being affected by the common issues associated with RTq-PCR, such as extraction of RNAs, generation of cDNA and amplification. Generally, for the quantification by RT-qPCR, it is assumed that all the sample preparation steps are effective at 100%. Unfortunately, in practice this is rarely the case, due to variable recovery rates of RNAs during an extraction, as well as a poor reverse transcription in generating cDNA. This can result in a misreading of absolute initial mature miRNAs, not being translated to cDNA and therefore amplified. Whereas, with the DCL system there are no longer laborious sample preparation steps with errors/ variability, being a direct method that allows read-outs of the absolute number of mature miRNAs, requiring neither pre-amplification nor pre-labelling of target nucleic acids.

DCL ELISA delivers a number of advantages over RT-qPCR for detection of miRNA in the research environment (Table 2.9). DCL ELISA provides a consistent method to detect not only intra-erythropoietic miRNA-451a, but also other relevant miRNAs with level of expressions comparable to the sensitivity achieved in this study. By reducing the dilution of biological fluids to release free-miRs, if compared to this proof of concept, plus using more advanced platforms with higher sensitivity (e.g. SIMOA HD-1), (84, 88) DCL ELISA will be able to detect miRNA found in biological fluids at low concentrations.

Table 2.9 – Comparison between DCL ELISA and RT-qPCR.

Method	Time to Result	Extraction Required	Amplification Required	Direct Quantification	Inter-experiment repeatability	Overall test Cost	Specimen Collection Flexibility	Sample Size Required
DCL ELISA	≈ 3 h	No	No	Yes	High	Mod.	All collection tubes	≥ 2 µL
RT-qPCR	≈ 6 h	Yes	Yes	No	Mod.	High	EDTA Only	≥ 100 µL

Mod.: Moderate.

2.5. Conclusions

1. The development of a rapid, cost-effective and robust, bead-based assay for the detection and quantification of nucleic acids using DCL in combination with a conventional multimode micro-plate reader, has been successfully accomplished, creating the so called “DCL ELISA platform”.
2. The DCL ELISA platform allows profiling miRNAs with single base resolution, without needing to neither extract RNA molecules, amplifying them (PCR-free) nor adding a modification to native mature miRNA (label-free).
3. This direct detection method overcomes the various limitations of conventional methods for analysing miRNAs, such as: a) the challenges associated with the pre-extraction of RNAs and; b) the problems related to both the reverse transcription and amplification.
4. The system was used to generate a calibration curve so to determine the instrumental LoD, resulting in ± 20 pM.
5. By using calibration curves it is now possible to absolute quantify miRNAs levels. This was validated by measuring miR-451a concentrations using blood samples with concentrations ranging from 22.86 nM to 30.20 nM.
6. The samples used for this proof of concept study were haemolysed in order to liberate intra-erythropoietic miR-451a, while not haemolysed plasma samples were used as controls and in these, miR-451a was not detected. However, when using RT-qPCR, miR-451a was detected also in the not haemolysed plasma samples. This indicated there is free miR-451a also in not haemolysed plasma, which were not detectable via the plate reader due to insufficient.
7. The DCL method is likely not being affected by the common issues associated with RT-qPCR, since it has shown superior: a) inter-experimental repeatability through

the two experimental days and, (b) correlation between the RBC/μL and the measured concentration of miRNA-451a.

8. The DCL method presented here has also been merged, with ultra-sensitive platforms such as the SIMOA HD-1 instead of a plate reader, presenting LoD of about 500 fM. In that way, the detection of miR-451a in not haemolysed plasmas will be possible.

Chapter 3:

Amplification-free profiling of microRNA-122 biomarker in DILI patient serums, using the

Luminex MAGPIX system

Chapter 3: Amplification-free profiling of microRNA-122 biomarker in DILI patient serums, using the Luminex MAGPIX system

3.1 Introduction

In this chapter we have interrogated circulating miRNA-122 and DILI as the clinical paradigm to test whether the DCL method can sensitively and specifically measure microRNA directly from serum with no need for microRNA extraction or amplification. For this purpose, the DCL method was combined with the Luminex MAGPIX system (139) to generate a unique assay for the direct measurement of miRNA-122 in DILI patients. The Luminex MAGPIX was chosen as it is a validated system for clinical use. The DCL protocol includes a unique buffer 'Stabiltech' that enables lysing, liberation and stabilisation of the miRNA under interrogation, without requiring the samples to be prepared, transported and stored under refrigerated conditions. Particularly, our group has recently reported a stability study of miRNA-122, using serum from a patient with DILI (ALT > 1000 U/L after acetaminophen overdose). (88)

3.1.1 Drug Induced Liver Injury

Adverse drug reactions (ADR) are a primary concern for patients, healthcare professionals and the pharmaceutical industry with an estimated annual cost to the EU of €79 B. DILI is the second most common ADR and a leading cause of acute liver failure (ALF) in the western world.

ALF is a life-threatening condition and identifying patients at risk for ALF is a priority task. DILI incidence depends on the drug itself and host/patient-specific factors such as sex, ethnicity, and genetic polymorphism in the detoxification of drugs and so on. For instance, for the antibiotic amoxicillin-clavulanate, approximately 1 out of 2300 patients will develop DILI. Also, DILI is one of the leading causes of drug attrition throughout all stages of the drug discovery process. In early development, 50% of all pre-clinical candidate drugs display effects upon the liver at supra-therapeutic doses and over the last 50 years, DILI was responsible for 18% of all medicines retracted post-marketing (the main reason for withdrawal). From 1997 to 2016, only in EU and USA, eight drugs have been withdrawn because of DILI related incidents including liver transplants and deaths. The interpretation of laboratory findings of suspected hepatotoxicity cases in clinical trials is complex, as increased levels of hepatic enzymes are not necessarily due to DILI but from other underlying liver diseases.

According to surveys in France and Iceland, DILI occurs with an annual incidence of about 14–19 per 100,000 inhabitants. (140) Paracetamol (acetaminophen) overdose is one of the most common poisonings worldwide. Although it is safe in small doses, paracetamol can be dangerous or even deadly if taken in larger quantities. In the United States, paracetamol is the most common cause of acute liver failure, and the second most common cause of liver failure requiring a transplant. In Europe, paracetamol poisoning is still the most common cause of listing for a liver transplant after drug overdose, involving about the 96% of such cases. In the UK, it is estimated that paracetamol overdose accounts for 48% of all poisoning admissions to hospitals. (141) In Asian countries like China, DILI is believed to be significantly underdiagnosed. The high frequency of DILI cases is associated with an extensive use of traditional Chinese medicines, herbal and dietary supplements and anti-tuberculosis drugs. In a recent retrospective study, it has been estimated an annual incidence in the general population to be 23.80 per 100,000 persons, (142) much higher than in Western countries. The unmet need going forward is, therefore, to develop an assay that enables a more rapid and accurate identification of DILI, so as to make improved and earlier clinical decisions on whether to start antidote therapy and therefore optimise therapies to reduce adverse events. (143)

Current diagnosis of DILI depends on expert opinion that is based on patient data and the typical ‘signatures’ associated with certain drugs. Causality scores such as the Roussel-Uclaf Causality Assessment Method (RUCAM) (144) are intended to confirm or exclude the suspicion of DILI. (141) Although the RUCAM approach is the current screening gold standard, the initial screening (RUCAM) comes along with several drawbacks, listed in Table 3.1.

Over the past several years, many animal and clinical studies have been published showing that miRNAs have an advantage over the conventional biomarkers for DILI. They are exceptionally stable, can be highly liver-specific and remarkably altered in pathologic states, are readily detectable in easily accessible bodily fluids, and are strictly conserved among species. Liver-specific miRNA-122 has been shown to be involved in various processes of liver development, differentiation, metabolism and stress responses. Compared with the conventional hepatotoxic markers, circulating miR-122 can effectively and consistently distinguish intrahepatic from extrahepatic damage with higher sensitivity and specificity. Thus, miRNA-122 is expected to be a preclinical and clinical biomarker of DILI.

Table 3.1 – RUCAM main drawbacks.

Problem	Description of the problem	Consequences
No specific screening examination	Early symptoms are generally non-specific, while early diagnoses are crucial to the treatment of drug overdoses	May limit the time in which results for analytical studies can be obtained
Arbitrary and complex scoring	RUCAM has limitations that include poor inter-rater reliability and arbitrary scoring. Besides, is difficult to apply in the clinical context due to its complexity (89)	Consensus opinion carries the risk of overruling a more insightful minority opinion (141)
Cost of examination	Toxicology investigation cost (€154) and ingestion poisoning investigation in-patient episode cost (€644), giving a total of €798 (145)	Diagnosis is expensive due to the lack of a specific screening method to study DILI

3.1.2 MiRNA-122

MiRNA-122 is a well-known liver specific miRNA expressed in high concentration in hepatocytes, making it an ideal biomarker for testing for liver disease. (141) As described elsewhere, (146) miRNA-122 is released into the circulation when hepatocytes are injured. (147) In humans, miRNA-122 is found around 100-1000-fold higher in patient serum following paracetamol overdose. (148) Comparing with alanine transaminase (ALT) in the context of DILI, miRNA-122 has advantages to be used as biomarker. Firstly, miRNA-122 is highly specific for the liver. (149-151) In fact, muscle injury commonly results in an elevation in serum ALT activity without liver injury. By contrast, circulating miRNA-122 is not increased. This property can aid drug development by enhancing specificity. Secondly, miRNA-122 increases in the circulation soon after liver injury starts, before ALT increases. This has been repeatedly demonstrated in pre-clinical rodent models, where miRNA-122 peaks at 6 hours after overdose in comparison with ALT peaking at 24 hours, and also demonstrated in human studies. (151) This enhanced sensitivity early in the disease process allows early rule in/rule out of liver injury after a toxic insult. Circulating miRNA-122 is also increased in patients with cholestyramine-induced liver injury, (152) ischemic hepatitis, (153) viral hepatitis (154) and cholestatic liver injury. (155)

3.1.3 The Luminex MAGPIX system

Traditionally, single-analyte, or singleplex, protein detection methods such as ELISA have been used sequentially to analyze multiple intracellular and extracellular proteins. Although these methods are well-established, validated techniques, they can be time-consuming, sample-depleting, and costly when used to measure numerous markers

per sample. In the other hand, multiplex immunoassays confer several advantages over widely adopted singleplex immunoassays including increased efficiency at a reduced expense, greater output per sample volume ratios and higher throughput predicating more resolute, detailed diagnostics and facilitating personalised medicine. Nonetheless, to date, relatively few protein multiplex immunoassays have been validated for in vitro diagnostics in clinical/point-of-care settings. Several high-content protein microarrays for comparative profiling are available commercially, (156-164) however, between them, relatively few have been validated for IVD applications; moreover, despite the theoretical multiplexing capacities of the platforms, commercially available panels appear to only harness a fraction of this capacity, seldom exceeding 20 individual analytes. (165-168)

Alternatively, Luminex xMAP technology enables scientists to measure multiple proteins in a single reaction. The Luminex xMAP technology includes fluorescent-coded beads, where each individual antigen is covalently linked to specific colour-coded microspheres such that the reading device can classify each bead set separately. Luminex instrumentation generally quantifies laser-induced fluorescent signals from each bead using flow cytometric technology but, more recently, a convenient developed alternative is the Luminex MAGPIX system. The MAGPIX system uses colour-coded magnetic beads displayed in a monolayer, which are detected with a light-emitting diode (LED) instead of laser system and imaged using a charge-coupled device (CCD) camera (Figure 3.1). This platform considerably reduces the costs of the multiplex approach since antigen is immobilized on a much smaller surface area compared to microplate wells, and sample volumes are reduced compared to ELISA. (169)

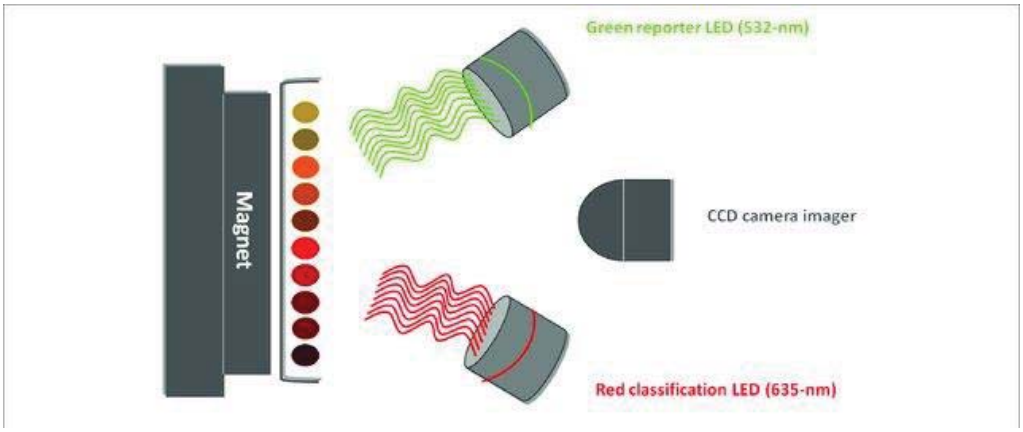

Figure 3.1 - Principle of analysis by the MAGPIX fluorescent imager. Magnetic microspheres immobilized on a magnet are recognized by LEDs and a CCD camera records the picture (LED, light-emitting diode; CCD, charge-coupled device). (170) (*Copyright under CC BY 4.0*).

3.2. Material and Methods. Integration of DCL into the Luminex MAGPIX system: The DCL/ MAGPIX assay

We used our DCL technology in combination with the Luminex MAGPIX system to generate a unique assay for the direct measurement of miRNA-122 in DILI patients. The DCL protocol includes a unique buffer 'Stabiltech' that enables lysing, liberation and stabilisation of the miRNA under interrogation, without requiring the samples to be prepared, transported and stored under refrigerated conditions. Particularly, our group has recently reported a stability study of miRNA-122, using serum from a patient with DILI (ALT > 1000 U/L after acetaminophen overdose). (88)

3.2.1 Materials

Synthetic mimic miRNA-122 oligomer was purchased from Integrated DNA Technologies (Table 3.2). Concentrations of RNA and DNA solutions were determined using a ThermoFisher NanoDrop1000 Spectrophotometer. MagPlex microspheres were purchased from Luminex Corporation (1.25 x 10^7/mL). Streptavidin-R-Phycoerythrin (SA-PE, 1mg/mL) was purchased from Moss Biotech Inc. Chemicals for couplings were purchased from Sigma-Aldrich. DGL 122 abasic PNA probe (Table 3.2), the aldehyde-modified biotinylated cytosine nucleobase (Figure 2.4) and buffers (including the Stabiltech buffer) for DCL reactions were provided by DESTINA Genomica S.L. Wash buffer contains 0.1% Tween 20 in PBS 1X. DESTINA reaction buffer is a solution of 30 mM trisodium citrate and 300 mM sodium chloride with 1% w/v of BSA (pH is adjusted to 6.0 using HCl). DGL 122 was coupled with the Luminex MagPlex microspheres (capture microspheres DGL 122) according to the protocol optimised by DESTINA Genomica S.L. and reported in section 3.3.4.

Table 3.2 – Sequences.

Sequence ID	**Name**	**Peptide with abasic position (N'-C')**
1	DGL 122	xx-CACCATT*GT*_AC*ACT*CCA
		miRNA sequence (5'-3')
2	Target miRNA-122	UGGAGUGU**G**ACAAUGGUGUUUG

xx = amino-PEG-linker; "*" = propanoic acid side chain at the gamma position; "_" = abasic unit containing a propanoic acid side chain at the gamma position. The underlined sequence miRNA-122 is the region that hybridises with the DGL 122. The "G" in position 9 from 5' (in bold) is opposite to the abasic unit monomer and allows the specific incorporation of the aldehyde-modified biotinylated cytosine (Figure 3.1).

3.2.2 Design, synthesis and characterization of DGL 122

Probe design was done using the public database miRbase.org, where has-miR122-5p has the miRbase Accession Number MIMAT0000421 and considering the antiparallel hybridization necessary to clamp mature miRNA 122. Two amino-miniPEG spacers are included in the N-terminal, and some negatives charges are distributed across the backbone using proprietary monomers as these are needed when immobilised on solid supports. The abasic site has a L-Serine monomer at gamma (γ) position and the probe also has a C-terminal primary amide.

DGL probes synthesis was based on standard solid-phase peptide chemistry and was done in an INTAVIS AG robotic synthesiser. The sequences were purified using an Agilent 1260 Infinity Agilent HPLC and a Jupiter Proteo C12 semipreparative column in reverse phase mode. The molecular weight of these DGL probes were confirmed by MALDI-TOF using a UltrafleXtreme mass spectrometer (Bruker). Synthesis and characterization was done by the Chemistry department of DESTINA.

3.2.3 Collection and ALT analysis of clinical samples

Alanine transaminase (ALT) activity in clinical samples were analysed elsewhere, (141) using a commercial serum ALT kit (Alpha Laboratories Ltd., Eastleigh, UK) adapted for use on either a Cobas Fara or Cobas Mira analyser (Roche Diagnostics Ltd, Welwyn Garden City, UK). Adult patients (16 years old and over) were recruited if they fulfilled the study inclusion and exclusion criteria. (140) Full informed consent was obtained from every participant, and ethical approval was given by the South East Scotland Research Ethics Committee and the East of Scotland Research Ethics Committee, via the South East Scotland Human Bioresource. Blood samples were taken at first presentation to hospital and centrifuged immediately at 11,000 x g for 15 min at 4ºC. Then, serum was separated into aliquots and stored at -80 ºC. Just prior to analysis, serum aliquots were thawed at room temperature for approximately 30 minutes. The primary endpoint for the study was acute liver injury, pre-defined as a peak hospital stay serum ALT activity greater than 100U/L.

3.2.4 Magplex microspheres coupling with abasic probe

Five million of microspheres were suspended in MES Buffer (50 µL, 0.1 M, pH 5) in an eppendorf tube and added with (i) a solution with 200 pmoles of abasic probe (2 µL, 100 µM), (ii) EDC (2.5 µL, 10 mg/mL in de-ionised water). The solution was vortexed and incubated for 30 min at RT under shaking in darkness. 2.5 µL of a second EDC solution (10 mg/mL freshly prepared) was added, and incubated for further 30 min at

RT in darkness. Microspheres were washed once with 1 mL of 0.02% Tween 20 and once with 1 mL of 0.1% SDS. Following the microspheres were resuspended and incubated with 200 µL of Ethanolamine (50 mM) in 0.1% Tween 20 for 1h under vortexing at RT in darkness. Microspheres were washed once more time in 1 mL of 0.02% Tween 20 solution, and 1 mL of 0.1% SDS solution. Finally, microspheres were resuspended in 100 µL of PBS solution with 0.1% Tween20 and 10% PEG10K.

3.2.5 Assay reaction

A volume of 10 µL of test solution (either serum sample or calibrator) was mixed with 25 µL of Stabiltech buffer containing 1,250 microspheres DGL 122. This first step, to hybridise the miRNA-122, was performed in a 96-well plate using a microplate orbital shaker (VWR) at 700 rpm for 1 h at 40 °C. After the hybridization, microspheres DGL 122 were washed 3 times with the wash buffer. Microspheres DGL 122 were resuspended in 50 µL of reaction buffer containing 5 µM aldehyde-modified biotinylated cytosine and 1 mM sodium cyanoborohydride. The 96-well plate was shaken at 700 pm at 40 °C for 1 h. Microspheres were washed 3 further times and incubated with 70 µL of 2 µg/mL SA-PE for 5 min at 40 °C while being shaken at 700 rpm. Microspheres were then washed with the wash buffer and analysed on the Luminex MAGPIX system to determine the Mean of Fluorescence Intensity (MFI) values (Figure 3.2).

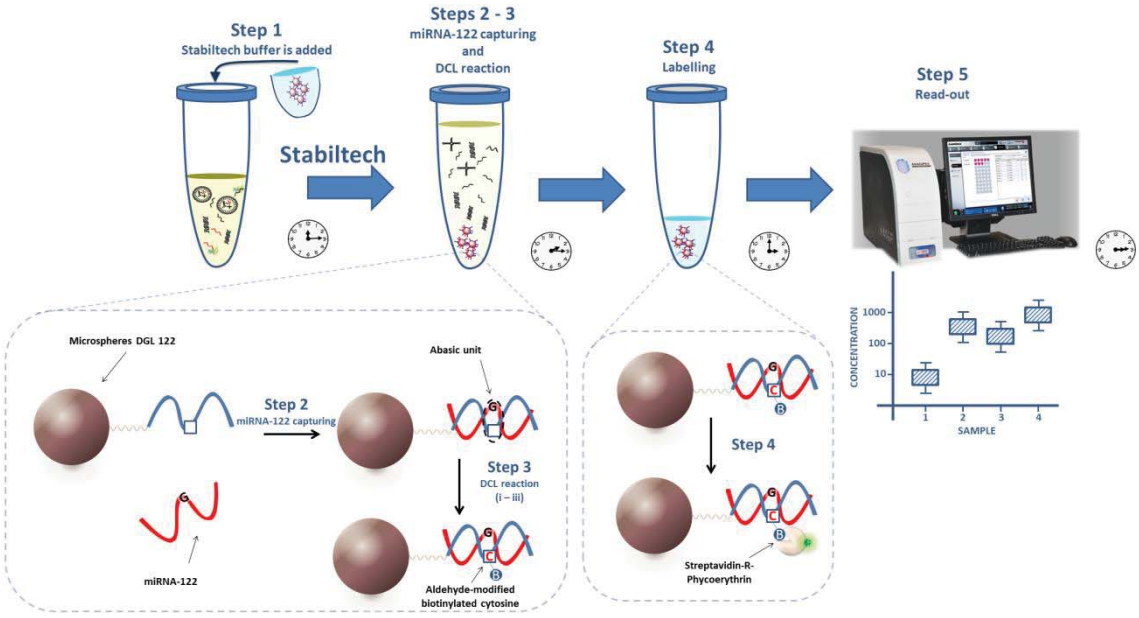

Figure 3.2 – Merging of dynamic chemical labelling assay with Luminex MAGPIX system. Fluorescence microspheres are read out by measuring the values of Median Fluorescence Intensity (MFI) – Phycoerythrin with λ excitation 488 nm and λ – emission 585 nm.

3.3. Results. DCL/ MAGPIX assay for the direct detection and quantification of miRNA-122

3.3.1 Assay sensitivity

The analytical sensitivity of the assay was determined by creating a calibration curve using known quantities of spike-ins (synthetic miRNA-122 oligomers) as follow: 40.5, 13.5, 4.5, 1.5 and 0.5 fmoles, in hybridization volumes of 35 µL, equal to 115.7, 38.6, 12.9, 4.3, and 1.4 pM respectively. Non spike-in was added as the negative control and experiments were performed in triplicate. The MFI values obtained for the five quantities of spike-ins were, respectively, 2763.3 ± 180.3 FI, 1154.8 ± 38.5 FI, 449.8 ± 16.5 FI, 181.0 ± 6.1 FI, 86.7 ± 2.5, and 32.0 ± 2.0 for the negative control (Table 3.3).

Table 3.3 – MFI measured by Luminex MAGPIX

Fmoles	MFI 1	MFI 2	MFI 3	Average MFI	SD	CV
40.5	2896.0	2836.0	2558.0	2763.3	180.3	6.53%
13.5	1168.0	1111.5	1185.0	1154.8	38.5	3.33%
4.5	433.0	450.5	466.0	449.9	16.5	3.67%
1.5	185.0	184.0	174.0	181.0	6.1	3.36%
0.5	89.0	84.0	87.0	86.7	2.5	2. 90%
Non spike-in	32.0	34.9	31.0	32.0	2.0	3.13%

Using the Formula 1 described below, the cut-off MFI value (describe as LoB in the formula) result in ±38.

The curves were obtained by plotting the MFI Average values versus the logarithm with the base of 10 of the quantity of spike-in(s) in fmoles, see Figure 3.3. The limit of detection (LoD) was determined according to the formula reported below [formula (1) and (2)]. It was calculated the Limit of Blank (LoB), formula (1) and it was substituted to the y value in the 4PL regression formula, formula 2. The resultant LoD was of ±11.1 amoles in a sample volume of 10 µL equal to ±1.11 pM (±6.68 x 10^5 molecules).

LoB=Average of blank+3 X SD of blank (1)

y= 〖c ((a+d)/(y-d)-1)〗 ^(1/b) (2)

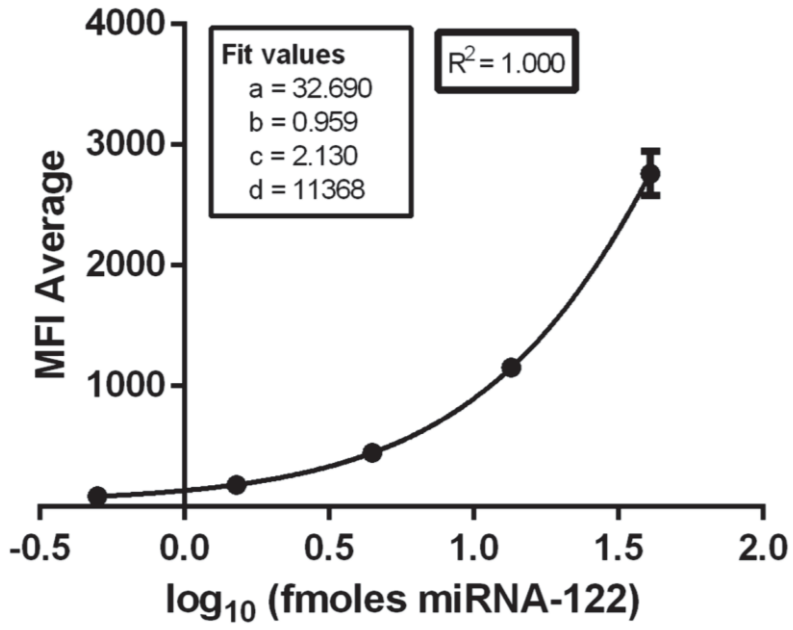

Figure 3.3 – Calibration curve. Using a 4PL non-lineal regression model, the MFI Average values plotted *vs.* the logarithm base of 10 of the quantity of synthetic miRNA-122 fmoles. Error bars (±1 s.d.) based on triplicate measurements; Fit values used for the LoD calculation represented. R^2 = 1.000. The error bars are smaller than the size of some data points. n=3.

3.3.2 Analysis of DILI patients

The assay was employed for profiling levels of miRNA-122 in nine serum samples of patients with DILI, and seven samples from healthy volunteers (as controls). For this study, the samples were treated as described in the section 3.3.5. The assay enabled us to profile levels of miRNA-122 in DILI patients (Table 3.4). As shown in Figure 3.4, most of the patients with DILI have increased levels of miRNA-122, while, and as expected, control healthy volunteers do not show significant levels of miRNA-122. The absolute miRNA-122 quantification was possible by extrapolating respective concentration levels (number of moles) from the calibration curve of Figure 3.3. Concentrations of miRNA-122 for all samples are reported in Table 3.5. Additionally, in Figure 3.5 was studied the correlation between levels of miRNA-122 and ALT for the nine DILI patients. When both molecules were compared by receiver operating characteristic (ROC), area under the curve (AUC) value was very high (0.94). This indicated that both tests were able to distinguish between negative and positive serum samples using ROC analysis (Figure 3.6), demonstrating the high accuracy of miRNA-122.

Table 3.4 – MFI measured for each sample

Sample code	MIF 1	MIF 2	MIF 3	Average MFI	SD	CV
Patient 1	90.0	94.5	95.0	93.2	2.7	2.96%
Patient 2	201.0	206.0	205.0	204.0	2.6	1.30%
Patient 3	41.0	41.0	40.0	40.6	0.6	1.42%
Patient 4	51.0	47.0	50.0	49.3	2.1	4.22%
Patient 5	855.5	876.0	789.5	840.3	45.2	5.38%
Patient 6	219.0	207.0	215.0	213.7	6.11	2.86%
Patient 7	206.0	197.0	203.0	202.0	4.6	2.27%
Patient 8	1169.0	1072.0	1112.0	1117.7	48.7	4.36%
Patient 9	755.0	730.0	713.5	732.3	20.9	2.85%
Control 1	32.0	31.0	32.0	31.7	0.6	1.82%
Control 2	32.0	34.0	34.0	33.3	1.2	3.46%
Control 3	35.0	33.0	34.0	34.0	1.0	2.94%
Control 4	33.0	33.0	33.0	33.0	0.0	0.00%
Control 5	34.0	33.0	32.0	33.0	1.0	3.03%
Control 6	29.0	28.0	30.0	29.0	1.0	2.35%
Control 7	32.0	32.0	33.0	32.3	0.6	1.79%

Control = Healthy volunteer

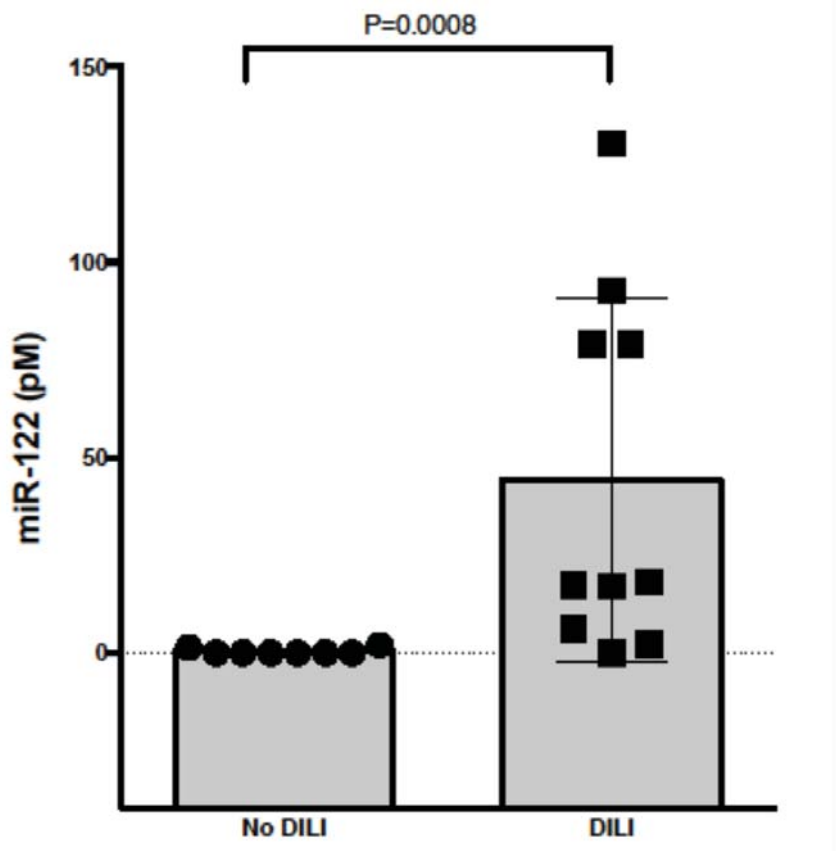

Figure 3.4 – Levels of miRNA-122 in DILI and No DILI patients. Those with liver injury after paracetamol overdose (ALT>100 – predefined in protocol of trial) and those without liver injury. Note: The samples analysed were from first presentation to hospital whereas the diagnosis of DILI was subsequent to first presentation. P calculated by Mann-Whitney. Bar = mean, error bars are SD

Table 3. 5 – miRNA-122 quantities corresponding to the average of MFI values.

Sample code	Average MFI	Sample fmoles	Sample concentration (pM)
Patient 1	93.2 ± 2.7	2.14	6.11
Patient 2	204.0 ± 2.6	6.08	17.38
Patient 3	40.6 ± 0.6	0.47	1.35
Patient 4	49.3 ± 2.1	0.74	2.11
Patient 5	840.3 ± 45.2	32.44	92.68
Patient 6	213.7 ± 6.11	6.43	18.37
Patient 7	202.0 ± 4.6	6.03	17.22
Patient 8	1117.7 ± 48.7	45.61	130.32
Patient 9	732.3 ± 20.9	27.67	79.07

Control 1	31.7 ± 0.6	n.d.	n.d.
Control 2	33.3 ± 1.2	n.d.	n.d.
Control 3	34.0 ± 1.0	n.d.	n.d.
Control 4	33.0 ± 0.0	n.d.	n.d.
Control 5	33.0 ± 1.0	n.d.	n.d.
Control 6	29.0 ± 1.0	n.d.	n.d.
Control 7	32.3 ± 0.6	n.d.	n.d.

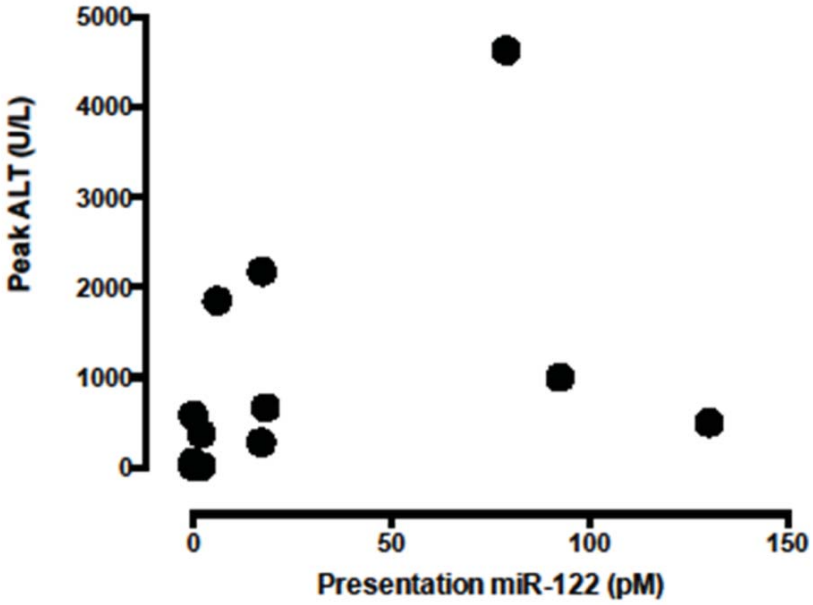

Figure 3.5 – Plot of first presentation to hospital miRNA-122 against peak ALT. Spearman r = 0.71 (95% CI 0.34 to 0.89). P = 0.001.

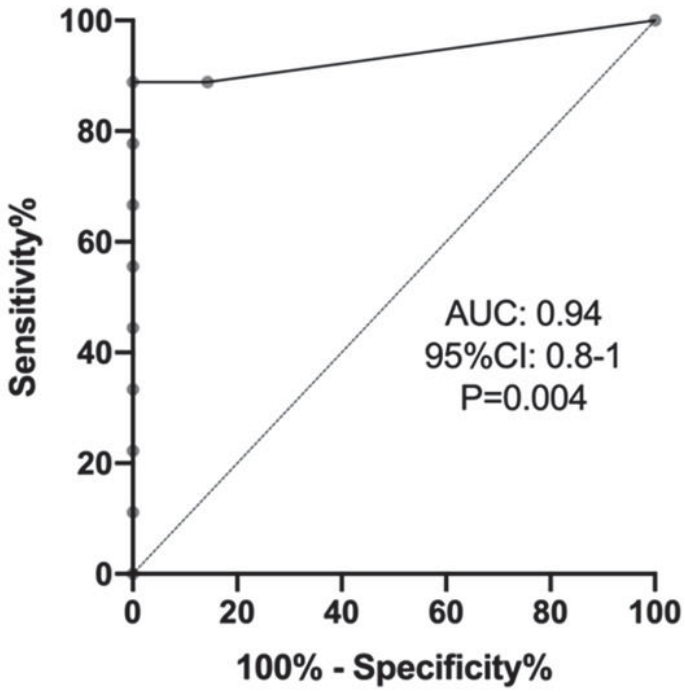

Figure 3.6 – ROC curves of miRNA-122 and ALT. The AUC was 0.94 (95% CI 0.8 – 1). ROC, receiver operating curve; ALT, alanine aminotransferase; AUC, area under the curve

3.4. Discussion

Current assays for the diagnosis of DILI are essentially based on exclusion methods that require quantification of several circulating proteins, some of them non-specific, lengthening the time until physicians can complete a diagnosis. In this chapter, we report a unique assay that allows the detection and quantification of the liver specific miRNA-122, a liver biomarker found to be substantially elevated in the serum of patients with DILI. The assay presented here is based on the integration of the above described DCL method with Luminex MAGPIX system. Used in combination, the new assay enables profiling of miRNA-122 with high specificity. The assay includes the unique Stabiltech buffer that allows liberation and stabilisation of miRNA-122 in serum samples with advantage of sample preparation, shipment and storage through to analysis at room temperatures. (88) As described elsewhere, (88) the stabilization of miRNA-122 is achieved through its hybridization with the DGL 122 capture microspheres, forming a high stability complex. The formation of this double-stranded complex between the target RNA and DGL probe protects the miRNA-122 molecules from enzymatic degradation, and thus its protection and stabilization. This novel assay overcomes the various limitations of current methods for analysing miRNAs, such as: (a) the challenges associated with the pre-extraction of RNAs and; (b) the problems related to both reverse transcription and amplification of miRNAs.

In the current study, the assay has been validated using spike-ins into serum samples, reaching a LoD of ±11.1 amoles (±1.11 pM in 10 µL of sample), a LoD sufficient to interrogate levels of miRNA-122 in clinical samples for patients with DILI. DILI serum samples from patients recruited at the Royal Infirmary of Edinburgh were tested using the new assay. MiRNA-122 was detected in all samples, as shown in Figure 3.5, with concentrations ranging from 1.3 to 130.3 pM. MiRNA-122 was non-detected (n.d.) in the healthy volunteers. The assay was also compared with the ALT test, as shown in Figure 3.6.

In conclusion, the assay was successfully used for an accurate, direct quantification of miRNA-122 in serum samples of DILI patients. It was free of errors in distinguishing DILI patients *vs.* healthy volunteers. The study was carried out in parallel and compared with the gold standard ALT test. With these features and results in mind, we propose this assay can be reliably used for direct detection and quantification of miRNA-122 in DILI patients. This new method could also be used to detect other circulating miRNA biomarkers of research and clinical importance, using the multiplex assay capability of the Luminex MAGPIX system.

3.5. Conclusions

1. The development of an assay that allows the direct detection and quantification of the liver specific miRNA-122 biomarker, using DCL in combination with Luminex MAGPIX system, has been successfully accomplished.
2. The assay includes the Stabiltech buffer developed by DESTINA that allows liberation and stabilisation of miRNA-122 in serum samples This offers several advantages if compare with other lysis buffers, as sample preparations, shipments and storage can now be performed at room temperatures.
3. This novel assay offer the same advantages than the one presented in Chapter 2 when compared to RT-qPCR gold standard assays.
4. The assay presents an analytical LoD of 11.1 amoles (1.11 pM in 10 µL of sample). This LoD allows identifying patients with acute DILI by measuring their levels of miRNA-122 in circulation.
5. DILI serum samples from patients recruited at the Royal Infirmary of Edinburgh were tested using the new assay, and miRNA-122 was detected in all samples with concentrations ranging from 1.3 to 130.3 pM.
6. miR-122 was non-detected (n.d.) in the healthy volunteers, therefore the assay was free of errors in distinguishing DILI patients *vs.* healthy volunteers.

7. The assay was also compared with the ALT test, reaching an optimal AUC value of 0.95.

Chapter 4:

Simultaneous Detection of Drug-Induced Liver Injury Protein and microRNA biomarkers using dynamic chemical

labelling on a Luminex MAGPIX system

Chapter 4: Simultaneous Detection of a DILI related microRNA and Protein using Dynamic Chemical Labelling on Luminex MAGPIX

4.1 Introduction

As described in the previous chapter, DILI is a potentially fatal adverse event to prescription drug intake, and a leading cause for pre and post-market drug withdrawal. Several international initiatives such as the Safer and Faster Evidence-based Translation (SAFE-T) consortium or, more recently, TransBioLine and the Pro-Euro DILI NETWORK have been seeking and validating DILI biomarkers as means to better diagnose DILI. (171, 172) A recent letter of support from the EMA (30) established that the lack of sensitive and specific assays to diagnose, predict and monitor idiosyncratic DILI remains a severe hurdle in drug development. All the scientific evidence points out that an innovative combination of biomarkers combining proteins and miRNAs would probably be optimal to clearly identify DILI, predict the course of the liver injury, and may help in assigning causality.

To the best of our knowledge, the combination of related protein and miRNA DILI biomarkers into a single assay has not been achieved. With the advances made by our team with dynamic chemical labelling (DCL) technology for the direct detection of miRNAs, the deliverable of a combo-multiplexed assay is now possible. The DCL approach for nucleic acid testing is particularly well suited to directly analyse miRNAs in biological fluids. (85-88, 95, 139, 173) As reported in the previous chapter, the technology delivers consistent and reliable quantitative readings of miRNA-122 in human samples when used with the Luminex MAGPIX system. (95) By removing multiple steps in the workflow, especially extraction/isolation steps, DCL enables the direct detection of miR-122 in enzyme-linked immunosorbent assay (ELISA) type format, overcoming the current limitation issue that inhibits development of simultaneous detection of protein and miRNA DILI biomarkers, with high specificity and accuracy, on the same machine.

The Luminex MAGPIX system provides an analytical tool capable of efficient multiple biomarker detection. This concept of “multiplexing”, or reading multiple test results in a single sample volume, has revolutionized diagnostic opportunities. (174) Parallel measurement of different biomarkers from a single sample allows more data from the same volume, reduction of processing time per assay, and consumables. It is a more a

more cost effective technique, and improve accuracy of data analysis. Currently, the Luminex MAGPIX system has multiplex assays for diagnosing numerous diseases, (175, 176) including the current global issue with the COVID-19 pandemic. (177) All of the multiplex-panel assays are multi-marker panels based on the detection of multiple molecules of the same nature, namely multiplex of proteins or multiplex of nucleic acids. However, the possibility to move closer both proteomic and genomic fields into a single platform having the capacity to interrogate these two class of molecules is unimaginable to date.

In this chapter, the DCL method was combined with the Luminex MAGPIX system to deliver a unique simultaneous detection of DILI related protein and miRNA with high sensitivity and specificity. This multiplex system, that has been named "seqCOMBO", was applied to profile levels of liver-type arginase 1 (ARG1) and miR-122 in serum samples from a DILI patient. Serum samples from no DILI patient were use as the negative control. ARG1 is a highly abundant protein found in liver cytosol, used to improve the sensitivity of ALT to detect liver injury. (178, 179) Among all protein biomarkers, ARG1 was used for this PoC since it is part of the MILIPLEX MAP Human Liver Injury Magnetic Bead Panel.

4.2. Materials and methods. SeqCOMBO assay to detect simultaneously protein and miRNA from a single sample

4.2.1 Materials

MILLIPLEX MAP reagents for analysing ARG1 were purchased from Merck (MILIPLEX MAP Human Liver Injury Magnetic Bead Panel – Toxicity Multiplex Assay, Cat # HLINJMAG-75K) and were used as received. The MILIPLEX MAP kit includes Anti-ARG1 Beads with colour region 26, (169) assay buffer and detection antibody. Luminex MagPlex® carboxylated beads from colour region 12 were purchased from Luminex Corporation (1.25 x 10^7/mL).

The DGL 122 abasic PNA probe (Table 3.2), SMART-C Biotin (Figure 3.1) and buffers (including the Stabiltech buffer) for interrogating miRNA-122 were provided by DESTINA Genomica S.L. (see section 3.3.1). Luminex MagPlex microspheres from colour region 12 (169) were functionalised with DGL 122 abasic PNA, using the protocol optimised by DESTINA Genomica S.L. (see 3.3.2), to generate the DGL-122 Beads. Synthetic mimic miRNA-122 oligomer was purchased from Integrated DNA Technologies (Table 3.2). Concentrations of DNA solutions were determined using a

ThermoFisher NanoDrop1000 Spectrophotometer. Streptavidin-R-Phycoerythrin (SA-PE, 1mg/mL) was purchased from Moss Biotech Inc. Chemicals for microspheres coupling were purchased from Sigma-Aldrich.

4.2.2 Design, synthesis and characterization of DGL 122

See section 3.3.2

4.2.3 Clinical samples

For DILI serum information see Section 3.3.3. No DILI patient was human serum from male AB clotted whole blood and was purchased from Sigma Aldrich, Cat. No. H6914-20ML.

4.2.4 ARG1 singleplex assay

A volume of 10 µL of serum sample was mixed with 25 µL of assay buffer and 7.5 µL of Anti-ARG1 Beads 1:6 diluted from the stock. This first step, to capture the ARG1, was performed in a 96-well plate (Cat. # 249570, from Thermo Fisher) using a microplate orbital shaker (VWR Micro Plate Shaker, Cat. # 12620-926) at 700 rpm for 2 h at 25 °C. After the capturing of ARG1, Anti-ARG1 Beads were washed 3 times with the wash buffer. Anti-ARG1 Beads were resuspended in 50 µL of detection antibody diluted 1:2 with assay buffer. The 96-well plate was shaken at 700 pm at 25 °C for 1 h. Beads were washed 3 further times and incubated with 70 µL of 2 µg/mL SA-PE for 5 min at 40 °C while being shaken at 700 rpm. Beads were then washed two times with the wash buffer and analysed on the Luminex MAGPIX system to determine the Mean of Fluorescence Intensity (MFI) values.

4.2.5 MiR-122 singleplex assay

A volume of 10 µL of serum sample was mixed with 30 µL of assay buffer and 80 µL of Stabiltech buffer containing DGL-122 Beads functionalized with DGL 122. This first step, to hybridise the miR-122, was performed in a 96-well plate using a microplate orbital shaker at 700 rpm for 1 h at 40 °C. After the hybridization, DGL-122 Beads were washed 3 times with the wash buffer. DGL-122 Beads were resuspended in 50 µL of assay buffer containing 5 µM SMART-C Biotin and 1 mM sodium cyanoborohydride. The 96-well plate was shaken at 700 pm at 40 °C for 1 h. Beads were washed 3 further times and incubated with 70 µL of 2 µg/mL SA-PE for 5 min at 40 °C while being shaken at 700 rpm. Beads were then washed two times with the wash buffer and analysed on the Luminex MAGPIX system to determine the MFI values.

4.2.6 SeqCOMBO assay

A volume of 10 µL of serum sample was mixed with 25 µL of assay buffer and 7.5 µL of Anti-ARG1 Beads 1:6 diluted from the stock. This first step allows capturing the ARG1 and was performed in a 96-well plate using a microplate orbital shaker at 700 rpm for 2 h at 25 °C. After the capturing, the supernatant was removed and kept for the subsequent miR-122 hybridization. Anti-ARG1 Beads pellet was washed 3 times with the wash buffer, resuspended in 100 µL of assay buffer and reserved at 4 ºC. The supernatant containing the miR-122 was treated by adding 80 µL of Stabiltech buffer containing 1,250 DGL-122 Beads. The hybridization of the miR-122 is performed at 700 rpm for 1 h at 40 °C. After the hybridization, DGL-122 Beads were washed 3 times with the wash buffer. DGL-122 Beads were resuspended in 100 µL of wash buffer and merged with the reserved 100 µL solution containing the Anti-ARG1 Beads. Once both set of beads were mixed, the supernatant was removed and the beads were resuspended in 25 µL of detection antibody and 25 µL of assay buffer containing 5 µM of SMART-C Biotin and 1 mM sodium cyanoborohydride. The 96-well plate was shaken at 700 rpm at 40 °C for 1 h. Beads were washed 3 times and incubated with 70 µL of 2 µg/mL SA-PE for 5 min at 40 °C while being shaken at 700 rpm. Beads were then washed two times with the wash buffer and analysed on the Luminex MAGPIX system to determine the MFI values.

4.3. Results. Singleplex and seqCOMBO to simultaneously direct detect ARG1 and miRNA-122 in clinical samples

4.3.1 Singleplex analysis of ARG1 and miR-122 on Luminex MAGPIX system

DILI and no DILI patient samples were tested individually to analyse ARG1 and miR-122 levels. The individual analysis was carried out by the workflows illustrated in Figure 1. The MILLIPLEX assay for the detection of ARG1 and the DCL method for miR-122 require, respectively, 3 hours 15 minutes and 2 hours 15 minutes. Both workflows, described in Figure 4.1, consist of 5 main steps.

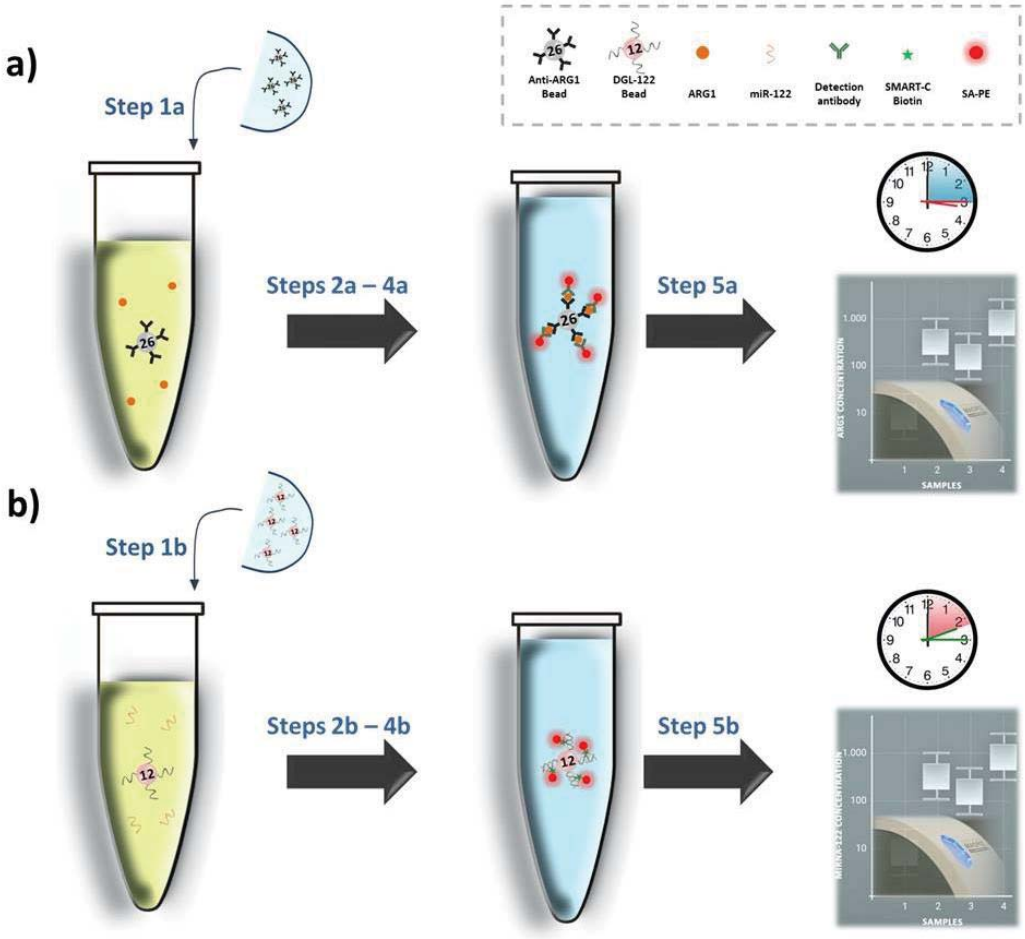

Figure 4.1 – Singleplex workflows. a) Analysis of ARG1: Step 1a – Anti-ARG1 Beads are added to the sample; Step 2a – Anti-ARG1 Bead captures ARG1; Step 3a – Detection antibody is added, recognizing the captured ARG1; Step 4a – Bead is labelled using SA-PE; Step 5a – Bead is read-out by measuring the values of MFI into the Luminex MAGPIX system. **b)** Analysis of miR-122: Step 1b – DGL-122 Beads are added to the sample; Step 2b – DGL-122 Bead hybridises miR-122; Step 3b – DCL reagents are added into the solution to incorporate the SMART-C Biotin; Step 4b – Bead is labelled using SA-PE; Step 5b – Bead is read-out by measuring the values of MFI into the Luminex MAGPIX system. Phycoerythrin with λ¬ excitation 488 nm and λ¬ emission 585 nm.

The two assays enabled us to profile levels of ARG1 and miR-122 in a DILI patient. As reported in Table 4.1, the patient with DILI presented high levels of both ARG1 and miR-122, while, and as expected, the no DILI patient has not shown significant levels of either ARG1 or miR-122.

Table 4.1 - – MFI measurement (in duplicate) of ARG1 and miR-122 in singleplex analysis and seqCOMBO. Levels of ARG1 and miR-122 correspond to a proportional MFI signal.

Assay	Sample	Analyte	MFI 1	MFI 2	Average MFI	SD	CV
ARG1 singleplex	**DILI**	ARG1	3257.0	3424.5	3340.5	118.9	3.54%
	No DILI		31.0	31.0	31.0	0.0	0.00%
miR-122 singleplex	**DILI**	miR-122	1440.0	1315.5	1376.8	89.5	6.50%
	No DILI		26.0	26.0	26.0	0.0	0.00%
seqCOMBO	**DILI**	ARG1	3374	3138	3256.0	166.9	5.13%
		miR-122	1328	1545	1436.5	153.4	10.7%
	No DILI	ARG1	53	52	52.5	0.7	1.35%
		miR-122	44	41	42.5	2.12	4.99%

4.3.2 SeqCOMBO assay on Luminex MAGPIX system

The two individual assays described in Figure 4.1a and 4.1b, were combined delivering the seqCOMBO to profile at the same time the levels of ARG1 and miR-122 in serum sample of a DILI patient. As shown in Figure 4.2, the seqCOMBO workflow consists in 9 main steps.

The seqCOMBO enables profiling levels of ARG1 and miR-122 in DILI patient. As reported in Table 4.1 and shown in Figure 4.3, the patient with DILI presented high levels of both ARG1 and miR-122, while, and as expected, the no DILI control has not shown significant levels of ARG1 or miR-122. No signal loss was observed when both protein and miRNA were analysed via seqCOMBO at the same time. To compare how the signal variability when singleplex or seqCOMBO is used, an inter-CV study was generated, comparing the MFI signals obtained for individual analysis vs. seqCOMBO, as shown in Table 4.2. These results indicate that the MILLIPLEX xMAP kit can be merged with the DCL method to analyse simultaneously ARG1 and miR-122 from the same sample, hence demonstrating that analysis of proteins and nucleic acids can be performed without differences if compared with individual tests.

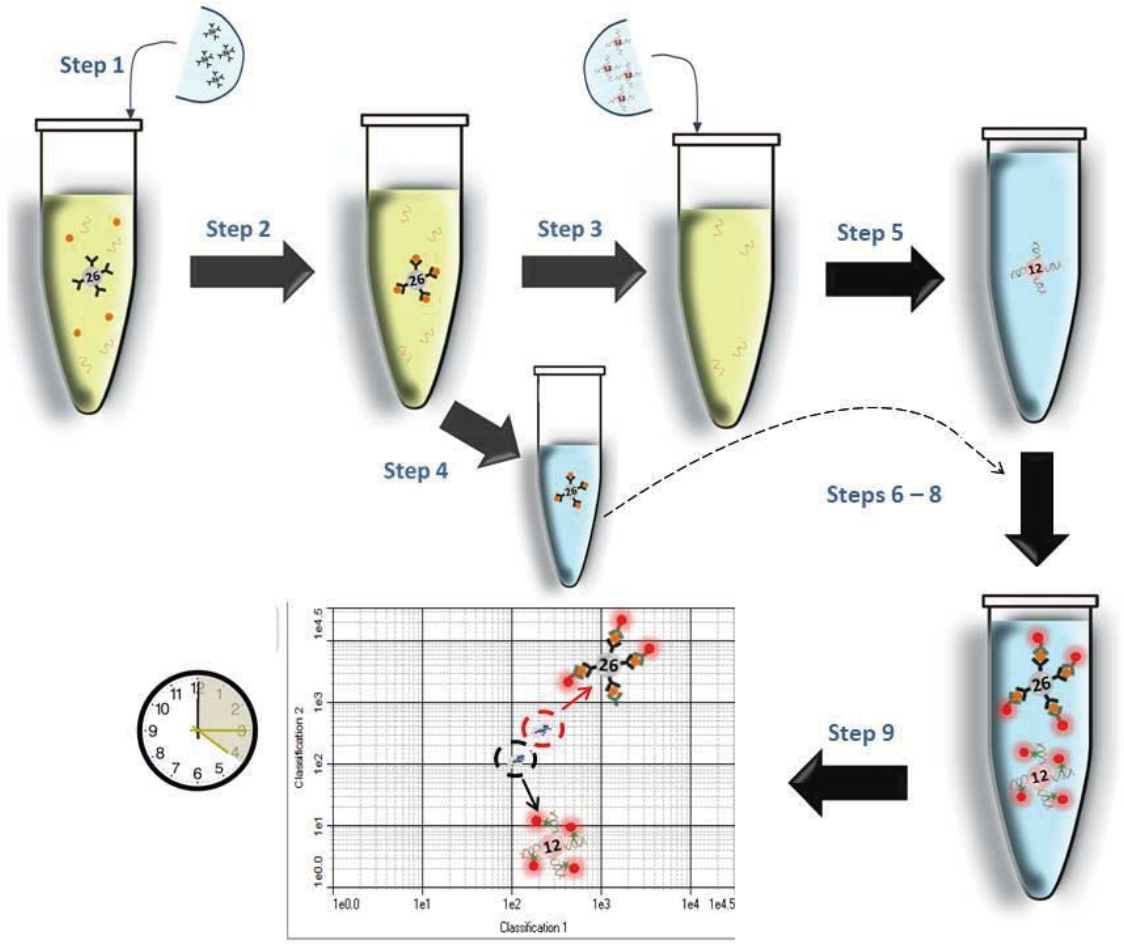

Figure 4. 2 – SeqCOMBO workflow. Step 1 – Anti-ARG1 Beads are added to the serum sample; Step 2 – Anti-ARG1 Bead capture the ARG1; Step 3 – Anti-ARG1 Beads are separated and reserved assay buffer; Step 4 – The supernatant is added with Stabiltech buffer containing the DGL-122 Beads; Step 5 – DGL-122 Bead hybridizes to the miR-122; Step 6 – Both sets of beads are merged; Step 7 – The detection antibody along with SMART-C Biotin are added to the mixture of Anti-ARG1 and DGL-122 Beads; Step 8 – Beads are labelled with SA-PE; Step 9 – Read-out of the two regions with MAGPIX instrument. Phycoerythrin with λ¬ excitation 488 nm and λ¬ emission 585 nm.

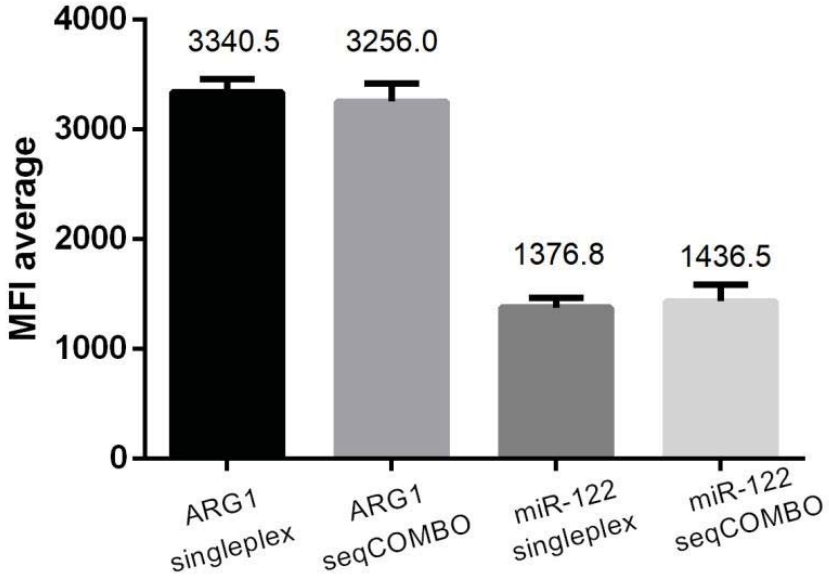

Figure 4.3 – Levels of ARG1 and miR-122 in DILI patient when measured via singleplex and seqCOMBO assays. n = 2

Table 4.2 – Inter-CV comparative analysis for singleplex vs. seqCOMBO

	Singleplex ARG1 MFI Average	Singleplex miR-122 MFI Average	seqCOMBO ARG1 MFI Average	seqCOMBMO miR-122 MFI Average	Average	SD	CV
ARG1	3340.5	----	3256.0	----	3298.0	59.8	1.81%
miR-122	----	1376.8	----	1436.5	1406.3	42.2	3.00%

4.4 Discussion

To date, it has not been possible to analyse protein and nucleic acid biomarkers of clinical relevance into a single assay on the same analytical platform. This is due to the technical peculiarities of handling RNA including: a) miRNA instability and degradation; b) RNA has until now required extraction, introducing variability and loss of target. Our team has transformed the way to interrogate miRNAs using its DCL technology (21-24, 31-34, 39-41). DCL enables direct detection of miRNAs in an ELISA type format, addressing current limitations that have inhibited until now the development of a combo assay (34).

In this study, we present the seqCOMBO, a first Luminex assay that enables, from a single sample, the profiling in a sequential manner proteins and miRNAs

simultaneously. In this manuscript, seqCOMBO was used to determine the levels of DILI related biomarkers. SeqCOMBO was validated using clinical samples from a patient with liver injury, successfully determining the levels of ARG1 and miR-122. When MFI values between both singleplex and seqCOMBO were compared, no signal differences are observed, demonstrating thus the high compatibility of the MILLIPLEX MAP kit with DCL reagents.

To the best of our knowledge, this is the first work that demonstrates profiling at the same time both protein and miRNA biomarkers for diagnosing DILI in a single step assay. The PoC is a first step towards the implementation of the present technology for the detection of other protein/miRNA signatures of predictive value, in pathologies such as cancer, or in evaluating drug-induced injuries affecting other organs (kidney, heart, lung, etc.). SeqCOMBO shows the way forward to simplified, more cost effective and robust multiplex tests in the future, with optimized protein/RNA biomarker combinations.

4.5. Conclusions

1. The developed seqCOMBO assay that enables, from a single sample, the quantification of proteins and miRNAs simultaneously. So far, this has not been possible due to the technical peculiarities of handling of proteins and miRNAs simultaneously. In order to achieve this, DCL reagents and MILLIPLEX MAP kits were combined to detect miRNA-122 and ARG1, respectively
2. SeqCOMBO was used to determine the levels of DILI related biomarkers using clinical samples from a patient with liver injury. In this way the levels of ARG1 and miR-122 were successfully determined.
3. When values of each biomarker using both singleplex and seqCOMBO assays were compared, no signal differences were observed, demonstrating thus the high compatibility of the MILLIPLEX MAP kit with DCL reagents.
4. The PoC is a first step towards the implementation of the present technology for the detection of other protein/miRNA signatures of predictive value in pathologies such as cancer and in evaluating drug-induced injuries affecting other organs (kidney, heart, lung, etc.).
5. SeqCOMBO shows the way forward to simplified, more cost effective and robust multiplex tests in the future, with optimized protein/RNA biomarker combinations.

Chapter 5:
Conclusions / Conclusiones

Chapter 5: Conclusions / Conclusiones

Conclusions

1. DCL assays have been developed for micro-plate reader and Luminex platforms. It has been demonstrated that these assays offer general advantages if compared to standard RT-qPCR.
2. These assays have allowed us to quantify miR-451a, which is related with erythropoiesis, miR-122 a liver-specific biomarker and a simultaneous analysis of ARG1 and miR-122 for liver diseases.
3. Reagents and protocols have been developed to use commercial reading platforms. This has allowed DESTINA to develop the first RUO kit named LiverAce for the detection of miR-122. Currently, the company is in the process of raising funds to develop the IVD LiverAce assay.
4. In this thesis, the use of DCL chemistry with different platforms has demonstrated its versatility and its adaptation to the sensitivity of the reading platform. Therefore, it can be said that DCL chemistry to quantify nucleic acid is as sensitive as the platform used.
5. The ultimate compatibility test is the development of the seqCOMBO assay. DCL reagents are fully compatible with standard immunoassays reagents used to detect protein, hence being able to develop a first simultaneous quantification of both a protein and a nucleic acid using the same sample. This open a range of business opportunities as these new assays will increase both the clinical specificity and sensitivity.
6. This thesis also shows how the industrial R&D work performed in industrial settings can be efficiently integrated with PhD programs offered by high academic institutions to produce shared know-how, scientific manuscripts and commercial products. The co-supervision of academic and industrial managers offers an opportunity to bring together both worlds.

Conclusiones

1. La química DCL se ha desarrollado tanto para un lector de placas convencional como para la plataforma de Luminex. Se ha demostrado que estos ensayos ofrecen ventajas generales en comparación con el estándar RT-qPCR.
2. Estos ensayos nos han permitido cuantificar miR-451a, que está relacionado con la eritropoyesis, miR-122 un biomarcador específico del hígado y un análisis simultáneo de ARG1 y miR-122 para enfermedades hepáticas.
3. Se han desarrollado reactivos y protocolos para utilizar plataformas de lectura comerciales. Esto ha permitido a DESTINA desarrollar el primer kit RUO llamado LiverAce para la detección de miR-122. Actualmente, la compañía está en proceso de recaudar fondos para desarrollar el ensayo IVD LiverAce.
4. En esta tesis, el uso de la química DCL con diferentes plataformas ha demostrado su versatilidad y su adaptabilidad a la sensibilidad de la plataforma de lectura. Por tanto, se puede decir que la química de DCL para cuantificar el ácido nucleico es tan sensible como la plataforma utilizada permita.
5. La prueba de compatibilidad definitiva es el desarrollo del ensayo seqCOMBO. Los reactivos DCL son totalmente compatibles con los reactivos de inmunoensayos estándar utilizados para detectar proteínas, por lo que por primera vez es posible la cuantificación simultánea de una proteína y un ácido nucleico utilizando la misma muestra. Esto abre una gama de oportunidades comerciales, ya que estos nuevos ensayos aumentarán tanto la especificidad clínica como la sensibilidad.
6. Esta tesis también muestra cómo el trabajo de I + D industrial realizado en entornos industriales puede integrarse de manera eficiente con los programas de doctorado ofrecidos por instituciones académicas de alto nivel para producir conocimientos técnicos compartidos, manuscritos científicos y productos comerciales. La co-supervisión de directores académicos e industriales ofrece una oportunidad para unir ambos mundos.

Chapter 6:
Industrial Impact

Chapter 6: Industrial Impact

6.1 Market type

The molecular diagnostic market can be divided into two, IVD and R&D market. Although the R&D molecular diagnostics market is a mature and fully developed one, no manufacturer has yet commercialized a regulatory cleared/approved miRNA-based diagnostic IVD kit being reimbursement by payers. The research program developed during this PhD aims to bring to Research Use Only (RUO) products to the market while also giving the first steps to produce IVD assays. Therefore, the DCL method in combination with different platforms will be sold as the first miRNA-based IVD test, a spin-off branch of the much bigger and well-established molecular diagnostics market.

6.2 Market size

The molecular diagnostics market is the fastest-growing segment of the overall clinical diagnostics market and is currently estimated to have a annual value of €8.5 B market (2019 growing to €12.5 B by 2024 with a CAGR of 8.6%). The two largest parts of the molecular diagnostics market are Infectious disease followed by cancer and have largely targeted DNA or RNA in the case of viral diagnostics. The tremendous interest and investigation in RNA as biomarkers for cancer and other syndromes is driving a need for improved test methodologies that enable reliable, routine clinical use of these biomarkers. Moreover, the approval in 2018 of Onpattro, “the first first-of-its kind targeted RNA-based therapy to treat a rare disease” [https://www.accessdata.fda.gov/drugsatfda_docs/nda/2018/210922Orig1s000TOC.cfm1] plus the development of mRNA-based vaccines for COVID19 by Moderna and Pfizer have tremendously increased the interest of pharmaceutical companies in using efficient methodologies to quantify RNA molecules.

The global miRNA market is currently a niche segment (12%) of the molecular diagnostic market, its expansion limited until now by inadequate detection tools. The global market for miRNA focused tools, services is estimated today as €1.02B, with most of it in the research, and drug discovery markets, other than a few laboratory-developed tests. Although there are currently no clinically approved kits for miRNA IVD tests, this market is expected to grow very significantly over the next 5 years. The growth will be driven by (a) The incorporation of hundreds of potential biomarkers into more routine clinical diagnostic assays once the tools to detect them such as the DCL technology is used more widely. (b) Liquid biopsies coming into mainstream use not

only for diagnosis but also for patient monitoring post clinical intervention. (c) The new clinical diagnostic test will also drive the fastest market growth in dollar terms, given their higher value/test delivered compared to research and pharmaceutical uses.

6.3 DCL and FLUOStar OMEGA, a platform to offer service to the new founded veterinary company VETSINA Animal Diagnostic – Chapter 2

VETSINA is a new company formed by DESTINA Genomics and Roslin Technologies to develop innovative diagnostics for animal health and veterinary use.

The new tests, based on the DCL method, can directly detect tissue- and disease-specific RNA and miRNA biomarkers in biological fluids. VETSINA will also have access under its exclusive licence to DESTINA's proprietary stabilisation buffer system, Stabiltech used in this Thesis.

VETSINA develop these new assays to form the basis of a new animal health diagnostic testing portfolio. The first assay, the miR-122 assay will be launched for reference laboratory use, and it is based on the work presented in Chapter 2 The development of the DCL ELISA platform, discussed in the Chapter 2 of the present doctoral thesis, bring to VETSINA the opportunity to count with a sensitive enough platform to interrogate animal serum/plasma samples for the diagnostic of veterinary diseases in a cost-effective way. Currently, the first one hundred dog samples are being tested to identify dogs with liver conditions

6.4 LiverAce: The miR-122 Assay – Towards the first IVD Assay of DESTINA – Chapter 3

miRNA-122 has shown to be an excellent candidate to detect early acute DILI patients. The DCL assay developed by DESTINA tick all the boxes required to bring it to clinical use. To do so, DESTINA needed to use a reading platform which was IVD approved. Looking at the available platforms, Luminex MAGPIX seems the most appropriated. Therefore, the work presented in Chapter 3 is being used by DESTINA to raise funds to develop the first IVD assay of the company. A total amount of €1.5m has been calculated as the cost to obtain the CE-IVD mark by the European Medical Agency (EMA). The company has used part of the data presented here to apply to the European Commission within its EIC Accelerator Project to obtain 60% of that amount

while the rest will be provided by DESTINA own resources. DESTINA is also looking at the private marker to raise these funds.

6.4 The COMBO Assay – European Consortium to improve RUCAM Screenings - Chapter 4

There is a clear opportunity for a reliable alternative to RUCAM screening if this alternative avoids the drawbacks mentioned in Table 3.1. Such an alternative approach must be trustworthy while addressing both the technical and financial aspects of the customer's pains. This approach must be fast and straightforward, helping physicians to reach the conclusion of requesting drug plasma concentrations swiftly (the critical quantitative study). Therefore, alternative technologies able to overcome customer pains have the potential not only to achieve a substantial market share but also to become the new standard of DILI initial diagnostic in hospitals.

As mentioned in Chapter 4, several multinational DILI initiatives have now suggested a panel of miRNA and protein biomarkers as the optimal combination for an assay to early detect liver injury, inform about mechanisms of liver injury and help in assigning causality. To overcome these limitations, it has been proposed the LiverAce solution by combining Luminex analytical platform, direct miRNA detection technology through DCL, protein multiplexing and clinical data analysis, as previously described in Chapters 3 and 4. This proposal has reach to get an Eurostar Application’s fundraising, in collaboration with prestigious European partners.

In Summary, this PhD has been aligned to the commercial interest of DESTINA to develop assays which are needed in the molecular market place.

Chapter 7:
Bibliography

Chapter 7: Bibliography

1. Ginsburg GS, McCarthy JJ. Personalized medicine: revolutionizing drug discovery and patient care. Trends Biotechnol. 2001;19(12):491-6.
2. Vogenberg FR, Isaacson Barash C, Pursel M. Personalized medicine: part 1: evolution and development into theranostics. P T. 2010;35(10):560-76.
3. Zenner HP. Individual Biomarkers Using Molecular Personalized Medicine Approaches. ORL J Otorhinolaryngol Relat Spec. 2017;79(1-2):7-13.
4. Salter H, Holland R. Biomarkers: refining diagnosis and expediting drug development - reality, aspiration and the role of open innovation. J Intern Med. 2014;276(3):215-28.
5. Strimbu K, Tavel JA. What are biomarkers? Curr Opin HIV AIDS. 2010;5(6):463-6.
6. Offit K. Personalized medicine: new genomics, old lessons. Hum Genet. 2011;130(1):3-14.
7. Bentley DR. The Human Genome Project--an overview. Med Res Rev. 2000;20(3):189-96.
8. Schmid SL. Molecular Biology of the Cell: It's Our Journal. Mol Biol Cell. 2005;16(1):i-ii.
9. Wang M, Yu G, Ressom HW. Integrative Analysis of Proteomic, Glycomic, and Metabolomic Data for Biomarker Discovery. IEEE J Biomed Health Inform. 2016;20(5):1225-31.
10. WATSON JD, CRICK FH. Molecular structure of nucleic acids; a structure for deoxyribose nucleic acid. Nature. 1953;171(4356):737-8.
11. Lodish H, Berk A, Zipursky SL, Matsudaira P, Baltimore D, Darnell J. Molecular Cell Biology, 4th edition2000.
12. Wang X, Lim HJ, Son A. Characterization of denaturation and renaturation of DNA for DNA hybridization. Environ Health Toxicol. 2014;29:e2014007.
13. Guil S, Esteller M. RNA-RNA interactions in gene regulation: the coding and noncoding players. Trends Biochem Sci. 2015;40(5):248-56.
14. García-Rubio M, Barroso SI, Aguilera A. Detection of DNA-RNA Hybrids In Vivo. Methods Mol Biol. 2018;1672:347-61.
15. Kriegel F, Matek C, Dršata T, Kulenkampff K, Tschirpke S, Zacharias M, et al. The temperature dependence of the helical twist of DNA. Nucleic Acids Res. 2018;46(15):7998-8009.
16. Lipfert J, Doniach S, Das R, Herschlag D. Understanding nucleic acid-ion interactions. Annu Rev Biochem. 2014;83:813-41.
17. Murphy D. Filter hybridization. Methods Mol Biol. 1993;18:449-51.
18. Auvinen E, Hukkanen V, Arstila P. Polyethylene glycol increases specificity of hybridization typing of HPV specimens. Mol Cell Probes. 1989;3(3):289-98.
19. Morange M. A new revolution? The place of systems biology and synthetic biology in the history of biology. EMBO Rep. 2009;10 Suppl 1:S50-3.
20. Micklefield J. Backbone modification of nucleic acids: synthesis, structure and therapeutic applications. Curr Med Chem. 2001;8(10):1157-79.
21. Nielsen CB, Singh SK, Wengel J, Jacobsen JP. The solution structure of a locked nucleic acid (LNA) hybridized to DNA. J Biomol Struct Dyn. 1999;17(2):175-91.
22. Karmakar S, Anderson BA, Rathje RL, Andersen S, Jensen TB, Nielsen P, et al. High-affinity DNA targeting using readily accessible mimics of N2'-functionalized 2'-amino-α-L-LNA. J Org Chem. 2011;76(17):7119-31.
23. Kauppinen S, Vester B, Wengel J. Locked nucleic acid: high-affinity targeting of complementary RNA for RNomics. Handb Exp Pharmacol. 2006(173):405-22.
24. Sørensen JJ, Nielsen JT, Petersen M. Solution structure of a dsDNA:LNA triplex. Nucleic Acids Res. 2004;32(20):6078-85.
25. McTigue PM, Peterson RJ, Kahn JD. Sequence-dependent thermodynamic parameters for locked nucleic acid (LNA)-DNA duplex formation. Biochemistry. 2004;43(18):5388-405.

26. Simeonov A, Nikiforov TT. Single nucleotide polymorphism genotyping using short, fluorescently labeled locked nucleic acid (LNA) probes and fluorescence polarization detection. Nucleic Acids Res. 2002;30(17):e91.
27. Crinelli R, Bianchi M, Gentilini L, Magnani M. Design and characterization of decoy oligonucleotides containing locked nucleic acids. Nucleic Acids Res. 2002;30(11):2435-43.
28. Nielsen PE, Egholm M, Berg RH, Buchardt O. Sequence-selective recognition of DNA by strand displacement with a thymine-substituted polyamide. Science. 1991;254(5037):1497-500.
29. Brown SC, Thomson SA, Veal JM, Davis DG. NMR solution structure of a peptide nucleic acid complexed with RNA. Science. 1994;265(5173):777-80.
30. Eriksson M, Nielsen PE. Solution structure of a peptide nucleic acid-DNA duplex. Nat Struct Biol. 1996;3(5):410-3.
31. Egholm M, Buchardt O, Christensen L, Behrens C, Freier SM, Driver DA, et al. PNA hybridizes to complementary oligonucleotides obeying the Watson-Crick hydrogen-bonding rules. Nature. 1993;365(6446):566-8.
32. Jensen KK, Orum H, Nielsen PE, Nordén B. Kinetics for hybridization of peptide nucleic acids (PNA) with DNA and RNA studied with the BIAcore technique. Biochemistry. 1997;36(16):5072-7.
33. Hyrup B, Nielsen PE. Peptide nucleic acids (PNA): synthesis, properties and potential applications. Bioorg Med Chem. 1996;4(1):5-23.
34. Karkare S, Bhatnagar D. Promising nucleic acid analogs and mimics: characteristic features and applications of PNA, LNA, and morpholino. Appl Microbiol Biotechnol. 2006;71(5):575-86.
35. Armitage B, Ly D, Koch T, Frydenlund H, Orum H, Schuster GB. Hairpin-forming peptide nucleic acid oligomers. Biochemistry. 1998;37(26):9417-25.
36. Betts L, Josey JA, Veal JM, Jordan SR. A nucleic acid triple helix formed by a peptide nucleic acid-DNA complex. Science. 1995;270(5243):1838-41.
37. Rasmussen H, Kastrup JS, Nielsen JN, Nielsen JM, Nielsen PE. Crystal structure of a peptide nucleic acid (PNA) duplex at 1.7 A resolution. Nat Struct Biol. 1997;4(2):98-101.
38. Eriksson M, Nielsen PE. PNA-nucleic acid complexes. Structure, stability and dynamics. Q Rev Biophys. 1996;29(4):369-94.
39. Hamilton SE, Simmons CG, Kathiriya IS, Corey DR. Cellular delivery of peptide nucleic acids and inhibition of human telomerase. Chem Biol. 1999;6(6):343-51.
40. Nielsen PE. Applications of peptide nucleic acids. Curr Opin Biotechnol. 1999;10(1):71-5.
41. Orum H, Nielsen PE, Egholm M, Berg RH, Buchardt O, Stanley C. Single base pair mutation analysis by PNA directed PCR clamping. Nucleic Acids Res. 1993;21(23):5332-6.
42. Abramson RD, Myers TW. Nucleic acid amplification technologies. Curr Opin Biotechnol. 1993;4(1):41-7.
43. Chen Y, Qian C, Liu C, Shen H, Wang Z, Ping J, et al. Nucleic acid amplification free biosensors for pathogen detection. Biosens Bioelectron. 2020;153:112049.
44. Southern EM. Detection of specific sequences among DNA fragments separated by gel electrophoresis. J Mol Biol. 1975;98(3):503-17.
45. Alwine JC, Kemp DJ, Stark GR. Method for detection of specific RNAs in agarose gels by transfer to diazobenzyloxymethyl-paper and hybridization with DNA probes. Proc Natl Acad Sci U S A. 1977;74(12):5350-4.
46. Sanger F, Nicklen S, Coulson AR. DNA sequencing with chain-terminating inhibitors. Proc Natl Acad Sci U S A. 1977;74(12):5463-7.
47. Mullis K, Faloona F, Scharf S, Saiki R, Horn G, Erlich H. Specific enzymatic amplification of DNA in vitro: the polymerase chain reaction. Cold Spring Harb Symp Quant Biol. 1986;51 Pt 1:263-73.

48. Weier HU, Gray JW. A programmable system to perform the polymerase chain reaction. DNA. 1988;7(6):441-7.
49. Higuchi R, Dollinger G, Walsh PS, Griffith R. Simultaneous amplification and detection of specific DNA sequences. Biotechnology (N Y). 1992;10(4):413-7.
50. Schena M, Shalon D, Davis RW, Brown PO. Quantitative monitoring of gene expression patterns with a complementary DNA microarray. Science. 1995;270(5235):467-70.
51. Jarvie T. Next generation sequencing technologies. Drug Discov Today Technol. 2005;2(3):255-60.
52. Mullegama SV, Alberti MO, Au C, Li Y, Toy T, Tomasian V, et al. Nucleic Acid Extraction from Human Biological Samples. Methods Mol Biol. 2019;1897:359-83.
53. Schy WE, Plewa MJ. Use of the diaminobenzoic acid fluorescence assay in conjunction with uv absorbance as a means of quantifying and ascertaining the purity of a DNA preparation. Anal Biochem. 1989;180(2):314-8.
54. Sederoff R. Availability of Taq polymerase. Science. 1993;259(5101):1521-2.
55. Cavanaugh SE, Bathrick AS. Direct PCR amplification of forensic touch and other challenging DNA samples: A review. Forensic Sci Int Genet. 2018;32:40-9.
56. Kwoh DY, Davis GR, Whitfield KM, Chappelle HL, DiMichele LJ, Gingeras TR. Transcription-based amplification system and detection of amplified human immunodeficiency virus type 1 with a bead-based sandwich hybridization format. Proc Natl Acad Sci U S A. 1989;86(4):1173-7.
57. Rifai N, Horvath AR, Wittwer CT. Principles and Applications of Molecular Diagnostics. Elsevier; 2018. p. 47-86.
58. Notomi T, Okayama H, Masubuchi H, Yonekawa T, Watanabe K, Amino N, et al. Loop-mediated isothermal amplification of DNA. Nucleic Acids Res. 2000;28(12):E63.
59. Hellyer TJ, Nadeau JG. Strand displacement amplification: a versatile tool for molecular diagnostics. Expert Rev Mol Diagn. 2004;4(2):251-61.
60. Zanoli LM, Spoto G. Isothermal amplification methods for the detection of nucleic acids in microfluidic devices. Biosensors (Basel). 2013;3(1):18-43.
61. Lutz S, Weber P, Focke M, Faltin B, Hoffmann J, Müller C, et al. Microfluidic lab-on-a-foil for nucleic acid analysis based on isothermal recombinase polymerase amplification (RPA). Lab Chip. 2010;10(7):887-93.
62. Tyagi S, Kramer FR. Molecular beacons: probes that fluoresce upon hybridization. Nat Biotechnol. 1996;14(3):303-8.
63. Tsourkas A, Behlke MA, Rose SD, Bao G. Hybridization kinetics and thermodynamics of molecular beacons. Nucleic Acids Res. 2003;31(4):1319-30.
64. Holland PM, Abramson RD, Watson R, Gelfand DH. Detection of specific polymerase chain reaction product by utilizing the 5'----3' exonuclease activity of Thermus aquaticus DNA polymerase. Proc Natl Acad Sci U S A. 1991;88(16):7276-80.
65. Lurquin PF. The use of intercalating dye molecules in the study of chromatin structure. Chem Biol Interact. 1974;8(5):303-12.
66. Ohler LD, Zollo M, Mansfield ES, Rose EA. Use of a sensitive fluorescent intercalating dye to detect PCR products of low copy number and high molecular weight. PCR Methods Appl. 1993;3(2):115-9.
67. Mokany E, Bone SM, Young PE, Doan TB, Todd AV. MNAzymes, a versatile new class of nucleic acid enzymes that can function as biosensors and molecular switches. J Am Chem Soc. 2010;132(3):1051-9.
68. Mokany E, Tan YL, Bone SM, Fuery CJ, Todd AV. MNAzyme qPCR with superior multiplexing capacity. Clin Chem. 2013;59(2):419-26.
69. Sun W, Qin P, Gao H, Li G, Jiao K. Electrochemical DNA biosensor based on chitosan/nano-V2O5/MWCNTs composite film modified carbon ionic liquid electrode and its application to the LAMP product of Yersinia enterocolitica gene sequence. Biosens Bioelectron. 2010;25(6):1264-70.

70. Wang K, Lei Y, Zhong GX, Zheng YJ, Sun ZL, Peng HP, et al. Dual-probe electrochemical DNA biosensor based on the "Y" junction structure and restriction endonuclease assisted cyclic enzymatic amplification for detection of double-strand DNA of PML/RARα related fusion gene. Biosens Bioelectron. 2015;71:463-9.
71. Pernagallo S, Ventimiglia G, Cavalluzzo C, Alessi E, Ilyine H, Bradley M, et al. Novel biochip platform for nucleic acid analysis. Sensors (Basel). 2012;12(6):8100-11.
72. Wang L, Chen X, Wang X, Han X, Liu S, Zhao C. Electrochemical synthesis of gold nanostructure modified electrode and its development in electrochemical DNA biosensor. Biosens Bioelectron. 2011;30(1):151-7.
73. Pan M, Li R, Xu L, Yang J, Cui X, Wang S. Reproducible Molecularly Imprinted Piezoelectric Sensor for Accurate and Sensitive Detection of Ractopamine in Swine and Feed Products. Sensors (Basel). 2018;18(6).
74. Lee Y, Lee YS. A New Submersion Detection Sensor Using Two Resistance Temperature Detectors Operating on the Thermal Equilibrium Principle. Sensors (Basel). 2019;19(19).
75. Sudo H, Mizoguchi A, Kawauchi J, Akiyama H, Takizawa S. Use of non-amplified RNA samples for microarray analysis of gene expression. PLoS One. 2012;7(2):e31397.
76. Socransky SS, Smith C, Martin L, Paster BJ, Dewhirst FE, Levin AE. "Checkerboard" DNA-DNA hybridization. Biotechniques. 1994;17(4):788-92.
77. Lefferts JA, Jannetto P, Tsongalis GJ. Evaluation of the Nanosphere Verigene System and the Verigene F5/F2/MTHFR Nucleic Acid Tests. Exp Mol Pathol. 2009;87(2):105-8.
78. Yu L, Bhayana S, Jacob NK, Fadda P. Comparative studies of two generations of NanoString nCounter System. PLoS One. 2019;14(11):e0225505.
79. Geiss GK, Bumgarner RE, Birditt B, Dahl T, Dowidar N, Dunaway DL, et al. Direct multiplexed measurement of gene expression with color-coded probe pairs. Nat Biotechnol. 2008;26(3):317-25.
80. Bowling AJ, Pence HE, Church JB. Application of a novel and automated branched DNA in situ hybridization method for the rapid and sensitive localization of mRNA molecules in plant tissues. Appl Plant Sci. 2014;2(4).
81. Baumeister MA, Zhang N, Beas H, Brooks JR, Canchola JA, Cosenza C, et al. A sensitive branched DNA HIV-1 signal amplification viral load assay with single day turnaround. PLoS One. 2012;7(3):e33295.
82. Horn T, Chang CA, Urdea MS. Chemical synthesis and characterization of branched oligodeoxyribonucleotides (bDNA) for use as signal amplifiers in nucleic acid quantification assays. Nucleic Acids Res. 1997;25(23):4842-9.
83. Bowler FR, Diaz-Mochon JJ, Swift MD, Bradley M. DNA analysis by dynamic chemistry. Angew Chem Int Ed Engl. 2010;49(10):1809-12.
84. Rissin DM, López-Longarela B, Pernagallo S, Ilyine H, Vliegenthart ADB, Dear JW, et al. Polymerase-free measurement of microRNA-122 with single base specificity using single molecule arrays: Detection of drug-induced liver injury. PLoS One. 2017;12(7):e0179669.
85. Marín-Romero A, Robles-Remacho A, Tabraue-Chávez M, López-Longarela B, Sánchez-Martín RM, Guardia-Monteagudo JJ, et al. A PCR-free technology to detect and quantify microRNAs directly from human plasma. Analyst. 2018.
86. Delgado-Gonzalez A, Robles-Remacho A, Marin-Romero A, Detassis S, Lopez-Longarela B, Lopez-Delgado FJ, et al. PCR-free and chemistry-based technology for miR-21 rapid detection directly from tumour cells. Talanta. 2019;200:51-6.
87. Detassis S, Grasso M, Tabraue-Chávez M, Marín-Romero A, López-Longarela B, Ilyine H, et al. New Platform for the Direct Profiling of microRNAs in Biofluids. Anal Chem. 2019;91(9):5874-80.
88. López-Longarela B, Morrison EE, Tranter JD, Chahman-Vos L, Léonard JF, Gautier JC, et al. Direct Detection of miR-122 in Hepatotoxicity Using Dynamic Chemical Labeling Overcomes Stability and isomiR Challenges. Anal Chem. 2020.

89. Gulmez SE, Larrey D, Pageaux GP, Bernuau J, Bissoli F, Horsmans Y, et al. Liver transplant associated with paracetamol overdose: results from the seven-country SALT study. Br J Clin Pharmacol. 2015;80(3):599-606.
90. Bowler FR, Reid PA, Boyd AC, Díaz-Mochón JJ, Bradley M. Dynamic chemistry for enzyme-free allele discrimination in genotyping by MALDI-TOF mass spectrometry. Analytical Methods. 2011;3(7):1656-63.
91. Li S, Peng Q, Liao S, Li W, Ma Q, Lu X. A reverse dot blot assay for the screening of twenty mutations in four genes associated with NSHL in a Chinese population. PLoS One. 2017;12(5):e0177196.
92. Schollen E, Vandenberk P, Cassiman JJ, Matthijs G. Development of reverse dot-blot system for screening of mitochondrial DNA mutations associated with Leber hereditary optic atrophy. Clin Chem. 1997;43(1):18-23.
93. Steinlein LM, Crawford JT. Reverse dot blot assay (insertion site typing) for precise detection of sites of IS6110 insertion in the Mycobacterium tuberculosis genome. J Clin Microbiol. 2001;39(3):871-8.
94. Tabraue-Chávez M, Luque-González MA, Marín-Romero A, Sánchez-Martín RM, Escobedo-Araque P, Pernagallo S, et al. A colorimetric strategy based on dynamic chemistry for direct detection of Trypanosomatid species. Sci Rep. 2019;9(1):3696.
95. Marín-Romero A, Tabraue-Chávez M, Dear JW, Sánchez-Martín RM, Ilyne H, Guardia-Monteagudo JJ, et al. Amplification-free profiling of microRNA-122 biomarker in DILI patient serums, using the luminex MAGPIX system. Talanta. 2020;219(121265).
96. Batta A, Kalra BS, Khirasaria R. Trends in FDA drug approvals over last 2 decades: An observational study. J Family Med Prim Care. 2020;9(1):105-14.
97. Winokur RS, Pua BB, Sullivan BW, Madoff DC. Percutaneous lung biopsy: technique, efficacy, and complications. Semin Intervent Radiol. 2013;30(2):121-7.
98. Li G, Liu M. Dr. Mari Mino-Kenudson: challenges and future developments in the field of biopsy. Transl Lung Cancer Res. 2017;6(Suppl 1):S97-S8.
99. Marrugo-Ramírez J, Mir M, Samitier J. Blood-Based Cancer Biomarkers in Liquid Biopsy: A Promising Non-Invasive Alternative to Tissue Biopsy. Int J Mol Sci. 2018;19(10).
100. Yoon JH, Kim EK, Kwak JY, Moon HJ. Effectiveness and limitations of core needle biopsy in the diagnosis of thyroid nodules: review of current literature. J Pathol Transl Med. 2015;49(3):230-5.
101. Buder A, Tomuta C, Filipits M. The potential of liquid biopsies. Curr Opin Oncol. 2016;28(2):130-4.
102. Diaz LA, Bardelli A. Liquid biopsies: genotyping circulating tumor DNA. J Clin Oncol. 2014;32(6):579-86.
103. Heitzer E, Auer M, Ulz P, Geigl JB, Speicher MR. Circulating tumor cells and DNA as liquid biopsies. Genome Med. 2013;5(8):73.
104. Finotti A, Allegretti M, Gasparello J, Giacomini P, Spandidos DA, Spoto G, et al. Liquid biopsy and PCR-free ultrasensitive detection systems in oncology (Review). Int J Oncol. 2018;53(4):1395-434.
105. Yang M, Forbes ME, Bitting RL, O'Neill SS, Chou PC, Topaloglu U, et al. Incorporating blood-based liquid biopsy information into cancer staging: time for a TNMB system? Ann Oncol. 2018;29(2):311-23.
106. Veldore VH, Choughule A, Routhu T, Mandloi N, Noronha V, Joshi A, et al. Validation of liquid biopsy: plasma cell-free DNA testing in clinical management of advanced non-small cell lung cancer. Lung Cancer (Auckl). 2018;9:1-11.
107. Izzotti A, Carozzo S, Pulliero A, Zhabayeva D, Ravetti JL, Bersimbaev R. Extracellular MicroRNA in liquid biopsy: applicability in cancer diagnosis and prevention. Am J Cancer Res. 2016;6(7):1461-93.
108. Kleppe M, Levine RL. Tumor heterogeneity confounds and illuminates: assessing the implications. Nat Med. 2014;20(4):342-4.

109. Coombs CC, Zehir A, Devlin SM, Kishtagari A, Syed A, Jonsson P, et al. Therapy-Related Clonal Hematopoiesis in Patients with Non-hematologic Cancers Is Common and Associated with Adverse Clinical Outcomes. Cell Stem Cell. 2017;21(3):374-82.e4.
110. Bartel DP. MicroRNAs: genomics, biogenesis, mechanism, and function. Cell. 2004;116(2):281-97.
111. Bartel DP. MicroRNAs: target recognition and regulatory functions. Cell. 2009;136(2):215-33.
112. Krol J, Loedige I, Filipowicz W. The widespread regulation of microRNA biogenesis, function and decay. Nat Rev Genet. 2010;11(9):597-610.
113. Nilsen TW. Mechanisms of microRNA-mediated gene regulation in animal cells. Trends Genet. 2007;23(5):243-9.
114. Romero-Cordoba SL, Salido-Guadarrama I, Rodriguez-Dorantes M, Hidalgo-Miranda A. miRNA biogenesis: biological impact in the development of cancer. Cancer Biol Ther. 2014;15(11):1444-55.
115. Chim SS, Shing TK, Hung EC, Leung TY, Lau TK, Chiu RW, et al. Detection and characterization of placental microRNAs in maternal plasma. Clin Chem. 2008;54(3):482-90.
116. Hanke M, Hoefig K, Merz H, Feller AC, Kausch I, Jocham D, et al. A robust methodology to study urine microRNA as tumor marker: microRNA-126 and microRNA-182 are related to urinary bladder cancer. Urol Oncol. 2010;28(6):655-61.
117. Park NJ, Zhou H, Elashoff D, Henson BS, Kastratovic DA, Abemayor E, et al. Salivary microRNA: discovery, characterization, and clinical utility for oral cancer detection. Clin Cancer Res. 2009;15(17):5473-7.
118. Weber JA, Baxter DH, Zhang S, Huang DY, Huang KH, Lee MJ, et al. The microRNA spectrum in 12 body fluids. Clin Chem. 2010;56(11):1733-41.
119. Kosaka N, Izumi H, Sekine K, Ochiya T. microRNA as a new immune-regulatory agent in breast milk. Silence. 2010;1(1):7.
120. Wang K, Zhang S, Weber J, Baxter D, Galas DJ. Export of microRNAs and microRNA-protective protein by mammalian cells. Nucleic Acids Res. 2010;38(20):7248-59.
121. Hunter MP, Ismail N, Zhang X, Aguda BD, Lee EJ, Yu L, et al. Detection of microRNA expression in human peripheral blood microvesicles. PLoS One. 2008;3(11):e3694.
122. Arroyo JD, Chevillet JR, Kroh EM, Ruf IK, Pritchard CC, Gibson DF, et al. Argonaute2 complexes carry a population of circulating microRNAs independent of vesicles in human plasma. Proc Natl Acad Sci U S A. 2011;108(12):5003-8.
123. Turchinovich A, Weiz L, Langheinz A, Burwinkel B. Characterization of extracellular circulating microRNA. Nucleic Acids Res. 2011;39(16):7223-33.
124. Turchinovich A, Weiz L, Burwinkel B. Extracellular miRNAs: the mystery of their origin and function. Trends Biochem Sci. 2012;37(11):460-5.
125. Kang K, Peng X, Luo J, Gou D. Identification of circulating miRNA biomarkers based on global quantitative real-time PCR profiling. J Anim Sci Biotechnol. 2012;3(1):4.
126. Chen Y, Gelfond JA, McManus LM, Shireman PK. Reproducibility of quantitative RT-PCR array in miRNA expression profiling and comparison with microarray analysis. BMC Genomics. 2009;10:407.
127. Moldovan L, Batte KE, Trgovcich J, Wisler J, Marsh CB, Piper M. Methodological challenges in utilizing miRNAs as circulating biomarkers. J Cell Mol Med. 2014;18(3):371-90.
128. Poel D, Buffart TE, Oosterling-Jansen J, Verheul HM, Voortman J. Evaluation of several methodological challenges in circulating miRNA qPCR studies in patients with head and neck cancer. Exp Mol Med. 2018;50(3):e454.
129. Lujambio A, Lowe SW. The microcosmos of cancer. Nature. 2012;482(7385):347-55.
130. Masaki S, Ohtsuka R, Abe Y, Muta K, Umemura T. Expression patterns of microRNAs 155 and 451 during normal human erythropoiesis. Biochem Biophys Res Commun. 2007;364(3):509-14.

131. Khordadmehr M, Jigari-Asl F, Ezzati H, Shahbazi R, Sadreddini S, Safaei S, et al. A comprehensive review on miR-451: A promising cancer biomarker with therapeutic potential. J Cell Physiol. 2019;234(12):21716-31.
132. Patrick DM, Zhang CC, Tao Y, Yao H, Qi X, Schwartz RJ, et al. Defective erythroid differentiation in miR-451 mutant mice mediated by 14-3-3zeta. Genes Dev. 2010;24(15):1614-9.
133. Rasmussen KD, Simmini S, Abreu-Goodger C, Bartonicek N, Di Giacomo M, Bilbao-Cortes D, et al. The miR-144/451 locus is required for erythroid homeostasis. J Exp Med. 2010;207(7):1351-8.
134. Svasti S, Masaki S, Penglong T, Abe Y, Winichagoon P, Fucharoen S, et al. Expression of microRNA-451 in normal and thalassemic erythropoiesis. Ann Hematol. 2010;89(10):953-8.
135. Pase L, Layton JE, Kloosterman WP, Carradice D, Waterhouse PM, Lieschke GJ. miR-451 regulates zebrafish erythroid maturation in vivo via its target gata2. Blood. 2009;113(8):1794-804.
136. Pan X, Wang R, Wang ZX. The potential role of miR-451 in cancer diagnosis, prognosis, and therapy. Mol Cancer Ther. 2013;12(7):1153-62.
137. Tsuchiya S, Oku M, Imanaka Y, Kunimoto R, Okuno Y, Terasawa K, et al. MicroRNA-338-3p and microRNA-451 contribute to the formation of basolateral polarity in epithelial cells. Nucleic Acids Res. 2009;37(11):3821-7.
138. Wang R, Wang ZX, Yang JS, Pan X, De W, Chen LB. MicroRNA-451 functions as a tumor suppressor in human non-small cell lung cancer by targeting ras-related protein 14 (RAB14). Oncogene. 2011;30(23):2644-58.
139. Venkateswaran S, Luque-González MA, Tabraue-Chávez M, Fara MA, López-Longarela B, Cano-Cortes V, et al. Novel bead-based platform for direct detection of unlabelled nucleic acids through Single Nucleobase Labelling. Talanta. 2016;161:489-96.
140. Kullak-Ublick GA, Andrade RJ, Merz M, End P, Benesic A, Gerbes AL, et al. Drug-induced liver injury: recent advances in diagnosis and risk assessment. Gut. 2017;66(6):1154-64.
141. Dear JW, Clarke JI, Francis B, Allen L, Wraight J, Shen J, et al. Risk stratification after paracetamol overdose using mechanistic biomarkers: results from two prospective cohort studies. Lancet Gastroenterol Hepatol. 2018;3(2):104-13.
142. Shen T, Liu Y, Shang J, Xie Q, Li J, Yan M, et al. Incidence and Etiology of Drug-Induced Liver Injury in Mainland China. Gastroenterology. 2019;156(8):2230-41.e11.
143. Tajiri K, Shimizu Y. Practical guidelines for diagnosis and early management of drug-induced liver injury. World J Gastroenterol. 2008;14(44):6774-85.
144. Danan G, Benichou C. Causality assessment of adverse reactions to drugs--I. A novel method based on the conclusions of international consensus meetings: application to drug-induced liver injuries. J Clin Epidemiol. 1993;46(11):1323-30.
145. Bateman DN, Carroll R, Pettie J, Yamamoto T, Elamin ME, Peart L, et al. Effect of the UK's revised paracetamol poisoning management guidelines on admissions, adverse reactions and costs of treatment. Br J Clin Pharmacol. 2014;78(3):610-8.
146. Vliegenthart ADB, Berends C, Potter CMJ, Kersaudy-Kerhoas M, Dear JW. MicroRNA-122 can be measured in capillary blood which facilitates point-of-care testing for drug-induced liver injury. Br J Clin Pharmacol. 2017;83(9):2027-33.
147. Vliegenthart AD, Starkey Lewis P, Tucker CS, Del Pozo J, Rider S, Antoine DJ, et al. Retro-orbital blood acquisition facilitates circulating microRNA measurement in zebrafish with paracetamol hepatotoxicity. Zebrafish. 2014;11(3):219-26.
148. Starkey Lewis PJ, Dear J, Platt V, Simpson KJ, Craig DG, Antoine DJ, et al. Circulating microRNAs as potential markers of human drug-induced liver injury. Hepatology. 2011;54(5):1767-76.
149. Vliegenthart AD, Shaffer JM, Clarke JI, Peeters LE, Caporali A, Bateman DN, et al. Comprehensive microRNA profiling in acetaminophen toxicity identifies novel circulating biomarkers for human liver and kidney injury. Sci Rep. 2015;5:15501.

150. Antoine DJ, Dear JW, Lewis PS, Platt V, Coyle J, Masson M, et al. Mechanistic biomarkers provide early and sensitive detection of acetaminophen-induced acute liver injury at first presentation to hospital. Hepatology. 2013;58(2):777-87.
151. Dear JW, Antoine DJ, Starkey-Lewis P, Goldring CE, Park BK. Early detection of paracetamol toxicity using circulating liver microRNA and markers of cell necrosis. Br J Clin Pharmacol. 2014;77(5):904-5.
152. Singhal R, Harrill AH, Menguy-Vacheron F, Jayyosi Z, Benzerdjeb H, Watkins PB. Benign elevations in serum aminotransferases and biomarkers of hepatotoxicity in healthy volunteers treated with cholestyramine. BMC Pharmacol Toxicol. 2014;15:42.
153. Ward J, Kanchagar C, Veksler-Lublinsky I, Lee RC, McGill MR, Jaeschke H, et al. Circulating microRNA profiles in human patients with acetaminophen hepatotoxicity or ischemic hepatitis. Proc Natl Acad Sci U S A. 2014;111(33):12169-74.
154. Zhang Y, Jia Y, Zheng R, Guo Y, Wang Y, Guo H, et al. Plasma microRNA-122 as a biomarker for viral-, alcohol-, and chemical-related hepatic diseases. Clin Chem. 2010;56(12):1830-8.
155. Shifeng H, Danni W, Pu C, Ping Y, Ju C, Liping Z. Circulating liver-specific miR-122 as a novel potential biomarker for diagnosis of cholestatic liver injury. PLoS One. 2013;8(9):e73133.
156. Hansson M, Mathsson L, Schlederer T, Israelsson L, Matsson P, Nogueira L, et al. Validation of a multiplex chip-based assay for the detection of autoantibodies against citrullinated peptides. Arthritis Res Ther. 2012;14(5):R201.
157. Seyfarth F, Schliemann S, Wiegand C, Hipler UC, Elsner P. Diagnostic value of the ISAC(®) allergy chip in detecting latex sensitizations. Int Arch Occup Environ Health. 2014;87(7):775-81.
158. Onell A, Hjälle L, Borres MP. Exploring the temporal development of childhood IgE profiles to allergen components. Clin Transl Allergy. 2012;2(1):24.
159. Röckmann H, van Geel MJ, Knulst AC, Huiskes J, Bruijnzeel-Koomen CA, de Bruin-Weller MS. Food allergen sensitization pattern in adults in relation to severity of atopic dermatitis. Clin Transl Allergy. 2014;4(1):9.
160. Prosperi MC, Belgrave D, Buchan I, Simpson A, Custovic A. Challenges in interpreting allergen microarrays in relation to clinical symptoms: a machine learning approach. Pediatr Allergy Immunol. 2014;25(1):71-9.
161. King EM, Filep S, Smith B, Platts-Mills T, Hamilton RG, Schmechel D, et al. A multi-center ring trial of allergen analysis using fluorescent multiplex array technology. J Immunol Methods. 2013;387(1-2):89-95.
162. Sander I, Zahradnik E, Kraus G, Mayer S, Neumann HD, Fleischer C, et al. Domestic mite antigens in floor and airborne dust at workplaces in comparison to living areas: a new immunoassay to assess personal airborne allergen exposure. PLoS One. 2012;7(12):e52981.
163. Earle CD, King EM, Tsay A, Pittman K, Saric B, Vailes L, et al. High-throughput fluorescent multiplex array for indoor allergen exposure assessment. J Allergy Clin Immunol. 2007;119(2):428-33.
164. Fu Q, Zhu J, Van Eyk JE. Comparison of multiplex immunoassay platforms. Clin Chem. 2010;56(2):314-8.
165. Chowdhury F, Williams A, Johnson P. Validation and comparison of two multiplex technologies, Luminex and Mesoscale Discovery, for human cytokine profiling. J Immunol Methods. 2009;340(1):55-64.
166. Backen AC, Cummings J, Mitchell C, Jayson G, Ward TH, Dive C. 'Fit-for-purpose' validation of SearchLight multiplex ELISAs of angiogenesis for clinical trial use. J Immunol Methods. 2009;342(1-2):106-14.
167. Brookes K, Cummings J, Backen A, Greystoke A, Ward T, Jayson GC, et al. Issues on fit-for-purpose validation of a panel of ELISAs for application as biomarkers in clinical trials of anti-Angiogenic drugs. Br J Cancer. 2010;102(10):1524-32.

168. Bastarache JA, Koyama T, Wickersham NE, Ware LB. Validation of a multiplex electrochemiluminescent immunoassay platform in human and mouse samples. J Immunol Methods. 2014;408:13-23.
169. Perraut R, Richard V, Varela ML, Trape JF, Guillotte M, Tall A, et al. Comparative analysis of IgG responses to Plasmodium falciparum MSP1p19 and PF13-DBL1α1 using ELISA and a magnetic bead-based duplex assay (MAGPIX®-Luminex) in a Senegalese meso-endemic community. Malar J. 2014;13:410.
170. Reslova N, Michna V, Kasny M, Mikel P, Kralik P. xMAP Technology: Applications in Detection of Pathogens. Front Microbiol. 2017;8:55.
171. SAFE-T consortium. Novel clinical biomarkers of Drug-Induced Liver Injury 2016 [Available from: http://www.imi-safe-t.eu/files/files-inline/DILI%20BM%20Summary%20Data%20Package%20-%2020170105_final_updated.pdf.
172. Comission E. Translational Safety Biomarker Pipeline (TransBioLine): Enabling development and implementation of novel safety biomarkers in clinical trials and diagnosis of disease 2019 [Available from: https://cordis.europa.eu/project/id/821283.
173. Garcia-Fernandez E, Gonzalez-Garcia MC, Pernagallo S, Ruedas-Rama MJ, Fara MA, López-Delgado FJ, et al. miR-122 direct detection in human serum by time-gated fluorescence imaging. Chem Commun (Camb). 2019;55(99):14958-61.
174. Elshal MF, McCoy JP. Multiplex bead array assays: performance evaluation and comparison of sensitivity to ELISA. Methods. 2006;38(4):317-23.
175. Esposito S, Scala A, Bianchini S, Presicce ML, Mori A, Sciarrabba CS, et al. Partial comparison of the NxTAG Respiratory Pathogen Panel Assay with the Luminex xTAG Respiratory Panel Fast Assay V2 and singleplex real-time polymerase chain reaction for detection of respiratory pathogens. Diagn Microbiol Infect Dis. 2016;86(1):53-7.
176. Shi X, Wu R, Shi M, Zhou L, Wu M, Yang Y, et al. Simultaneous detection of 13 viruses involved in meningoencephalitis using a newly developed multiplex PCR Mag-array system. Int J Infect Dis. 2016;49:80-6.
177. Li Y, Yao L, Li J, Chen L, Song Y, Cai Z, et al. Stability issues of RT-PCR testing of SARS-CoV-2 for hospitalized patients clinically diagnosed with COVID-19. J Med Virol. 2020.
178. Bailey WJ, Holder D, Patel H, Devlin P, Gonzalez RJ, Hamilton V, et al. A performance evaluation of three drug-induced liver injury biomarkers in the rat: alpha-glutathione S-transferase, arginase 1, and 4-hydroxyphenyl-pyruvate dioxygenase. Toxicol Sci. 2012;130(2):229-44.
179. Murayama H, Ikemoto M, Fukuda Y, Nagata A. Superiority of serum type-I arginase and ornithine carbamyltransferase in the detection of toxicant-induced acute hepatic injury in rats. Clin Chim Acta. 2008;391(1-2):31-5.